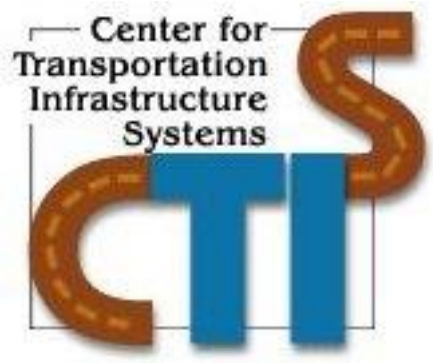

INTELLIGENT COMPACTION ROLLER RETROFIT KIT VALIDATION

Conducted for
Texas Department of Transportation
in cooperation with
Federal Highway Administration

August 2015

Center for Transportation Infrastructure Systems
The University of Texas at El Paso
El Paso, TX 79968
(915) 747-6925
http://ctis.utep.edu

TECHNICAL REPORT STANDARD TITLE PAGE

1. Report No.	2. Government Accession No.	3. Recipient's Catalog No.

4. Title and Subtitle	5. Report Date
Intelligent Compaction Roller Retrofit Kit Validation	August 2015
	6. Performing Organization Code

7. Author(s)	8. Performing Organization Report No.
Soheil Nazarian, Mehran Mazari, George Chang, Raed Aldouri, Jorge Beltran	

9. Performing Organization Name and Address	10. Work Unit No.
Center for Transportation Infrastructure Systems The University of Texas at El Paso El Paso, Texas 79968-0516	11. Contract or Grant No.

12. Sponsoring Agency Name and Address	13. Type of Report and Period Covered
Texas Department of Transportation Research and Technology Implementation Office P.O. Box 5080, Austin, Texas 78763-5080	Draft Final Report
	14. Sponsoring Agency Code

15. Supplementary Notes

Research Performed in cooperation with TxDOT and the Federal Highway Administration
Research Study Title: Intelligent Compaction Roller Retrofit Kit Validation

16. Abstract

The main goals of this project were to evaluate and validate intelligent compaction (IC) retrofit (after market) kits for use in the field compaction of asphalt pavements, bases, and subgrade materials. This project was a part of the second phase of Every Day Counts (EDC2) program by the Federal Highway Administration (FHWA) to nationally deploy the use of IC technology to improve compaction quality and managing compaction data. Under this study, the intelligent compaction measurement values (ICMV) obtained from the mounted IC retrofit kits were compared with the Original Equipment Manufacturer (OEM) IC rollers and other spot test methods. In addition, a verification process was developed to ensure that the retrofit kit was mounted properly to capture the drum rebound. Two equipment rodeos, one in California for asphalt materials and another one in Texas for soils materials, were conducted for side-by-side comparison of IC-retrofitted rollers to the OEM IC rollers. Finally, the data collected at the two rodeos were utilized to evaluate the performance of each participating IC equipment regarding measurement reliability on asphalt pavement, base, and subgrade materials. In general, the performance of the IC retrofit kit utilized in this study seemed reliable as long as the hardware and software were installed properly. The calibration/validation of the vibration sensor and the global positioning system (GPS) of the retrofit kit is crucial to obtain dependable and reliable IC data.

17. Key Words	18. Distribution Statement
Intelligent compaction, Retrofit kit, Geomaterials, IC Measurement Value	No restrictions. This document is available to the public through the National Technical service, 5285 Port Royal Road, Springfield, Virginia 22161, www.ntis.gov

19. Security Classif. (of this report)	20. Security Classif. (of this page)	21. No. of Pages	22. Price
Unclassified	Unclassified		

Form DOT F 1700.7 (8-69)

INTELLIGENT COMPACTION ROLLER RETROFIT KIT VALIDATION

by

Soheil Nazarian, PhD, PE
Mehran Mazari, PhD, EIT
George Chang, PhD, PE
Raed Aldouri, PhD
Jorge Beltran, BSCE

Conducted for

Texas Department of Transportation
in cooperation with
Federal Highway Administration

Center for Transportation Infrastructure Systems
The University of Texas at El Paso
El Paso, TX 79968-0516

DISCLAIMERS

The contents of this report reflect the view of the authors who are responsible for the facts and the accuracy of the data presented herein. The contents do not necessarily reflect the official views or policies of the Texas Department of Transportation or the Federal Highway Administration. This report does not constitute a standard, a specification or a regulation.

The material contained in this report is experimental in nature and is published for informational purposes only. Any discrepancies with official views or policies of the Texas Department of Transportation or the Federal Highway Administration should be discussed with the appropriate Austin Division prior to implementation of the procedures or results.

NOT INTENDED FOR CONSTRUCTION, BIDDING, OR PERMIT PURPOSES

Soheil Nazarian, PhD, PE (66495)
Mehran Mazari, PhD, EIT
George Chang, PhD, PE
Raed Aldouri, PhD
Jorge Beltran, BSCE

ACKNOWLEDGEMENTS

The authors would like to express their sincere appreciation to the Project Management Committee of this project, consisting of Jimmy Si and Richard Izzo from Texas Department of Transportation and Antonio Nieves, Michael Arasteh, and Richard Duval from the Federal Highway Administration (FHWA) for their support.

We are grateful to Ebi Fini and Chuck Suszko from California Department of Transportation (CalTrans) and Granite Construction for their cooperation in arrangement of California field tests and Richard Williammee from Texas Department of Transportation (TxDOT) and Lone Star Civil Construction for helping with planning the Texas field tests. The help and support from the IC roller vendors (Caterpillar, Wirtgen Group/HAMM and SAKAI) and their partners (TOPCON and Trimble) are also acknowledged.

We are also grateful to a number of undergraduate and graduate students from The University of Texas El Paso (UTEP) for their assistance in the project.

ABSTRACT

The main goals of this project were to evaluate and validate intelligent compaction (IC) retrofit (after market) kits for use in the field compaction of asphalt pavements, bases, and subgrade materials. This project was a part of the second phase of Every Day Counts (EDC2) program by the Federal Highway Administration (FHWA) to nationally deploy the use of IC technology to improve compaction quality and managing compaction data. Under this study, the intelligent compaction measurement values (ICMV) obtained from the mounted IC retrofit kits were compared with the Original Equipment Manufacturer (OEM) IC rollers and other spot test methods. In addition, a verification process was developed to ensure that the retrofit kit was mounted properly to capture the drum rebound. Two equipment rodeos, one in California for asphalt materials and another one in Texas for soils materials, were conducted for side-by-side comparison of IC-retrofitted rollers to the OEM IC rollers. Finally, the data collected at the two rodeos were utilized to evaluate the performance of each participating IC equipment regarding measurement reliability on asphalt pavement, base, and subgrade materials. In general, the performance of the IC retrofit kit utilized in this study seemed reliable as long as the hardware and software were installed properly. The calibration/validation of the vibration sensor and the global positioning system (GPS) of the retrofit kit is crucial to obtain dependable and reliable IC data.

EXECUTIVE SUMMARY

The intelligent compaction (IC) retrofit kits have been recently introduced as an economic alternative to the original equipment manufacturer (OEM) IC systems. Although IC retrofit kits have been employed in many projects nationwide, their performance and reliability on asphalt, soils and base materials has not been evaluated in a comprehensive manner. The Federal Highway Administration (FHWA), as a part of the second Every Day Counts (EDC2) initiative, funded this research study through the Texas Department of Transportation (TxDOT) to evaluate the performance of intelligent compaction (IC) roller retrofit kits. A data acquisition system was developed to validate the vibration data collection process parallel to the IC retrofit kit and the OEM IC systems. As one of the main parts of this study, two equipment rodeos were conducted for field evaluations. One of these equipment rodeos was dedicated to asphalt materials which was performed along a construction site near Sacramento, California. The second equipment rodeo was dedicated to study the soil layers on a test section near Cleburne, Texas. Three IC roller vendors including Caterpillar (CAT), Wirtgen Group-Hamm (HAMM), and Sakai America (SAKAI), participated in both rodeos. The IC systems on the CAT rollers are similar to the Trimble aftermarket IC (retrofit) kits for single- and double-drum rollers. The IC systems on the SAKAI rollers are provided by SAKAI and TOPCON. The TOPCON also recently launched an IC retrofit kit. TOPCON retrofit kit was not evaluated in this study because it was not available during our field studies. HAMM utilizes its OEM IC system known as HAMM Compaction Quality (HCQ). Both the Trimble retrofit and CAT OEM systems produce Compacter Meter Values (CMV). The HAMM OEM produces HAMM Measurement Value (HMV), while the SAKAI OEM produces Compaction Control Value (CCV). These accelerometer-based measurement values, which are collectively called Intelligent Compaction Measurement Values (ICMVs), are generally related to the stiffness of the existing compacted materials with influence from underlying layers. This report along with the appendices present the findings from the evaluation of the IC roller retrofit kits. The findings of this study are briefly summarized as follows.

Equipment Rodeo on Hot Mix Asphalt

- The cumulative distributions of CMVs collected with the two retrofit systems installed on the HAMM and SAKAI rollers during the pre-mapping of the existing base layer were similar. However, the CAT roller showed a different trend for the cumulative distribution of the collected CMVs.
- The distributions of the ICMVs from the OEM system and retrofit kit on the HAMM roller, HMV and CMV respectively, were similar during the pre-mapping. The IC data from the SAKAI OEM system were not available for comparison purposes.
- The two retrofit systems mounted on the HAMM and SAKAI rollers showed different trends in terms of the CMV values during the mapping of the HMA layers. This could be due to the different coverage area and change of HMA stiffness between the breakdown and intermediate compaction during the HMA rodeo.

Equipment Rodeo on Geomaterials

- The CMVs during the pre-mapping of the existing embankment layer with the retrofit kit mounted on the HAMM roller and the OEM system on the CAT roller were similar. The CMVs collected from the retrofit kit mounted on the SAKAI roller were different than those reported by the HAMM retrofit and CAT OEM systems.

- The ICMV data from the retrofit kit and OEM system during the pre-mapping with the HAMM roller, CMV and HMV respectively, show similar trends with some differences that could be due to the data processing algorithms used by each of the two systems.
- The spatial distributions of the CMVs from the retrofit system on the HAMM roller and the OEM system on the CAT roller during mapping are similar as they identified similar less stiff areas.
- Even though the mapping of the compacted subgrade layer with the smooth drum CAT roller was performed about 18 hours after the compaction process using a CAT roller with a padfoot shell kit, the spatial distribution trends of the CMVs from the two operations were similar. However, the spatial distribution of the CMV from the smooth drum roller was clearer, than those from the padfoot roller and the amplitudes of CMVs from the smooth drum roller were greater than those from the padfoot roller.

The following points summarize comments regarding validation of the ICMV using a UTEP Vibration Data Acquisition (DAQ) System:

- The proper positioning of the accelerometers is crucial in capturing the proper vibration energy.
- Identifying the vibration frequencies and their multiple harmonics properly is essential in calculating the appropriate ICMVs.
- The vibration responses of the two accelerometers installed by the research team on the opposite sides of the drums were similar with typically less than 4% difference.
- The calculated cumulative distributions of the CMVs from the retrofit kit and DAQ system were similar with minor differences when the retrofit kit was installed properly.
- The influence depth of roller vibration underneath the drum depends on the layer stiffness as well as the vibration settings. Based on the field data in this study, the influence depth could be as shallow as 20 in. for a very stiff granular layer over bedrock and deeper than 5 ft for a less stiff clayey materials.

Spot Tests:

Correlations between the spot test values (including density and stiffness) and ICMVs were not significant which may be due to differences in test foot prints and influence depths.

In general, the performance of the IC retrofit kit utilized in this study seemed reliable as long as the hardware and software were installed properly. The calibration/validation of the vibration sensor and global positioning system (GPS) of the retrofit kit is crucial to obtain dependable and reliable IC data.

TABLE OF CONTENTS

LIST OF FIGURES

LIST OF TABLES

CHAPTER 1. INTRODUCTION

1.1 INTRODUCTION

Intelligent Compaction (IC) is an innovative technology for compaction quality control and acceptance of base, soil and hot mix asphalt (HMA). Two types of IC rollers are available in the market. One is original equipment manufacturer (OEM) IC rollers and the other one is retrofitted rollers. The Federal Highway Administration through the TxDOT sponsored a research project under the second Every Day Count (EDC2) program entitled "National Deployment of Intelligent Compaction." The main goal of this project was to conduct a comprehensive evaluation of the candidate intelligent compaction (IC) retrofit kits for quality compaction of hot mix asphalt, base, and subgrade layers.

One key component of this project was to conduct two equipment rodeos. The main objectives of the equipment rodeos were to:

- Demonstrate IC retrofit kit installation and operation to targeted departments of transportation (DOTs)
- Recommend the proper installation of the retrofit kits
- Determine the measurement variability of each specific IC roller as well as retrofitted rollers with respect to inherent field and material variations, and
- Investigate the correlation between selected nondestructive test (NDT) results and IC data collected from retrofitted and OEM IC rollers

A number of roller manufacturers have implemented IC technology in their compaction equipment for both HMA and soils. Each of these OEM systems employ different instrumentation to collect vibration data and use different methods to estimate the stiffness of the compacted layer. As an alternative option to an OEM system, a retrofit system (after-market kit) can be installed on a regular roller to collect IC data. The performance of retrofit systems as compared with various OEM systems has not been documented to date. The main purpose of this research project was to evaluate the IC retrofit kits through equipment rodeos during actual field operations.

1.2 WORK PLAN OVERVIEW

Two separate rodeos were planned. The first rodeo was dedicated to HMA and the second to soil (subgrade) layers. The following activities were conducted during each equipment rodeo:

- Identifying and preparing test strips
- Setting up the GPS
- Retrofitting rollers
- Evaluating kit installation
- Mapping existing layers
- Performing spot tests
- Facilitating an open house
- Conducting a follow-up/feedback meeting

Three roller manufacturers participated in the field rodeos and the Trimble retrofit systems was employed to perform the data collection process.

As a part of this project, a data acquisition system (DAQ) was developed to evaluate and monitor the vibration of drums (using two accelerometers mounted on the rollers) as well as the response of the ground (using two 3-dimensional geophones buried at two different depths) during the compaction process.

1.3 ORGANIZATION OF REPORT

Besides the existing chapter which includes the introduction and structure of the research findings, this report contains four additional chapters. Chapter 1 (this chapter) includes the introduction and structure of the research findings, this report contains five additional chapters.

Chapter 2 includes a brief review of intelligent compaction systems and the retrofit kits as well as the definition of different IC measurement values.

Chapter 3 contains the description of field activities during the two equipment rodeos on HMA and soils. This chapter also includes the details of the DAQ system that was developed as a part of this research. The data reduction algorithms are further discussed in Appendix C.

Chapter 4 discusses the results of field tests for different IC rollers as well as the data collected by the DAQ system. The results of spot tests are also included in that chapter. The summary of field tests and data collection process during the two equipment rodeos are included in Appendices A and B.

Chapter 5 summarizes the major findings of this research, recommendations for the application of retrofit kits during IC data collection, and recommendations for future studies.

Appendix A contains the activities and results during the first rodeo dedicated to HMA materials in California.

Appendix B includes the data collection process and analyses of results regarding the second equipment rodeo on soils in Texas.

Appendix C is dedicated to the detailed process of reducing and analyzing vibration data from DAQ validation system.

Appendix D contains a multimedia presentation showing the step-by-step installation process for the retrofit kit.

Appendix E contains a list of FAQs for the installation and operation of an IC retrofit kit.

CHAPTER 2. LITERATURE REVIEW

2.1 INTRODUCTION

Intelligent compaction (IC) is an emerging technology for monitoring the compaction process for HMA, base and soil layers and for managing the compaction data to improve the quality of compacted layers and to avoid over/under compaction. The advantages of IC are reported as (Anderegg and Koufman, 2004; Hossian et al., 2006; Petersen et al., 2006; White et al., 2006; Mooney et al., 2010; Chang et al., 2011; and Gallivan et al., 2011):

- Improved quality and uniformity of compaction
- Reduced over/under compaction
- Identification of less stiff spots, and

The following section contains a literature survey of the IC retrofit kit, IC measurement values (ICMVs) and their definitions.

2.2 INTELLIGENT COMPACTION RETROFIT KIT

Intelligent compaction is a specific terminology for a wider concept of continuous compaction control (CCC) that was initiated by the Swedish Highway Administration in 1974. In 1975, Geodynamik continued the development of a roller-mounted compaction meter. Geodynamik and Dynapac later introduced the Compaction Meter Value (CMV) to monitor the roller-integrated compaction process. A number of roller manufacturers began offering CMV-enabled systems. In 1982, Bomag introduced the Omega value (which was a measure of compaction energy and time) and the Terrameter. With the introduction of mechanistic and performance-related soil properties, Bomag launched the Vibration Modulus that was a measure of dynamic soil stiffness. In 1999, Ammann introduced the Soil Stiffness Parameter followed by initiation of the Compaction Control Value (CCV) by SAKAI in 2004 (Mooney et al, 2010). The IC systems have been under continuous development since then. Even though the IC systems were considered original equipment manufacturer (OEM) systems, in 2008 Trimble introduced the IC retrofit (after-market) kit that can be installed on most regular vibratory rollers to collect IC data. With the advancement and improvement of the IC retrofit kit, its application has been growing during the past few years. Due to the increasing application of the IC retrofit kit, there was a need to evaluate the performance of the kit during the actual compaction process. This study was focused on addressing the need for such evaluation. TOPCON recently launched their IC retrofit kit. The TOPCON retrofit kit was not evaluated in this study because they become available after the two field studies were completed.

2.3 INTELLIGENT COMPACTION MEASUREMENT VALUES

Intelligent compaction is a form of roller-integrated continuous compaction control (CCC) that was initiated in late 1970s and has been under constant development. The concept of correlating stiffness of the compacted layer to the excitation frequency (Geodynamik, 1974) initiated the use of accelerometers to monitor the compaction process. This idea was further improved and became the basis of measurement for some of the roller vendors. CAT uses this concept as Compaction Meter Value (CMV) while HAMM utilizes that as HAMM Measurement Value (HMV). These measurement values are defined as (Mooney et al, 2010):

$$\boldsymbol{CMV\ or\ HMV = 300 \times (\frac{A_4}{A_2})} \quad (2.1.1)$$

where A_2 is the acceleration of the forcing component of the vibration and A_4 is the acceleration of the first harmonic of the vibration. As indicated in Figure 2.1.1, the CMV only takes the forcing frequency and first harmonic into account. However, if the compacted layer becomes stiffer, the other harmonics (A_1 through A_6 in Figure 2.1.2) could also be identified during the compaction process.

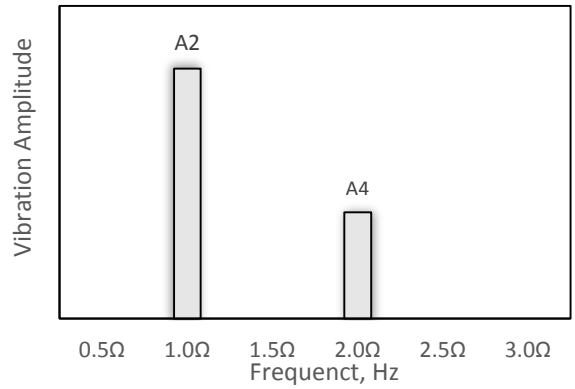

Figure 2.1.1. Forcing frequency and vibration harmonics for a less stiff

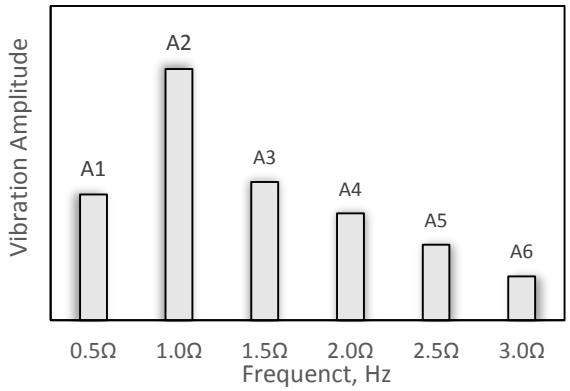

Figure 2.1.2. Forcing frequency and vibration harmonics for a stiff layer

The SAKAI Compaction Control Value (CCV) utilizes the following equation to estimate the layer stiffness:

$$CCV = 100 \times \left[\frac{A_1+A_3+A_4+A_5+A_6}{A_1+A_2}\right] \quad (2.1.2)$$

Assuming that the rotational frequency of the forcing mode of the vibration is Ω, parameters A_1 through A_6 in Equation 2.1.2 represent the acceleration of vibration at 0.5Ω, Ω, 1.5Ω, 2Ω, 2.5Ω and 3Ω, respectively.

Adam and Kopf (2000) introduced another index as the Resonant Meter Value (RMV) for dynamic rollers (using a vibration or oscillating mechanism) which is defined as:

$$RMV = \left(\frac{A_1}{A_2}\right) \quad (2.1.3)$$

The soil-drum interaction force of a dynamic roller can be simulated from the following equation:

$$F_b = -m_d a_d + m_u r_u \Omega^2 \cos(\Omega t) + \left(m_f + m_d\right) g \quad (2.1.4)$$

where m_d = mass of the drum, a_d = acceleration of the drum that is the second derivative of the vertical displacement of the drum, m_f = mass of the frame, m_u = unbalanced mass, r_u = radial distance at which the unbalanced mass is attached, Ω = vibration frequency, t =elapsed time and g = acceleration of gravity. Thereafter, K_b, the secant stiffness, could be estimated from the ratio of F_b and maximum vertical drum displacement.

Ammann (2003) introduced K_s as an estimate of the soil stiffness using drum and vibration parameters as:

$$K_s = \Omega^2 \left[m_d + \frac{m_0 e_0 \cos(\phi)}{z_d}\right] \quad (2.1.5)$$

where $m_{0.}e_0$ = eccentric mass moment, m_d = drum mass, Ω = excitation frequency, z_d = vertical drum displacement and ϕ = phase lag between the eccentric force and drum displacement.

Bomag initiated the Omega value (a measure of compaction energy and time) in the early 1980s and later introduced the vibration modulus (E_{vib}) as a measure of dynamic soil stiffness. This concept resembles the roller vibration as a cyclic plate load test and estimates the E_{vib} using the following equation (Briaud, 2004):

$$E_{vib} = 1.5r\left(\frac{1}{a_1+a_2\sigma_{1max}}\right) \quad (2.1.6)$$

where r = radius of loading plate (which is the contact width of a roller with the underlying layer), σ_{1max} = maximum average normal stress of the first loading cycle, a_1 and a_2 are calculated from plate load test results (using $s = \sigma_0 + a_1\sigma_0 + a_2\sigma_0^2$ in which s is the settlement of the center of the plate and σ_1 is the average nominal stress under the plate).

CHAPTER 3. FIELD EVALUATIONS

3.1 EQUIPMENT RODEOS

Two equipment rodeos were conducted for side-by-side comparisons of IC-retrofitted rollers with OEM rollers; the first rodeo was dedicated to HMA, while the second rodeo focused on soils. The project for the HMA rodeo was located in El Dorado County, California near El Dorado Hills (Figure 3.1.1). A 500 ft long by 25 ft wide test section was used for this rodeo. All IC rollers were used to compact the entire project area during the rodeo (Figure 3.1.2). The project contained a 6.5 in.-thick HMA layer (which was placed in two 2.5 in thick lifts and one 1.5 in thick surface course lift) on top of an 18-in.-thick base layer. The base layer was compacted prior to the rodeo and was pre-mapped with IC rollers prior to the HMA paving. The asphalt rodeo was performed during the third week of September 2014. The detailed field activity is included in Appendix A.

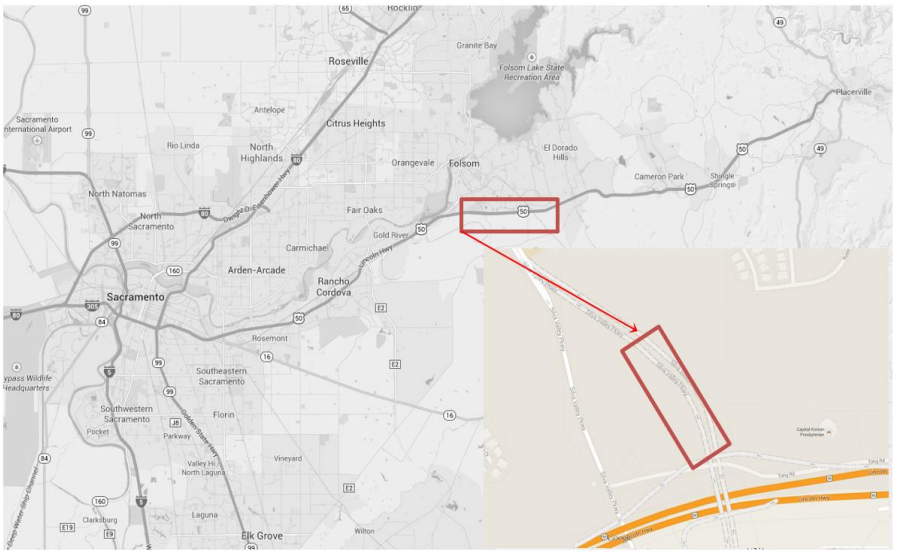

Figure 3.1.1. Location of HMA rodeo in El Dorado Hills, California

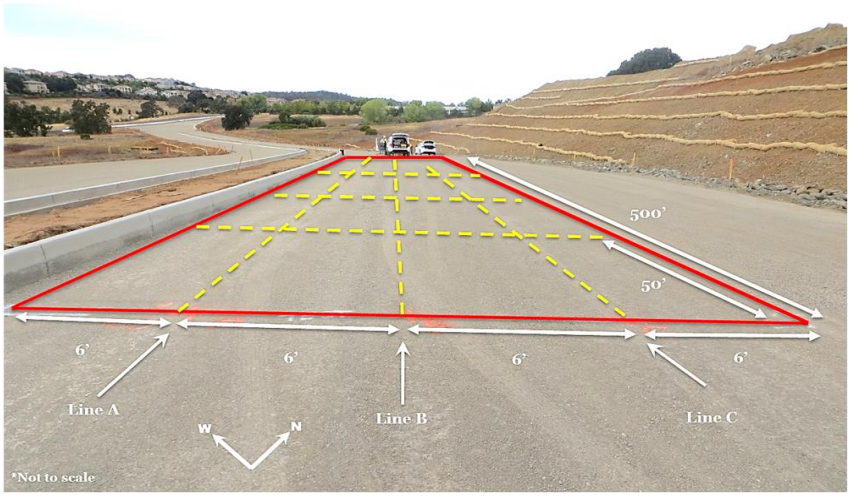

Figure 3.1.2. Testing section and test grid for HMA rodeo

The project location selected for the soils rodeo was at the junction of US 67-Business and County Road 801B near Cleburne, Texas (Figure 3.1.3). This test section was a part of the US 67 widening which included soils. The focus of this study was on pre-mapping the existing embankment and the compaction of a 12 in. clayey subgrade layer. Similar to the HMA rodeo, a 500 ft long and 25 ft wide test section was selected on the east bound frontage road to perform the IC data collection (Figure 3.1.4). This rodeo took place during the third week of November 2014. A detailed field activity is included in Appendix B.

Figure 3.1.3. Location of soils rodeo in Cleburne, Texas

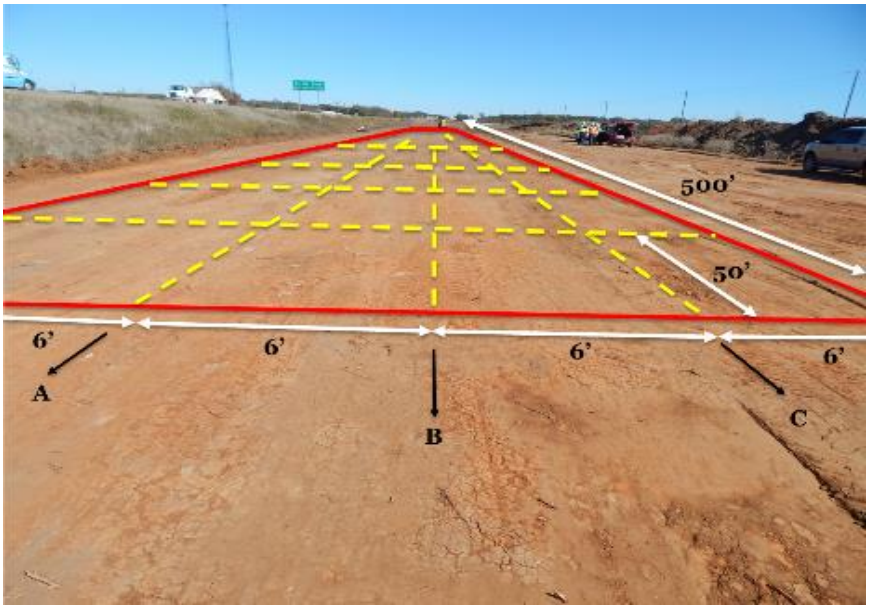

Figure 3.1.4. Testing section and test grid for soils rodeo

3.2 INTELLIGENT COMPACTION DATA COLLECTION

Three IC roller manufacturers, including Caterpillar (CAT), Wirtgen Group-Hamm (HAMM), and Sakai America (SAKAI), participated in this study. Two types of IC rollers are available in the market. The original equipment manufacturer (OEM) IC rollers with factory-installed IC system, and retrofitted IC rollers that use after-market (retrofit) IC kits mounted on conventional rollers. At the time of performing this research, the only commercially available retrofit kits were distributed by Trimble®. The evaluation of the TOPCON IC retrofit kits, introduced in March 2015, were not included in this study. One of the main objectives of this study was to evaluate the performance of IC retrofit kits relative to the performance of the OEM systems. To that end, the HAMM and SAKAI IC OEM systems were also retrofitted with Trimble retrofit kits. Since the CAT OEM systems are similar to that of Trimble's, the Trimble retrofit kits were not installed on those CAT rollers.

To further evaluate the vibration characteristics of the OEM and retrofit IC systems, a data acquisition system (DAQ) was developed at UTEP. A schematic of the system is depicted in Figure 3.2.1. The system consists of two accelerometers that are mounted on the two sides of the rollers (drums), a data acquisition box, a GPS antenna and receiver, a power supply and a laptop computer to monitor the data collection process (see Figure 3.2.2).

A similar data acquisition system was also developed to monitor the propagation of roller vibration within the geomaterials by embedding three-dimensional (3D) geophones at two different depths in the subsurface layers. A second GPS system was used to synchronize the collected data with this stationary system with the accelerometers mounted on the rollers. The two 3D geophones were embedded in the existing ground layer (before placement of the new test layer) at two different depths to monitor the soil layer responses during the IC operation. The 3D geophones recorded the vertical, transversal and longitudinal amplitudes of vibration, with the longitudinal response being in the same direction as the roller movement and the transversal response being perpendicular to the moving direction.

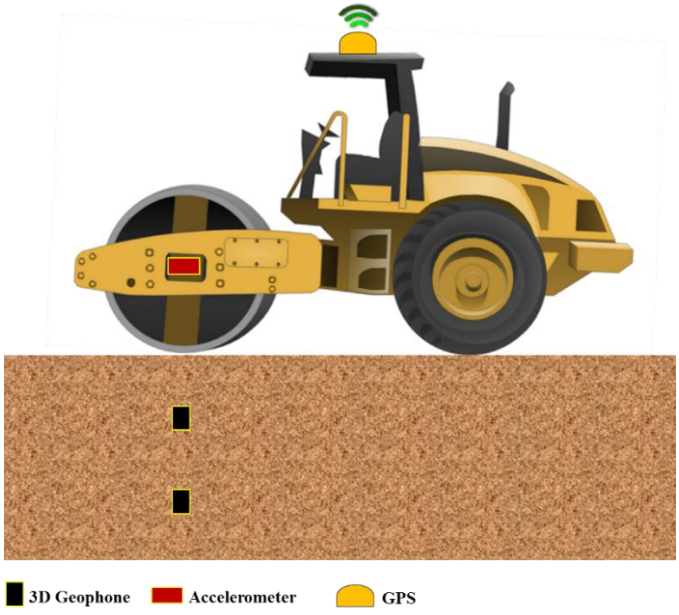

Figure 3.2.1. Schematic of the IC Validation System

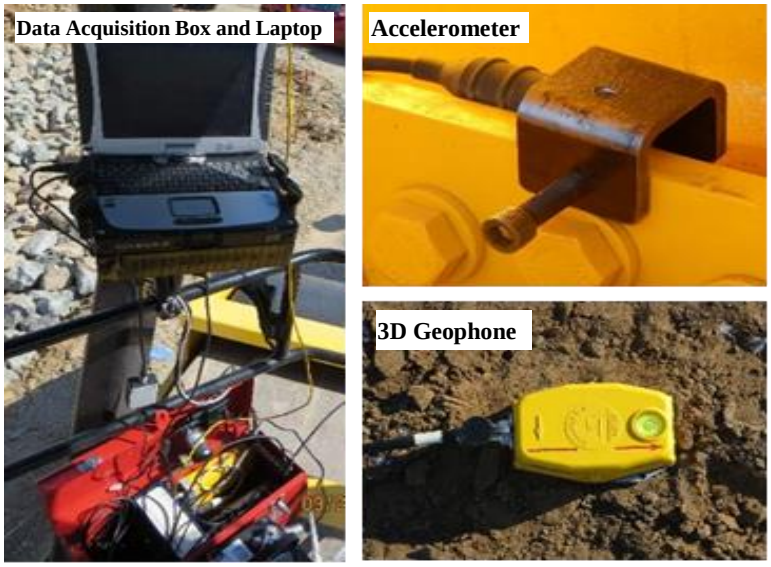

Figure 3.2.2. Components of the data acquisition system developed for this research

The DAQ was installed on each roller to collect data using the following two setups:

- Stationary vibration (with two accelerometers mounted on the roller, one on the drum surface and one inside the drum) with the following settings (see Figure 3.2.3):
    - Low-frequency and low-amplitude
    - High-frequency and low-amplitude
    - Low-frequency and high-amplitude
    - High-frequency and high-amplitude
- Moving vibration (see Figure 3.2.4) from 50 ft before to 50 ft after the location of embedded geophones while the two accelerometers were mounted on each side of the front drum.

Figures 3.2.5 and 3.2.6 illustrate typical vibration data from mounted accelerometers and embedded geophones, respectively. In both figures, the raw data are shown in the time domain. The frequency-domain data are also demonstrated to show the peak amplitudes, forcing and associated harmonic frequencies. The data reduction process will be explained in more details in Chapter 4.

Figure 3.2.7 illustrates the typical position of the mounted accelerometers on the front drums to monitor their performance. As noted earlier, three different data collection systems (retrofit kit, OEM and UTEP DAQ) were utilized to collect vibration data simultaneously during the compaction process. Figure 3.2.8 exhibits a typical result of the fast-Fourier transform (FFT) analysis that shows the forcing and first harmonic vibrating frequency of the mounted accelerometer as well as their corresponding amplitudes (A2 and A4).

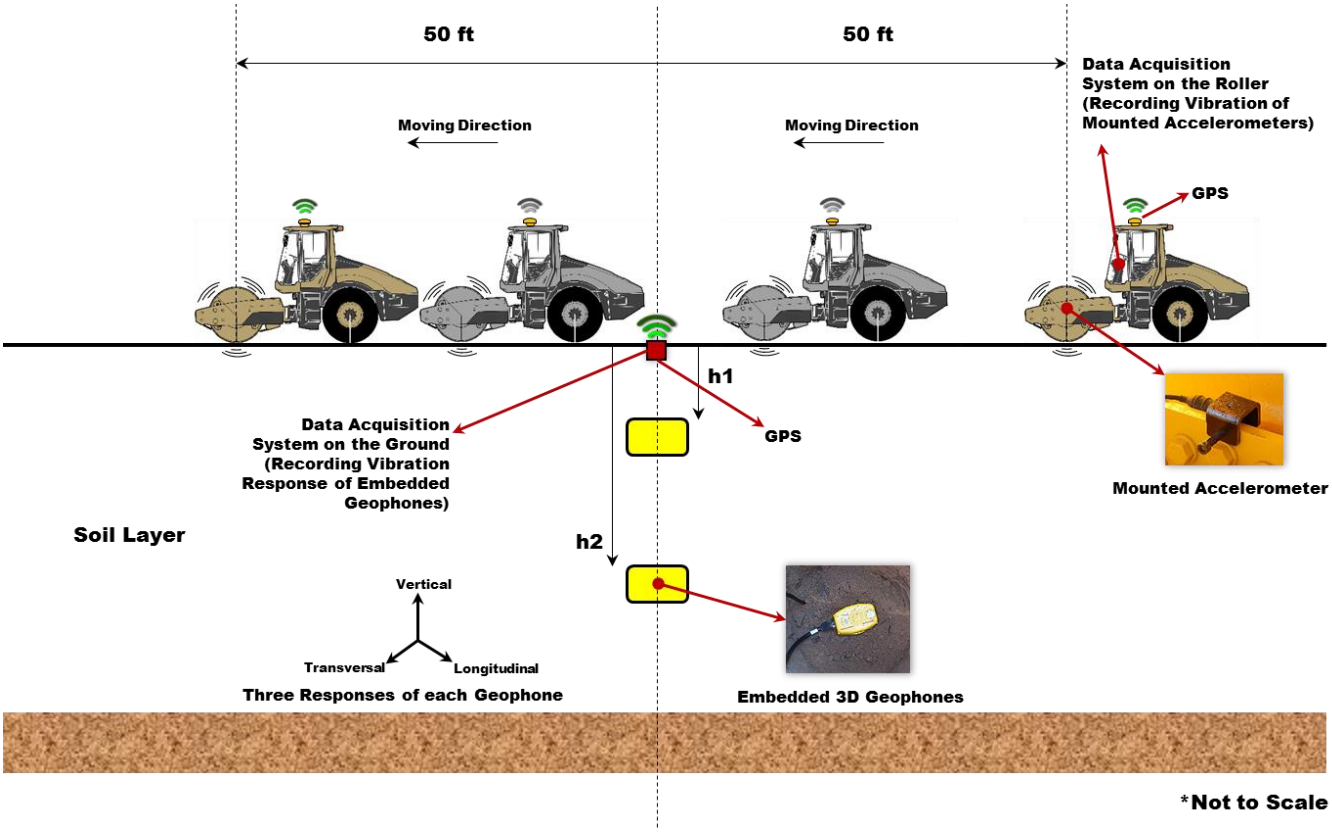

Figure 3.2.3. Data collection during moving vibration

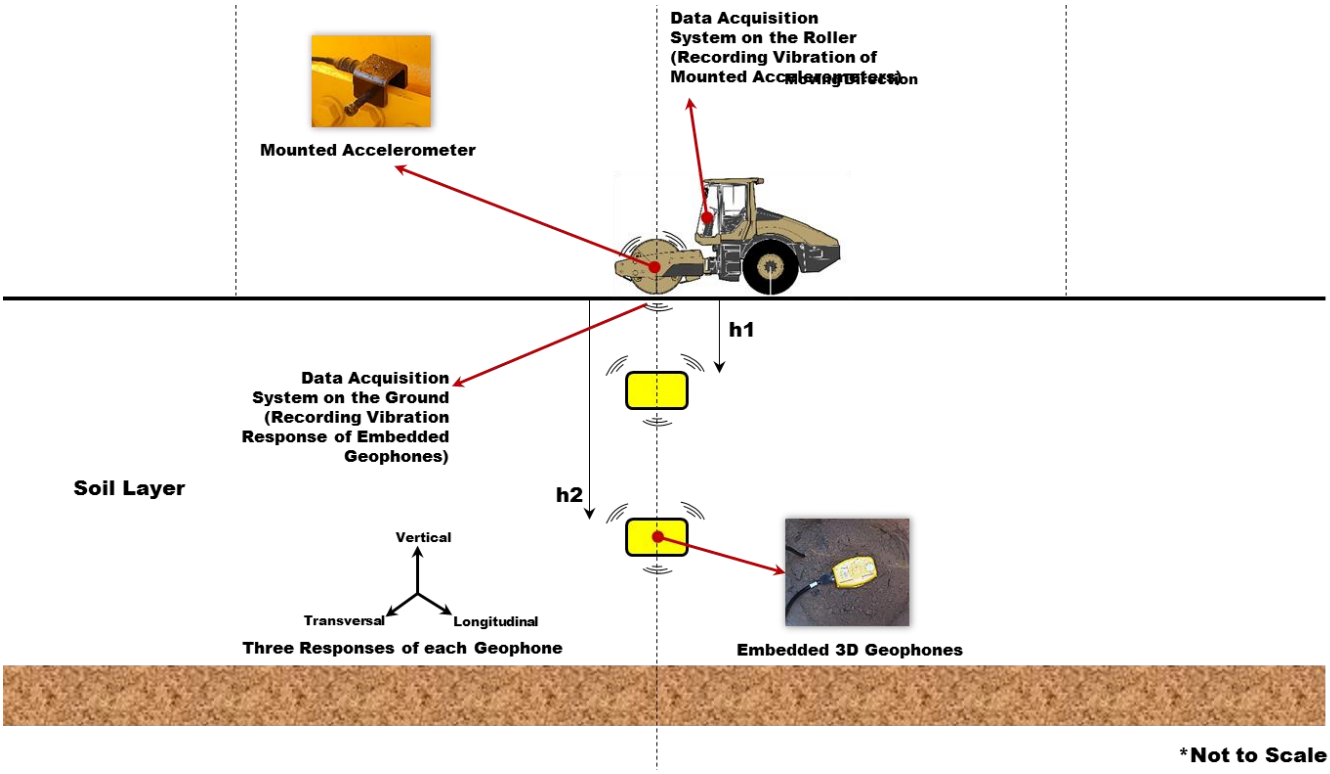

Figure 3.2.4. Data collection during stationary vibration

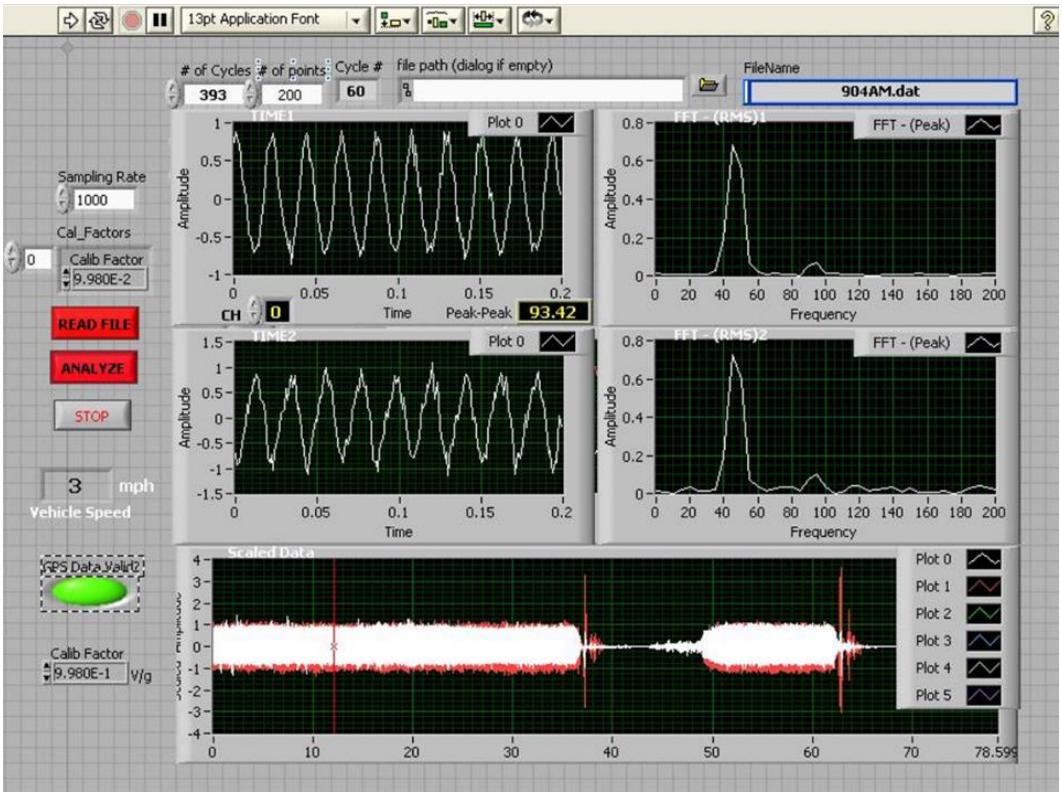

Figure 3.2.5. Typical vibration data collected with the mounted accelerometers

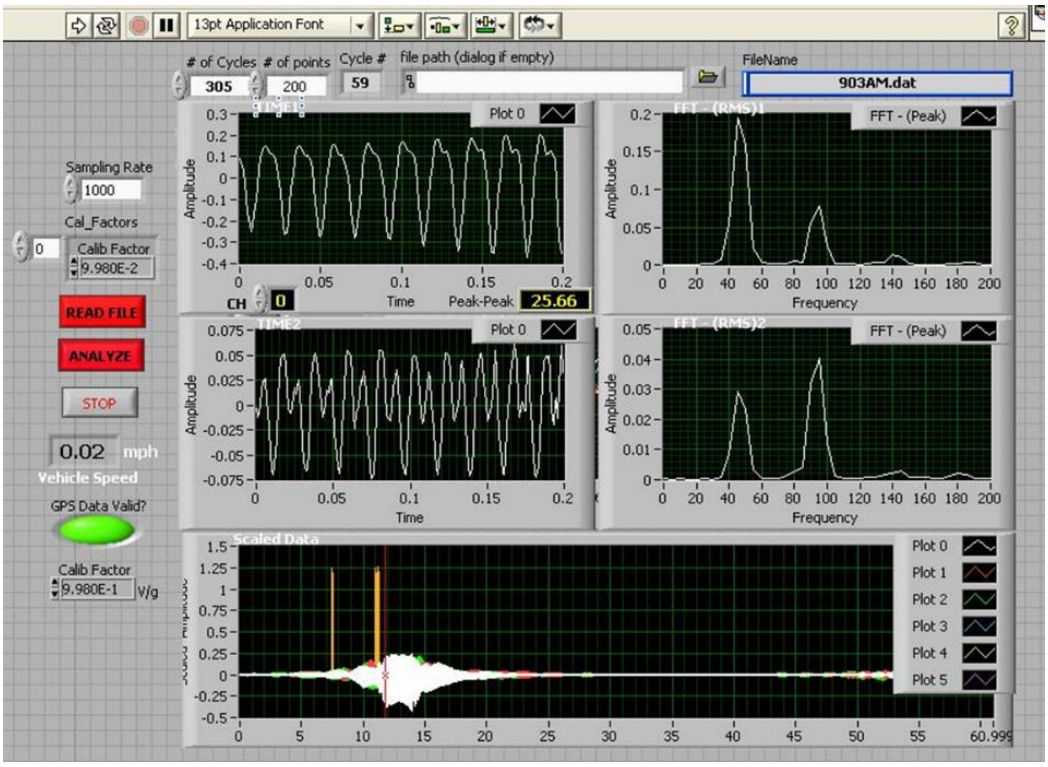

Figure 3.2.6. Typical vibration data collected with the embedded geophones

Figure 3.2.7. Mounted accelerometers on both sides of the drum

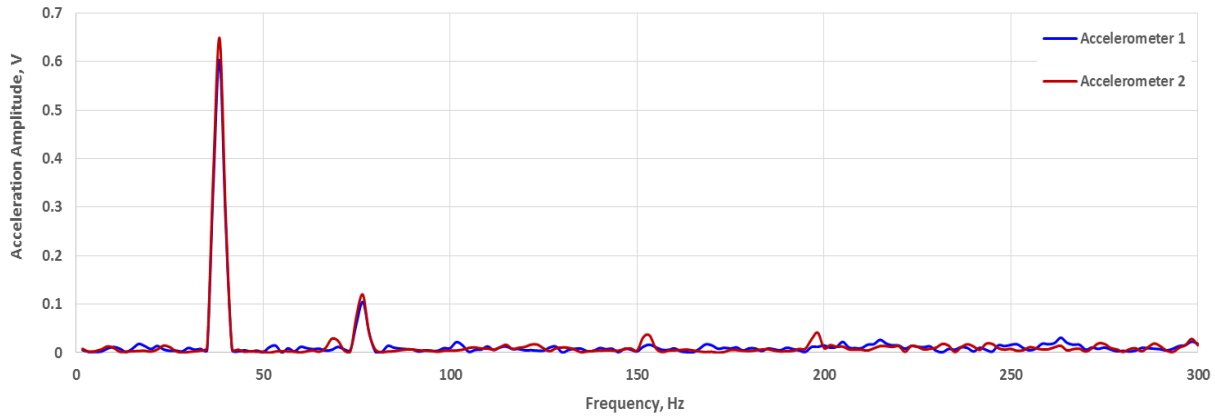

Figure 3.2.8. Example of acceleration amplitude data in frequency domain

3.3 SPECIFICATIONS OF THE OEM SYSTEMS AND RETROFIT KIT

Figure 3.3.1 shows the Trimble CCSFlex retrofit kit components. Figure 3.3.2 illustrates the components of a retrofit kit installed on a roller. The components include a GPS antenna and receiver, vibration sensor (accelerometer), connection cables and in-cab control box which provides the vibration data and system settings. The reliability of the collected data and their comparison with OEM systems has been the main focus of this research project.

The OEM intelligent compaction systems are installed on single-drum (for soils) or double-drum (for HMA) vibratory rollers to collect vibration data through accelerometers (vibration sensors) and a GPS unit. Tables 3.3.1 and 3.3.2 summarize the specifications of the three double-drum rollers employed in the HMA and the three single drum rollers employed in the soil compaction process in this project.

Figure 3.3.1. Components of the Trimble retrofit systems

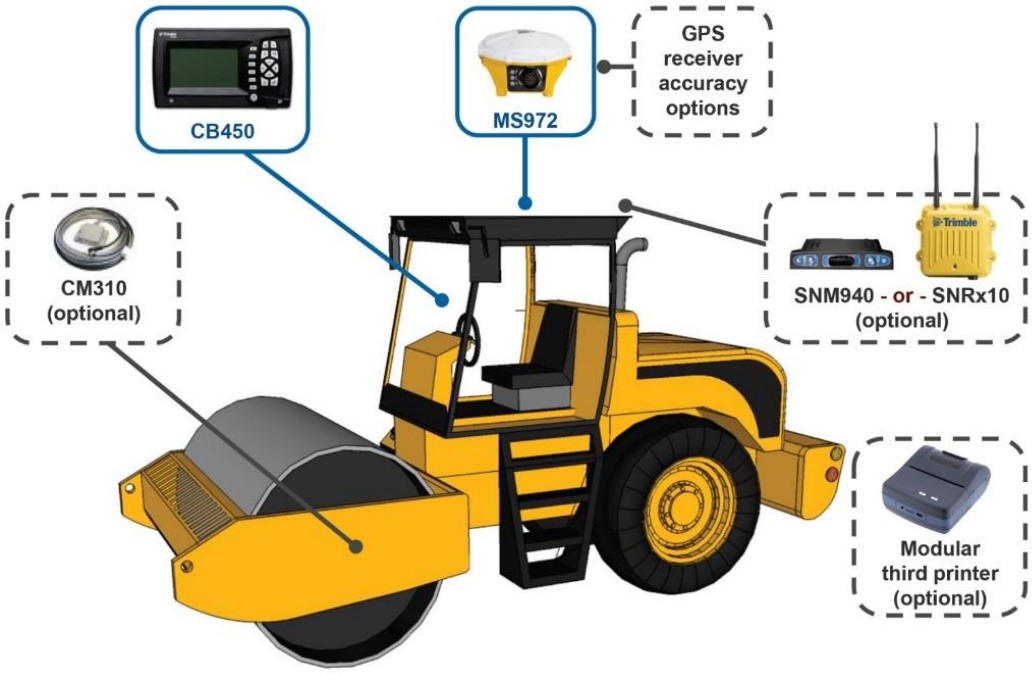

Figure 3.3.2. Components of the retrofit kit installed on a regular roller (courtesy of Trimble)

Table 3.3.1. Specification of double-drum rollers in the Asphalt rodeo

	CAT	SAKAI	HAMM
Vendor/ Manufacturer			
Model	CB54XW Asphalt Compactor	Asphalt Roller - SW880	HD+120 Vibratory Smooth Drum Roller
Compaction Width	79 in.	79 in.	78 in.
Operating Weight	26,230 lbs	29,560 lbs	26,488 lbs
Centrifugal Force	7,801 – 24,729 lbs	14,165 – 39,790 lbs	25,100 – 41,850 lbs
Nominal Amplitude	0.012 - 0.034 in.	0.013 - 0.022 in.	0.018 – 0.034 in.
Frequency	2520 - 3800 vpm	2520 - 4000 vpm	2520 – 3200 vpm
Temperature Sensor	Yes	Yes	Yes
Compaction Measurement Technology	Compaction Meter Value (CMV)	Compaction Control Value (CCV)	HAMM Measurement Value (HMV)

Table 3.3.2. Specification of single-drum rollers in the Soils rodeo

	CATERPILLAR	SAKAI	HAMM
Vendor/ Manufacturer			
Model	Single-drum IC roller with a padfoot shell kit - CS74B	Single-drum padfoot IC roller (with smooth drum shell kit) - SV540T	HD120 Vibratory Smooth Drum Roller
Compaction Width	84 in.	84 in.	84 in.
Operating Weight	35,264 lbs	24,450 lbs	24,857 lbs
Centrifugal Force	37,300 – 74,600 lbs	38,665 – 57,325 lbs	38,475 – 55,350 lbs
Nominal Amplitude	0.039 – 0.083 in.	0.037 – 0.076 in.	0.033 – 0.080 in.
Frequency	1400 – 1680 vpm	1700 – 2000 vpm	1800 – 2400 vpm
Temperature Sensor	No	No	No
Compaction Measurement Technology	Compaction Meter Value (CMV)	Compaction Control Value (CCV)	HAMM Measurement Value (HMV)

3.4 GPS VALIDATION PROCESS

Both the OEM and retrofit systems apply offset of the GPS positions from the GPS receivers to the centers of the drums where the ICMV system is installed. To meet the survey grade precision, the GPS readings from the OEM and retrofit systems were adjusted with correction signals from a land-based GPS base station or virtual reference stations.

The UTEP DAQ vibration sensors were installed on each side of the front drum while the retrofit and OEM sensors were installed on one side of the drum, as typically done with the OEM systems. The GPS readings from the UTEP DAQ were translated to the centerlines of the front drums to represent the vibration data, assuming one ICMV across the entire drum.

The process of GPS validation that was implemented in this project is shown in Figures 3.4.1 and 3.4.2. In order to obtain accurate GPS location, the roller moved slowly to a designated position to allow header computation to be stabilized. After the roller stopped, the last reading, which was associated with the center of the drum, was recorded. The coordinates of both sides of the drum (Figure 3.4.2) were then recorded using a handheld survey-grade GPS rover that was previously synched with the local base station. The coordinates of the drum center was interpolated from the coordinates of the two sides of the drum. The coordinates reported by the OEM and retrofit systems were compared with the coordinates estimated from the rover. If necessary, the OEM and retrofit systems' coordinates were transformed to match the same coordinate system. The tolerance of the differences is 12 in. in the northing and easting directions, as recommended in the FHWA generic IC specifications. Such validation process is strongly recommended before starting the IC data collection process to avoid data shifts or erroneous setup.

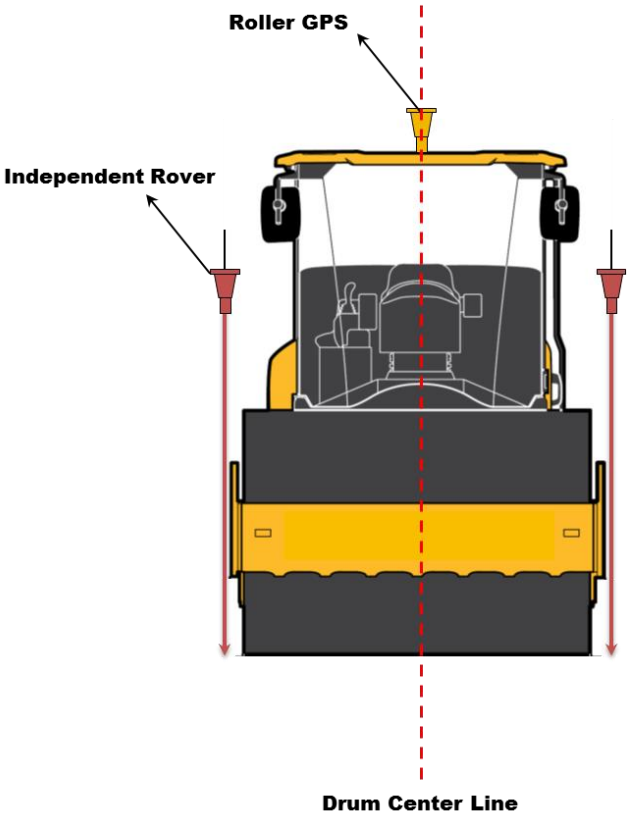

Figure 3.4.1. Schematic of the GPS validation process

Figure 3.4.2. GPS validation process

3.5 DATA MANAGEMENT

The desirable format for IC data that can be easily interpreted and analyzed, is comma separated (.csv) values. Since most roller vendors have their own proprietary formats for data collection and algorithms for data export, each vendor provides a tool to translate the data to csv format. Table 3.5.1 summarizes the format of collected data files for each roller vendor along with their corresponding tools.

Table 3.5.1. Different IC data formats and visualization tools

Roller Vendor	HAMM	CAT and Trimble	SAKAI
Native Data Format	*.hcqx	*.tag	*.ml3
Exported Gridded Data Format	*_amd.vexp, *_pmd.vexp	*.csv	*.pln and *.plns
Software	HCQ	VisionLink®	TOPCON SiteLink3D

No information about the data acquisition and analysis processes by the OEM or retrofit systems is available. The raw vibration data from the UTEP accelerometers and geophones were collected at a rate of 1000 data samples per second. A FFT was applied to 600 acceleration time series data samples every 0.2 seconds to obtain the acceleration, velocity and displacement spectra in frequency domain. Additionally, moving average was applied to a window of every 200 processed data points. The next step was to synchronize the accelerometer data with the geophone responses utilizing the GPS time stamps. This process provided the necessary vibration data within the specified range of the soil rodeo test section from 50 ft before to 50 ft after the location of the geophones (see Figure 3.2.3). That distance was 100 ft before and after the geophones location for

the HMA rodeo. Appendix C contains a detailed description of the trade-offs associated with the parameters stated above.

3.6 GEOSPATIAL ANALYSIS OF IC DATA

Geostatistical and geospatial data analyses were employed to visualize and interpret the IC data. The two common tools for presentation of the IC data and performing additional analyses are Veta and ArcGIS. Each tool has its own advantages and limitations. Veta is user-friendly and is required as a standard tool in FHWA, AASHTO, and many State DOT's specifications. ArcGIS provides more tools and flexibility required for a rigorous analysis and visualization to expert users. Both tools were employed in this project to represent collected IC data during each equipment rodeos. To perform advanced analyses, ArcMap 10.2.2 was employed in this project. The IC data was exported from the vendors' software to a csv format. The process of IC data analysis with ArcMap is summarized as follows:

- Importing the csv data file into ArcMap environment
- Displaying the IC data on the map based on the coordinate system used during data collection. The Universal Transverse Mercator (UTM) system uses Northing and Easting coordinates to locate the position of data points. The projected coordinate system uses Latitude and Longitude formats. Both UTM and projected coordinate systems were used to collect IC data in this project.
- Checking data formats and exporting the IC data as a shape file format (*.shp)
- Drawing specific boundaries to select the desired test section from the whole covered area and filtering IC data within the boundary limits
- Performing geostatistical analysis on the collected IC data and generating customized color-coded maps

3.7 SPOT TESTS

One of the advantages of intelligent compaction over conventional spot tests (density and/or modulus) is that IC provides a 100% coverage of the section while spot tests only evaluate random locations as defined by the quality control/quality assurance (QC/QA) process. To further evaluate the performance of the IC data, a number of modulus/stiffness-based devices were employed during the field evaluations. Figures 3.7.1 through 3.7.3 illustrate the employment of spot test devices in this project. These devices included:

- **Portable Seismic Property Analyzer (PSPA)** uses the Spectral-Analysis-of-Surface-Waves (SASW) method which is based upon measuring surface waves propagating in layered elastic media. The major advantage of seismic methods is that similar results are anticipated from the field and laboratory tests as long as the material is tested under comparable conditions. This unique feature of seismic methods in material characterization is particularly significant in QA operations. The depth of influence of PSPA is limited to the desired top layer of interest (Nazarian et al, 2000).
- **Light Weight Deflectometer (LWD)** is a portable Falling Weight Deflectometer that has been developed as an alternative in-situ testing device to the plate load test. Generally, the LWD consists of a loading device that produces a defined load pulse, a loading plate, one center displacement sensor (and up to two optional additional sensors) to measure the center deflection or a deflection bowl. Similar to FWD, the LWD determines the stiffness of the pavement system by measuring the material's response under the impact of a load

with a known magnitude and dropped from a known height. LWD reports the composite modulus of the layers with the estimated depth of influence of up to 6 ft (Tirado et al, 2014). The LWD tests were performed in this project following the ASTM E2583.

- **Dynamic Cone Penetrometer (DCP)** test involves driving a cone shaped probe into the soil or aggregate layer using a dynamic load and measuring the advancement of the device for each applied blow or interval of blows. The depth of penetration is a directly impacted by the drop height of the weight, cone size, and cone shape. Also, the resistance to penetration is dependent on the strength of the material. The strength, in turn, is dependent on density, moisture, and material type of the layer evaluated. The standard test method (ASTM D6951) was followed to perform DCP tests during field evaluation. The California Bearing Ratio (CBR) was determined from penetration index. Thereafter, the equation recommended by the UK Transportation Road Research Laboratory (TRRL) was used to estimate modulus from the CBR values.

The following moisture/density tests were also performed during the field activities:

- Nuclear Density Gauge (NDG) on HMA lifts as per ASTM D6938
- Field samples of base materials for estimation of index properties and oven dry (as per ASTM D2216) tests
- Bulk density tests for core samples from HMA lifts as per ASTM D5361 for the asphalt rodeo

The results of spot tests were employed to evaluate the IC data and establish any possible correlation with stiffness data reported by the IC systems. Detailed evaluation of spot test results during the two equipment rodeos are included in Appendices A and B.

Figure 3.7.1. Portable Seismic Property Analyzer (PSPA)

Figure 3.7.2. Light Weight Deflectometer (LWD)

Figure 3.7.3. Dynamic Cone Penetrometer (DCP)

CHAPTER 4. OBSERVATIONS FROM FIELD RODEOS

The IC data were collected with the OEM and retrofit systems employing three double drum IC rollers and three single drum IC rollers during the equipment rodeos in Texas and California sites, respectively. A validation system was also developed by UTEP to evaluate the vibration data during the roller operations at both rodeos. A summary of collected IC data are included in this chapter and further details are provided in Appendices A and B for the asphalt and soils rodeos, respectively. Appendix C is dedicated to the detailed process of reducing and analyzing vibration data from the validation system.

4.1 SPOT TESTS

Two modulus-based devices (PSPA and LWD) were employed during the pre-mapping of the existing base layer during the California HMA rodeo. Figures 4.1.1 and 4.1.2 illustrate the contour plots of the PSPA and LWD moduli along the test grid. Spot tests were performed at 33 points distributed along a 6 ft × 50 ft grid (see Appendices A and B). The Natural Neighbor interpolation (NNI) technique (Sibson, 1981) was employed to generate color maps of the spatial distribution of the moduli. To obtain the interpolated value for a given query point in that technique, the closest subset of input samples to that point were found and weights proportional to their areas were applied to them. The quantile method was used to classify the data into three classes represented by red, yellow and green. In the quantile method, the numbers of data points in the three classes are equal. Figure 4.1.3 summarizes the distributions of PSPA and LWD moduli along the centerline for the base layer. The PSPA moduli are expectedly higher than LWD moduli since PSPA estimates the low-strain elastic modulus of the layer. The LWD moduli on the base layer of the California HMA rodeo varied from 17 ksi to 32 ksi with a mean modulus of 23 ksi and a standard deviation of 4 ksi; while the PSPA moduli were in the range of 54 ksi to 222 ksi with a mean value of 121 ksi and a standard deviation of 43 ksi. The PSPA measurements point to a less stiff area around the center and towards the downhill northwestern part of the test section. The LWD results point to different less stiff areas. The depth of influence of the LWD penetrates into the subgrade layer providing a composite stiffness of the base and subgrade; while the PSPA estimates the stiffness of the base layer. Therefore, the less stiff areas from the PSPA could be associated with less stiff base layer and the less stiff areas from the LWD data could be due to the properties of either the base, subgrade or both layers.

The spatial distribution of the moduli from spot tests on the subgrade layer in the soils rodeo in Texas are summarized in Figures 4.1.4 through 4.1.6. Since the PSPA and DCP are layer-specific devices, they reflect the properties of layer of interest instead of a composite modulus. Therefore, the overall pattern of the PSPA and DCP results reflect the less stiff areas. However, the range of estimated moduli are different since PSPA measures the linear elastic low-strain modulus down to a depth of 12 in. (in this study) while DCP results are based on penetration of cone and relating the penetration index to CBR to further estimate the modulus utilizing experimental relationships. Since the influence depth of LWD device is deeper than PSPA, the less stiff areas reflected in Figure 4.1.4 might be an indicator of condition of deeper layers. Figure 4.1.7 summarizes the distributions of moduli from the PSPA, DCP and LWD on the embankment layer. Again, the PSPA shows higher estimated moduli while the DCP and LWD results seem to be in the same range and lower than the PSPA. Due to the different influence depths of these two devices, the LWD moduli reflect the condition of the lower layers while the DCP moduli are specific to the top layer.

Figure 4.1.1. Spatial variation of PSPA moduli on base layer at HMA site

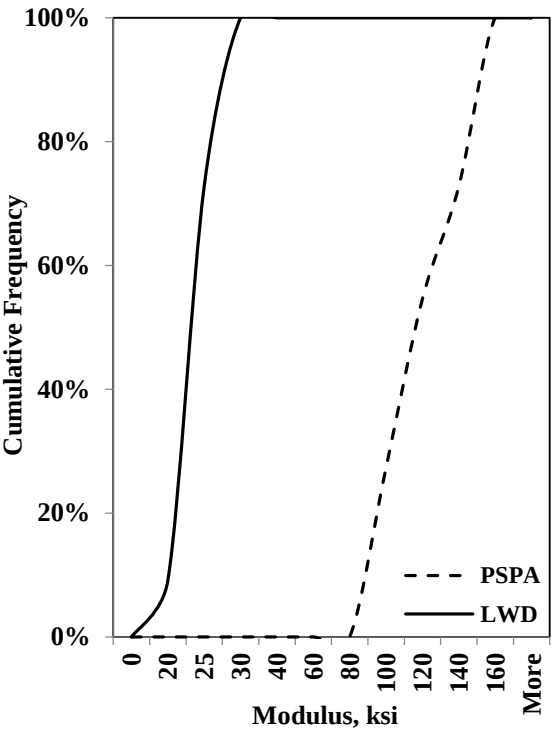

Figure 4.1.3. Distribution of PSPA and LWD moduli on base layer

Figure 4.1.2. Spatial variation of LWD moduli on base layer at HMA site

Figure 4.1.4. Spatial variation of PSPA modulus on embankment layer

Figure 4.1.5. Spatial variation of LWD modulus on embankment layer

Figure 4.1.6. Spatial variation of DCP modulus on embankment layer

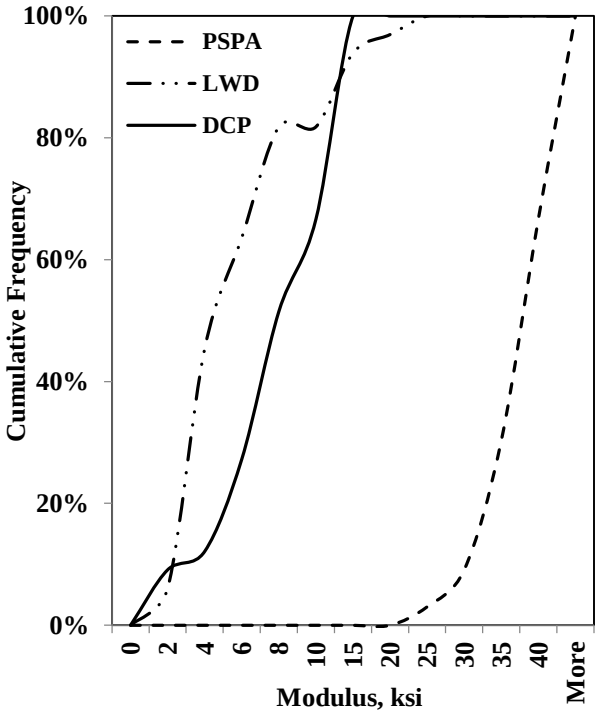

Figure 4.1.7. Distribution of PSPA, LWD and DCP moduli on embankment layer

Soil samples were extracted at each test station to estimate the oven-dry moisture contents in the laboratory. The moisture data were then interpolated using the Natural Neighbor interpolation to create a contour map as depicted in Figure 4.1.8. The red-colored areas show drier conditions while the green-colored areas represent wetter areas. The correlation of moisture content throughout the test section to the stiffness of compacted layer is discussed in Section 4.4.

Figure 4.1.8. Distribution of moisture content of subgrade layer

Table 4.1.1 summarizes the results of the spot tests during the pre-mapping process for the asphalt and soils rodeos. DCP tests were not performed during the asphalt rodeo because of the nature of the in-place materials. The differences between the PSPA and LWD moduli are because PSPA measures the low-strain elastic modulus of the top layer. Furthermore, due to the nature of seismic tests, the PSPA measurements typically show higher coefficient of variation as compared to LWD on the base layer of the HMA rodeo during pre-mapping. Similar differences in moduli are observed among the PSPA, LWD and DCP from the pre-mapping of the embankment layer during the soils rodeo. However, the DCP and LWD moduli are closer. The high coefficients of variation of the LWD and DCP test results reflect the variability of soil properties throughout the section. On the other hand, the COV of the PSPA device indicates that the top layer was fairly consistent while the properties of underlying soil layers, as reflected in the LWD and DCP results, were variable. Such variations should be reflected in the IC measurements given the depth of influence of the IC rollers.

Table 4.1.1. Descriptive Statistics of Spot Test Results during Pre-Mapping

Statistical Parameter	Modulus of Base Layer in Asphalt Rodeo, ksi		Modulus of Embankment Layer in Soils Rodeo, ksi		
	PSPA	LWD	PSPA	LWD	DCP
Minimum	85.9	19.3	23.0	1.2	1.6
Maximum	158.6	26.7	52.0	15.2	14.7
Average	120.5	23.1	38.3	5.8	8.4
Standard Deviation	26.1	2.4	6.4	3.8	3.8
COV, %	22%	10%	17%	67%	46%

4.2 ANALYSIS OF INFORMATION FROM OEM AND RETROFIT IC SYSTEMS

Table 4.2.1 includes a summary of data collected with the three rollers during the HMA rodeo in California. Due to technical difficulties, some portions of the IC data were not collected properly.

Table 4.2.1. Summary of IC data collected during HMA equipment rodeo

Date	HAMM			SAKAI			CAT*	
	OEM System	Retrofit System	Validation System	OEM System	Retrofit System	Validation System	OEM System	Validation System
Day 1	Available	Available	Available	Not Available	Available	Available	Available	Available
Day 2	Available	Available	Not Collected	Available	Available	Available	Partially Available	Not Collected
Day 3	Available	Available	Not Collected	Available	Available	Available	Available	Not Collected

* Since CAT rollers use Trimble systems, there is no need to install the retrofit system on them

The thorough analyses of the collected IC data during the HMA rodeo are included in Appendix A. The spatial variations of the ICMVs for the three rollers during the pre-mapping of the base layer of the HMA rodeo were established first. To generate the color-coded maps, the IC data were selected within the boundaries of the test section as illustrated in Figure 4.2.1. Any nonnumeric and zero values in the ICMV data were identified and removed from the data file. The Bayesian Empirical Kriging method was employed to interpolate the filtered IC data and generate the data for color-coded maps. The standard Quantile method was used for all color-coded maps for ease in visual comparison. Due to different data distributions, the range of color-coded classes are not the same between different figures.

The IC data from the retrofit systems installed on the SAKAI and HAMM rollers are compared with the IC data collected by the CAT OEM system in Figures 4.2.1 through 4.2.3. The blank areas in the color-coded maps correspond to the areas that IC data were not available in the data files. The overall distributions among the three rollers follow the same trends. The three color-coded maps demonstrate the less stiff area on the north-west segment of the test section. The distributions of the ICMVs during pre-mapping from the three systems are summarized in Figure 4.2.4. The maps demonstrate the less stiff area on the northwest segment of the test section. The histograms of the ICMVs from the two retrofit systems are similar, with minor differences due to different operational parameters used by the rollers. The ICMVs from the CAT OEM system are greater than the ICMVs from the other two retrofit systems.

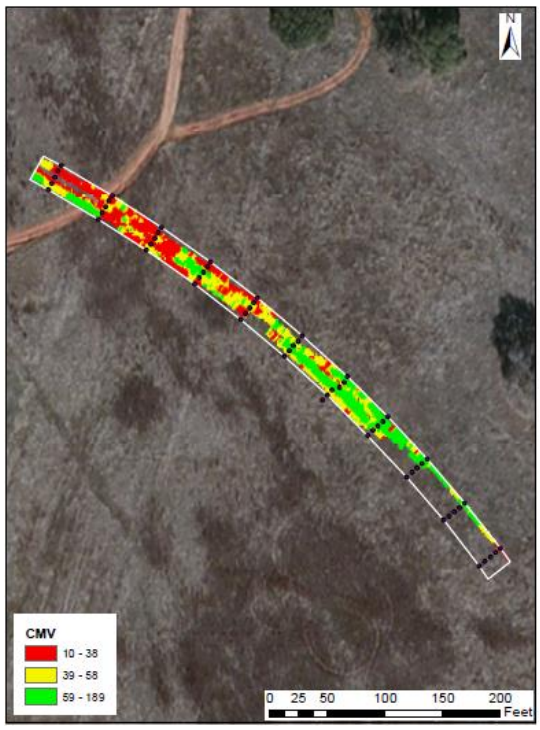

Figure 4.2.1. Spatial variation of CMV data from HAMM retrofit system during pre-mapping

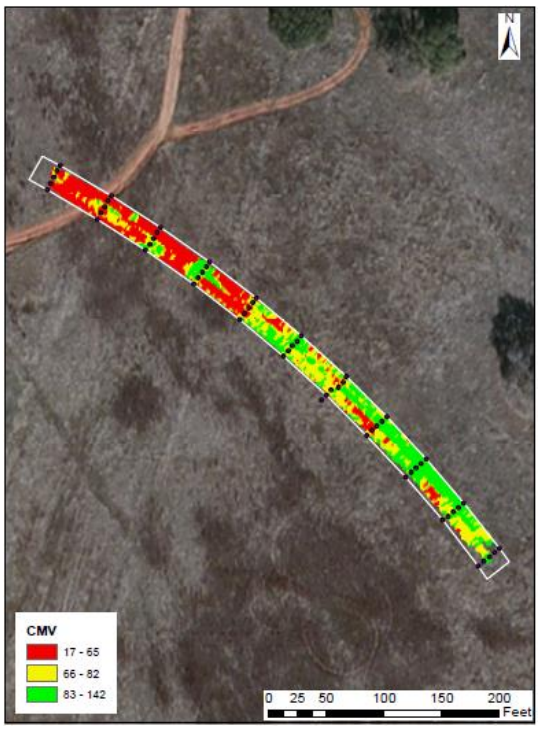

Figure 4.2.3. Spatial variation of CMV data from CAT system during pre-mapping

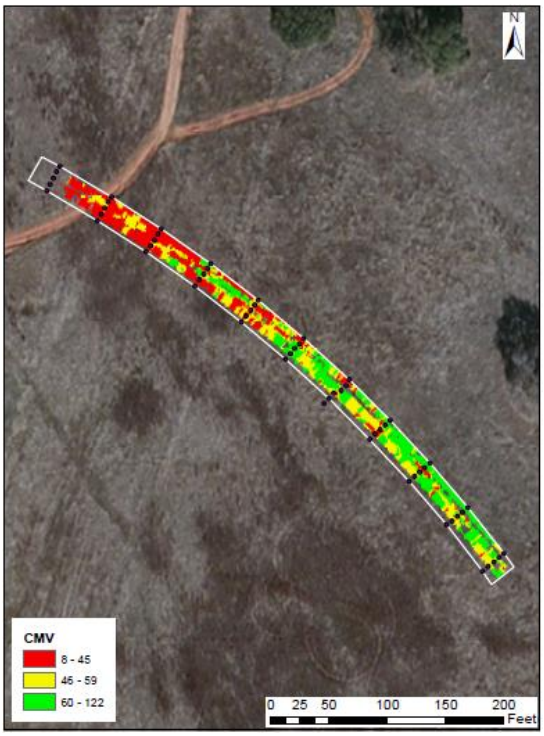

Figure 4.2.2. Spatial variation of CMV data from SAKAI retrofit system during pre-mapping

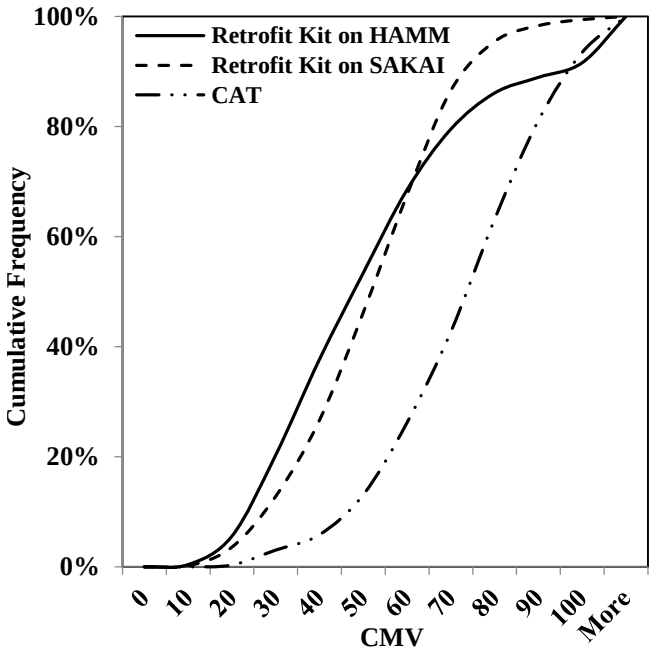

Figure 4.2.4. Comparison of CMV data from the retrofit systems on SAKAI and HAMM rollers with CMV data from CAT roller during pre-mapping of base layer

To further compare the results of the retrofit and OEM systems, the color-coded maps of the ICMVs from the OEM and retrofit systems on the HAMM roller are compared in Figures 4.2.5 and 4.2.6. The HMVs and CMVs were calculated using the same Equation 2.1.1. Figure 4.2.7a demonstrates the differences in the different ICMVs from the HAMM roller during pre-mapping. The CMVs from the retrofit system vary from 6 to 194 while the HMVs are in the range of 20 to 150. With an 80% confidence level, the CMVs are around 70 with a mean value of 55 while the HMVs are about 120 with a mean of 90. Aside from the fact that the two systems did not cover the same areas, the differences between these two sets of IC data could be associated with the differences in the vibration sensors and GPS systems or different proprietary filtering of the data carried out by the two systems' algorithms. These data will be further compared with the information collected with the UTEP data acquisition system.

Figure 4.2.7b illustrates the box plot of the ICMV data from the retrofit kit and OEM system on the HAMM roller. As illustrated in Figures 4.2.1 through 4.2.3, the coverage areas by different systems were dissimilar. The common coverage area among the three rollers is illustrated in Figure 4.2.8. This common area is about 47% of the total area of the test section.

Table 4.2.2 summarizes the ICMV data from the retrofit kit and OEM system on the HAMM roller during pre-mapping of the base layer. The coefficient of variation of ICMV data from the retrofit kit is greater than that from the OEM system. The average CMV is about 40% less than the average HMV. Such differences could be due to the fact the two systems did not cover the same areas due to difficulties with GPS unit of each system (see Figures 4.2.5 and 4.2.6). Also, the vibration sensors and the data reduction algorithms are different between the retrofit and OEM systems.

Figure 4.2.9a compares the cumulative distributions of the ICMVs within the common coverage area among the two retrofit systems mounted on the SAKAI and HAMM rollers and the CAT OEM system. The distributions of the SAKAI and HAMM IC data are similar with minor differences due to the positioning of the retrofit vibration sensors and operational differences in the vibration characteristics of the rollers. For an 80% confidence level, the CMV of the retrofit system on the HAMM roller is 75 while the same value for the SAKAI roller is 65. The CMV from the CAT roller at 80% confidence level is 90. The retrofit system on the HAMM roller reports CMVs as high as 180 while the corresponding values from the SAKAI and CAT rollers are less than 150.

Figure 4.2.9b illustrates the box plot of CMV data from the three rollers on the common area during pre-mapping. The box plot represents the minimum, 25^{th} percentile, 50^{th} percentile, 75^{th} percentile and maximum values from the bottom to the top, respectively. The spatial distributions of the results are included in Appendix A. The two retrofit systems on the rollers seem to give similar results although the range of the CMVs from the HAMM roller is more than the SAKAI roller. The range of the CAT ICMVs are close to the SAKAI ICMVs but with different median values. The range of ICMVs from retrofit kit on HAMM is greater than the other two rollers.

Table 4.2.3 summarizes the ICMV data from the common area collected by the CAT and the retrofit kits on the HAMM and SAKAI during pre-mapping of the base layer. Although the average ICMVs are fairly close between the retrofit systems on the HAMM and SAKAI, the coefficient of variation of the HAMM data is greater than that of the SAKAI data. The COVs of the CAT and SAKAI data are similar.

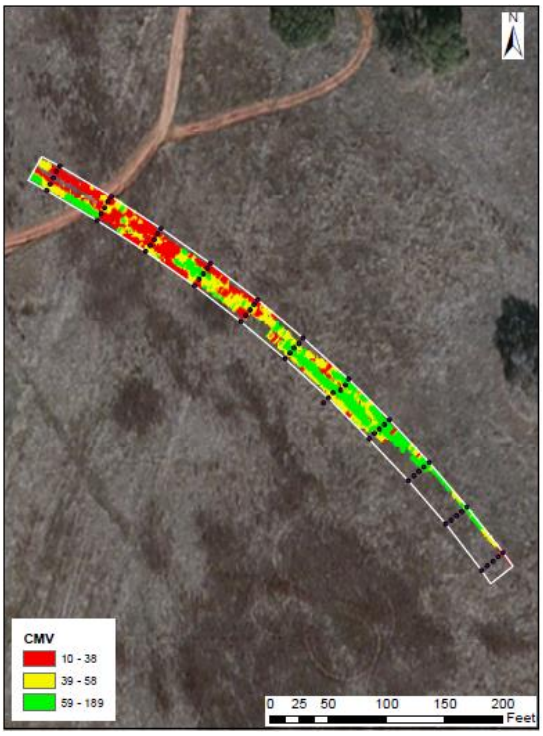

Figure 4.2.5. Spatial variation of CMV data from HAMM retrofit system during pre-mapping

Figure 4.2.6. Spatial variation of HMV data from HAMM OEM system during pre-mapping

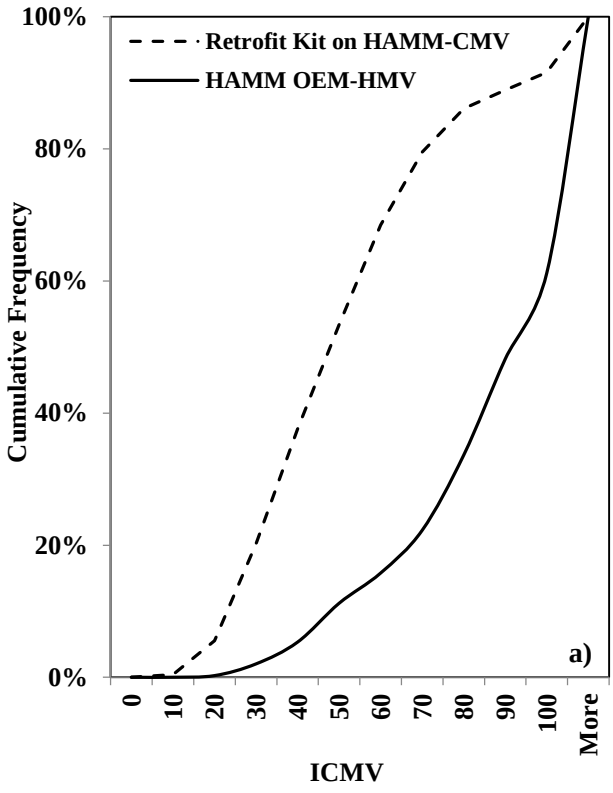

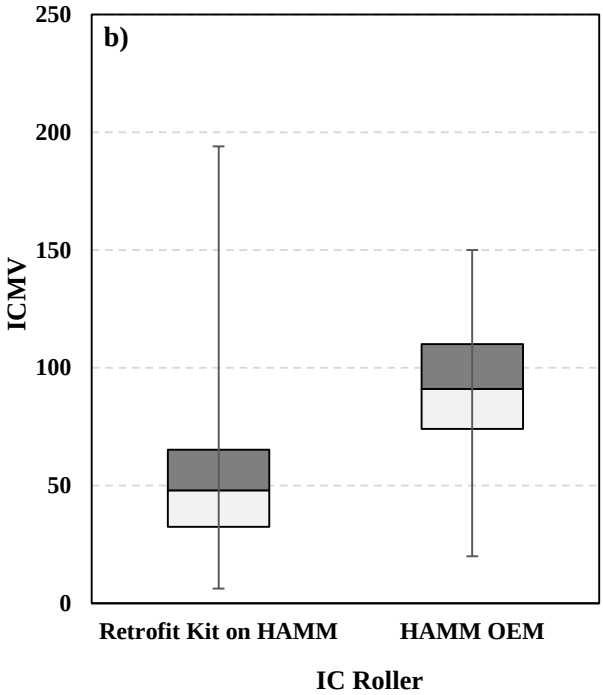

Figure 4.2.7. Comparison of ICMV data from the retrofit and OEM systems on HAMM roller during pre-mapping of base layer

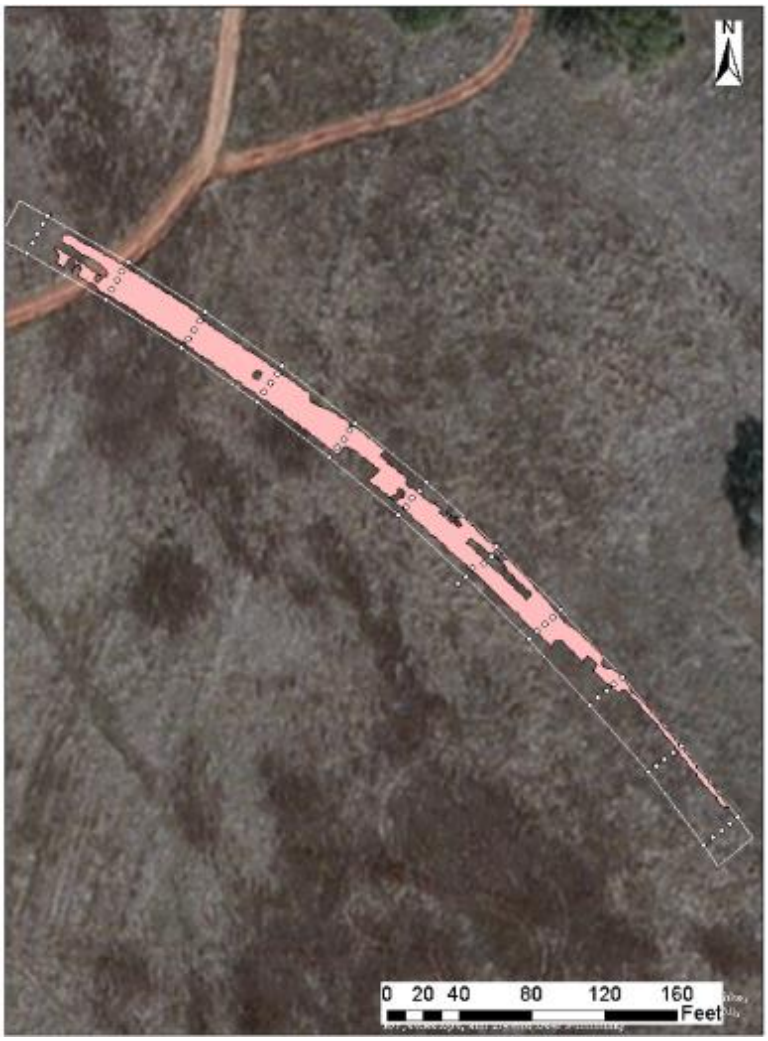

Figure 4.2.8. Common coverage area among two retrofit systems on HAMM and SAKAI and CAT system during pre-mapping

Table 4.2.2. Descriptive Statistics of ICMV data from Retrofit Kit and OEM systems on HAMM roller during Pre-Mapping of Base Layer

Statistical Parameter	CMV from Retrofit Kit	HMV from OEM System
Minimum	6	20
Maximum	194	150
Average	56	90
Standard Deviation	35	28
COV	62%	31%

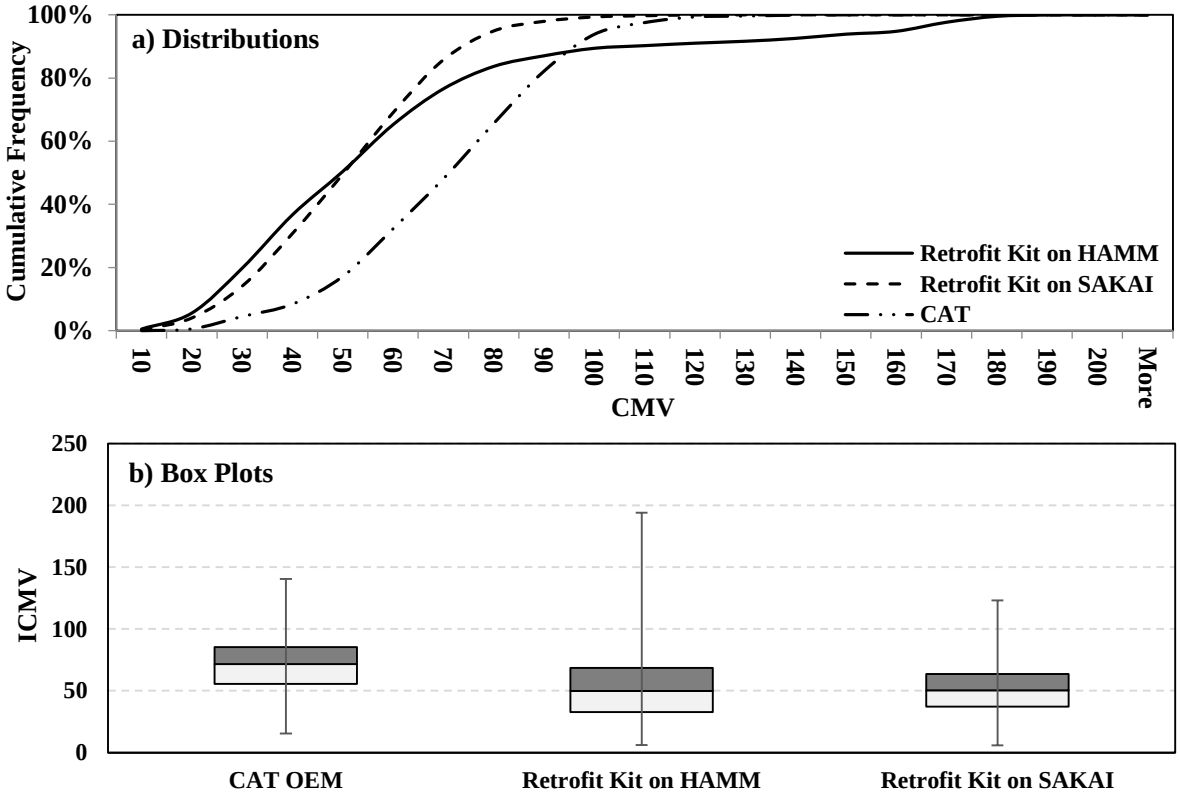

Figure 4.2.9. Comparison of ICMVs from the two retrofit systems on SAKAI and HAMM rollers with CMV data from CAT roller during pre-mapping of base on common area

Table 4.2.3. Descriptive Statistics of CMV data of Common Area during Pre-Mapping

Statistical Information	CAT	Retrofit Kit on HAMM	Retrofit Kit on SAKAI
Minimum	15.5	6.2	5.8
Maximum	140.5	194.1	123.2
Average	70.2	58.3	50.6
Standard Deviation	21.3	37.5	18.3
COV, %	30%	64%	36%

For the first lift of the HMA, the HAMM, SAKAI and CAT rollers were selected for breakdown, intermediate and finishing compaction, respectively. For the second lift, the CAT, SAKAI and HAMM rollers were selected for breakdown, intermediate and finishing, respectively. A nuclear density gauge (NDG) and an infrared thermometer were used to monitor the density and temperature after each pass of each roller at one test point within each lane. Figures 4.2.10 and 4.2.11 summarize the density and temperature changes between different passes of the rollers for one of the control points during the compaction of the first and second HMA lifts. Densities were not recorded during the finishing process by the CAT roller on the first HMA lift. The density increased as more passes of the rollers were applied. As a result of the cooling process, the temperature of the HMA lift decreased between the passes of the rollers.

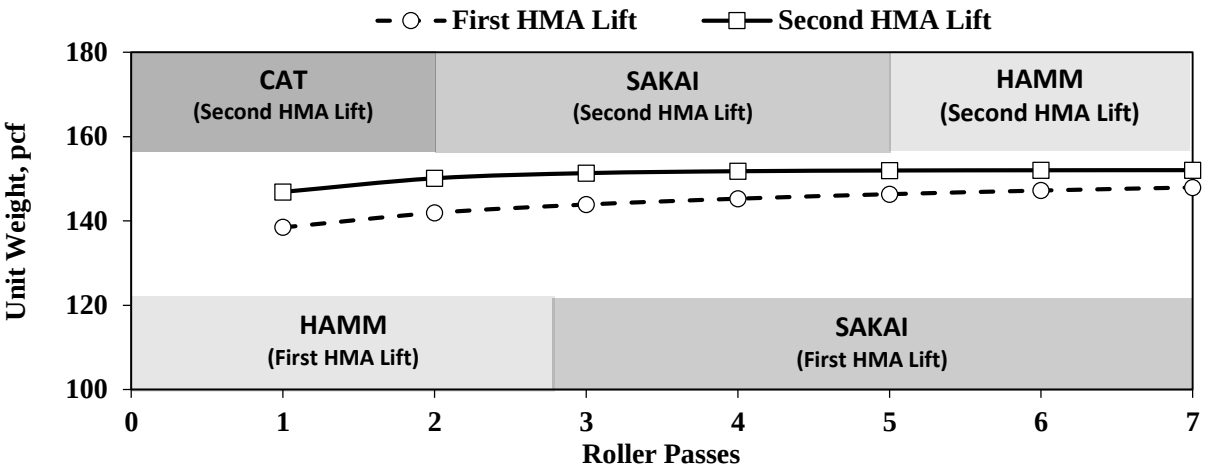

Figure 4.2.10. Variation of unit weight between roller passes (first and second HMA lifts)

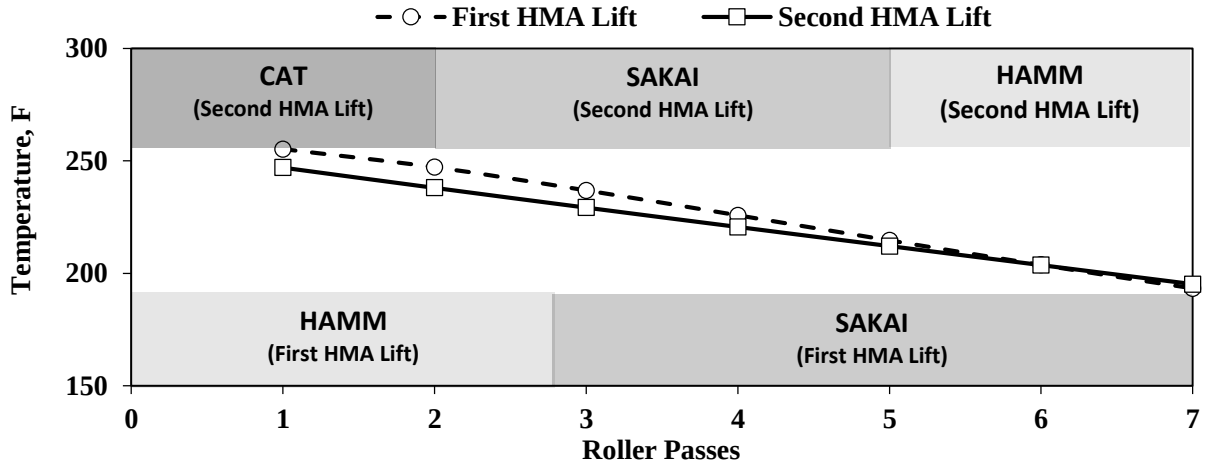

Figure 4.2.11. Variation of temperature between roller passes (first and second HMA lifts)

Figure 4.2.12 compares the CMVs from the two retrofit systems mounted on the HAMM and SAKAI rollers during the compaction process. The differences between the distributions of the CMVs between the two retrofit systems can be due to the fact that the HAMM roller was the breakdown roller and the SAKAI roller was the intermediate roller. The CMV data from the retrofit system on the HAMM roller has an average of 49 and a coefficient of variation of 34% while these values for the retrofit system on the SAKAI roller are 35 and 46%, respectively.

The retrofit and OEM systems gathered vibration data simultaneously on the HAMM and SAKAI rollers. Figure 4.2.13 summarizes the ICMVs from the retrofit and OEM systems on the HAMM roller during the mapping of the first HMA lift. About 75% of the data from the retrofit system have CMVs of 60 or less while about 95% of the OEM data have HMV of 60 or less. The standard deviations of both ICMVs are close while the average CMV for the retrofit system is 49 and for the HMV estimated by the OEM system is 37.

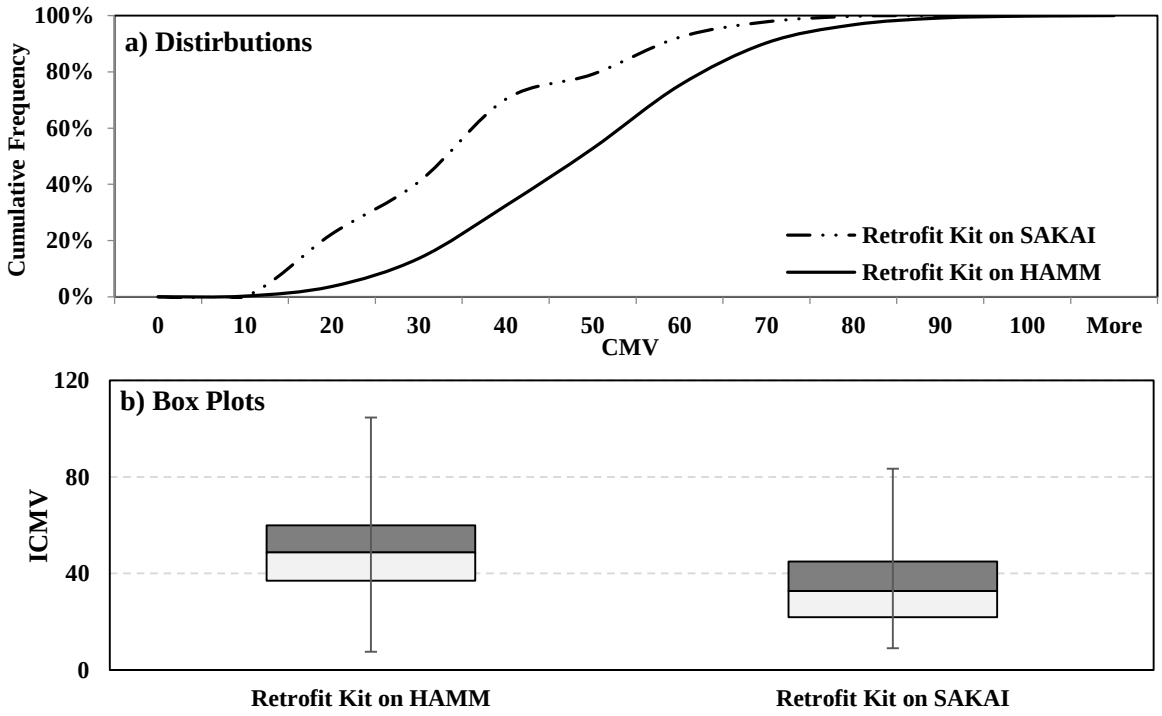

Figure 4.2.12. Comparison of CMV data from the two retrofit systems on HAMM (breakdown) and SAKAI (intermediate) rollers during mapping of first HMA lift

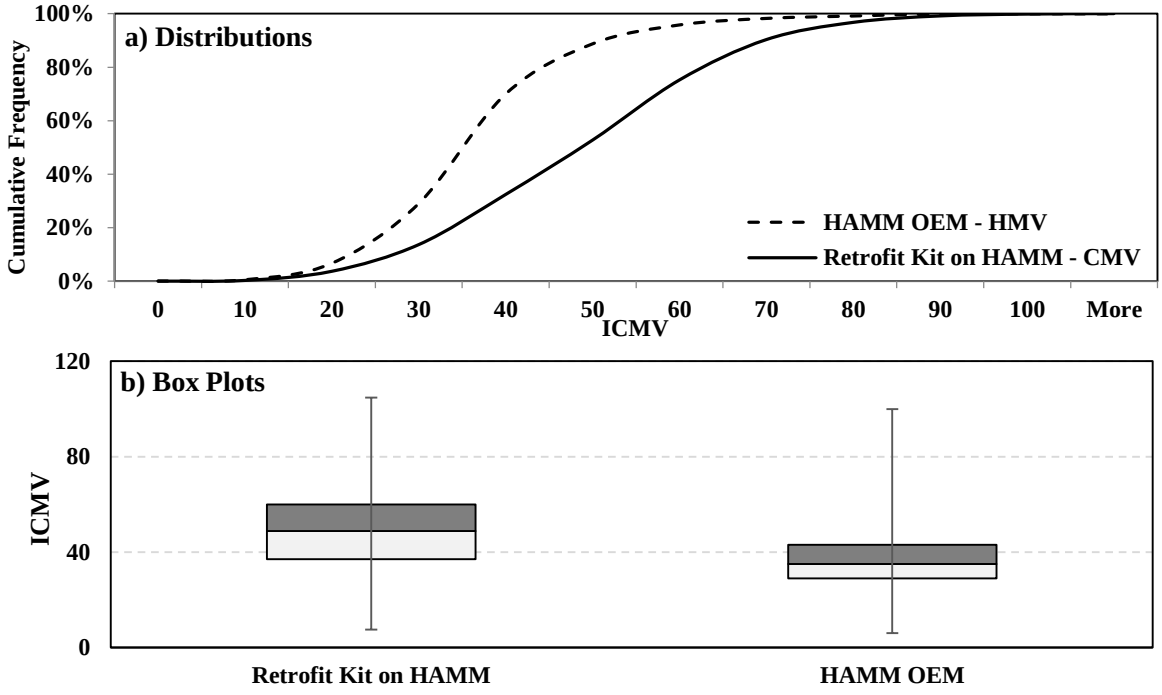

Figure 4.2.13. Comparison of ICMV data from OEM (HMV) and the Trimble retrofit system (CMV) on HAMM roller during mapping of first HMA lift

Figure 4.2.14 illustrates the CCV and CMV data during the compaction of the first HMA lift with the SAKAI roller. The average CCV is 3.2 with a coefficient of variation of 12% while these values for the CMV data from the retrofit system are 35 and 46%, respectively.

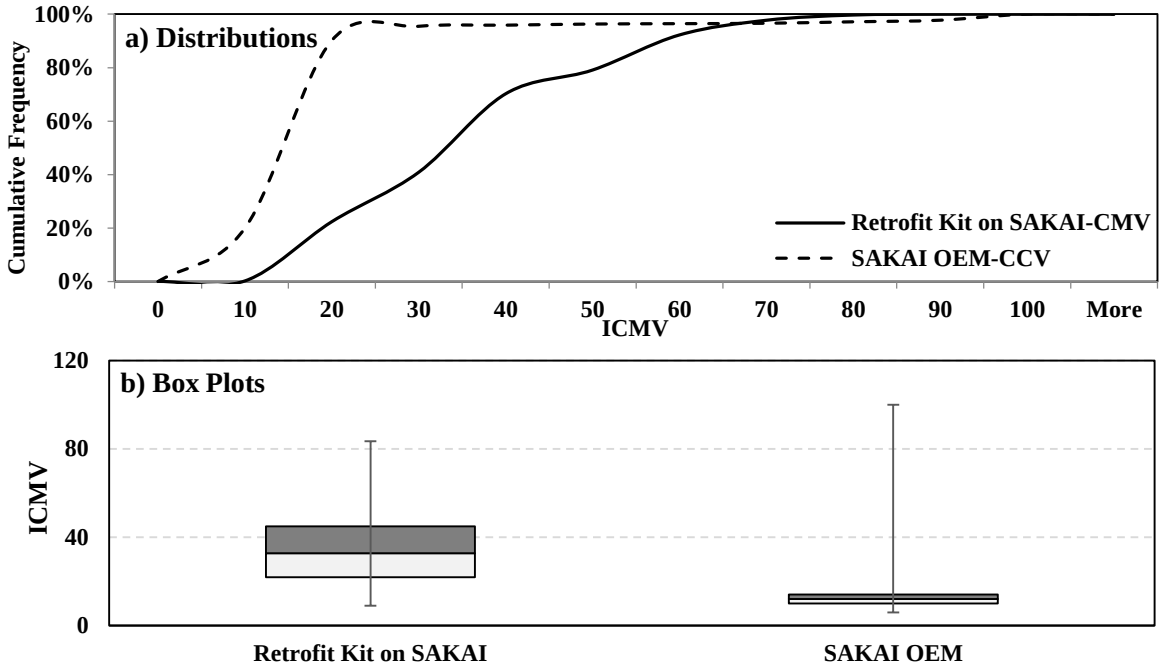

Figure 4.2.14. Comparison of ICMV data from OEM (CCV) and Trimble retrofit system (CMV) on SAKAI roller during mapping of first HMA lift

The IC data from the mapping with the retrofit system of the SAKAI roller and the OEM system on the CAT roller of the second HMA lift are summarized in Figure 4.2.15. At 95% confidence level, the CMVs from the CAT roller are less than 70 while for the retrofit system on the SAKAI roller, this value is about 40. The CAT CMV data show a coefficient of variation of 45% as compared to the CMV data from the retrofit system on the SAKAI roller which is 23%.

Figure 4.2.16 shows the differences between the OEM and retrofit systems' ICMVs on the SAKAI roller during the compaction process for the second HMA lift. The COV of the CMV data from the retrofit system on the SAKAI roller is 23% as compared to 50% for CCV data from the OEM system. The uncertainties associated with the reported CCV data are higher during the same compaction process.

Table 4.2.4 summarizes the ICMV data collected by the retrofit kits and OEM systems on the HAMM and SAKAI rollers as well as the data collected from the CAT roller. During the mapping of the first HMA lift, the results from the retrofit kit on the HAMM roller are similar to the results from the HAMM OEM system. On the other hand, the SAKAI OEM system shows high variation in the reported ICMVs as compared to the data collected by the retrofit kit on the same roller.

Direct comparison of the results from the HAMM and SAKAI rollers was not feasible since they were mapping different asphalt compaction processes (i.e., HAMM was the breakdown roller and SAKAI was the intermediate one). During the mapping of the second HMA lift, the retrofit kit on the SAKAI roller reflects the lowest coefficient of variation. However, the ICMVs collected from

the SAKAI OEM system were in a different range as compared to the CMVs collected by the retrofit kit considering the fact they are reporting two different measure of stiffness.

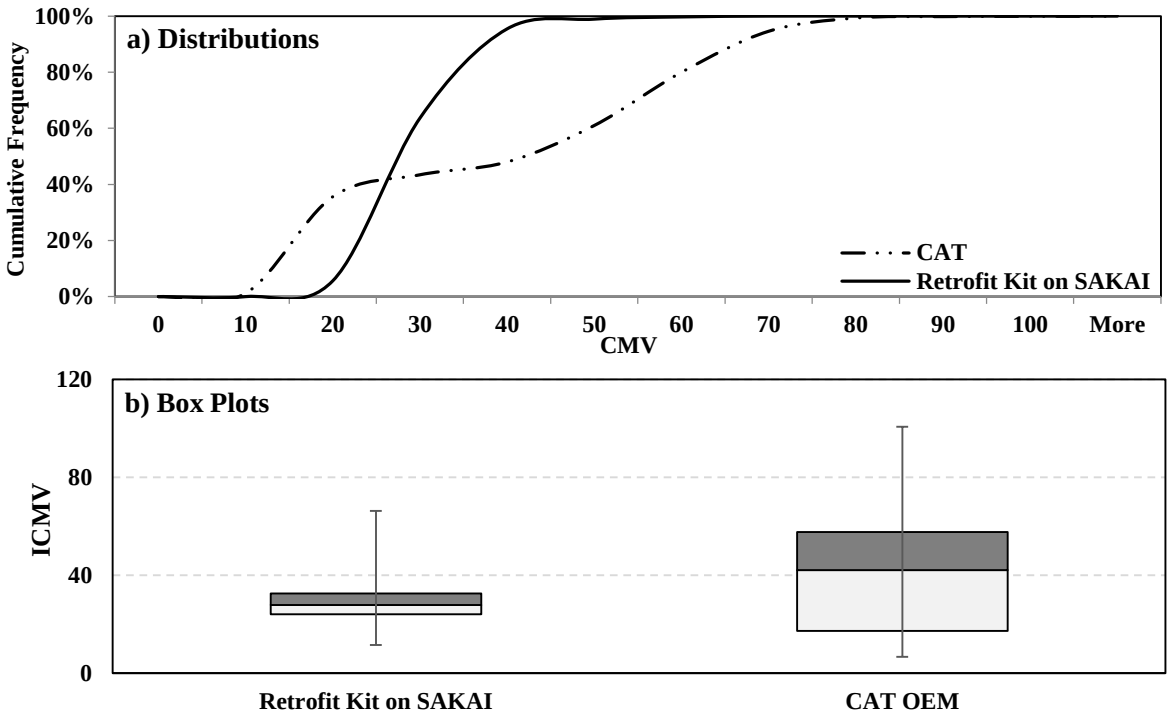

Figure 4.2.15. Comparison of ICMV data from CAT roller (breakdown) and SAKAI retrofit system (intermediate) during mapping of second HMA lift

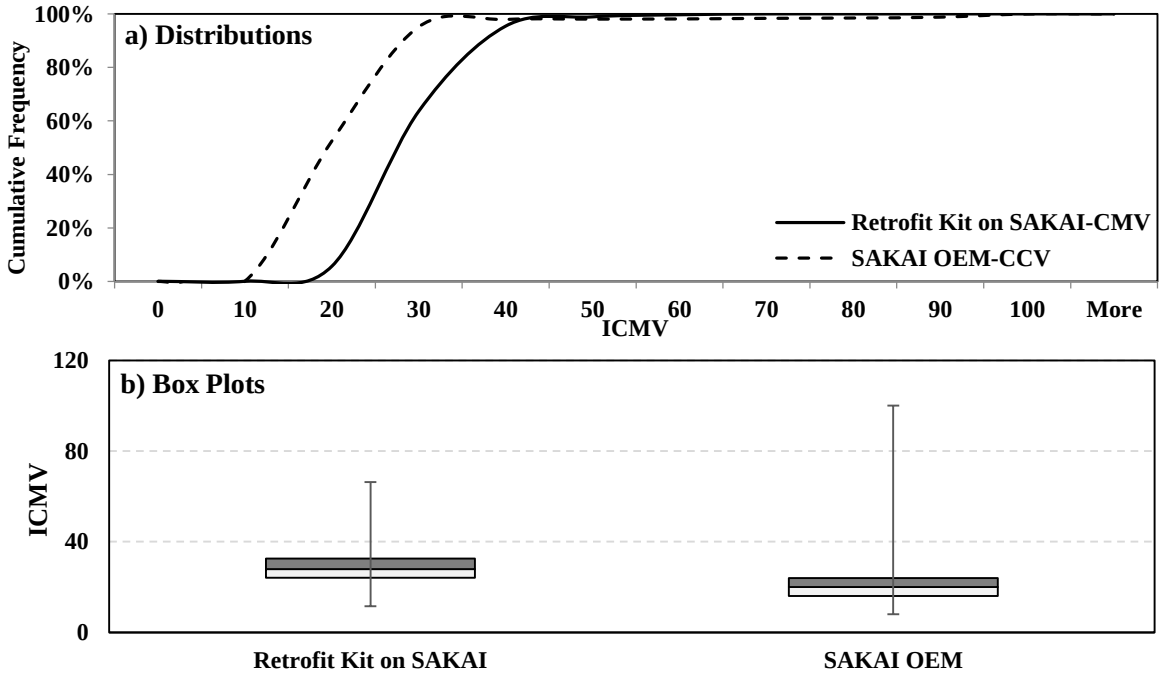

Figure 4.2.16. Comparison of CMV data from retrofit and OEM systems on SAKAI roller during mapping of second HMA lift

Table 4.2.4 summarizes the ICMV data collected by the retrofit kits and OEM systems on the HAMM and SAKAI rollers as well as the data collected from the CAT roller. During the mapping of the first HMA lift, the results from the retrofit kit on the HAMM roller are similar to the results from the HAMM OEM system. On the other hand, the SAKAI OEM ICMVs are more variable as compared to the data collected by the retrofit kit on the same roller. Direct comparison of the results from the HAMM and SAKAI rollers was not feasible since they were mapping different asphalt compaction processes (i.e., HAMM was the breakdown roller and SAKAI was the intermediate one). During the mapping of the second HMA lift, the retrofit kit on the SAKAI roller exhibited the lowest coefficient of variation. The SAKAI OEM ICMVs were in a different range as compared to the CMVs collected by the retrofit kit considering the fact they are reporting two different measure of stiffness.

Table 4.2.4. Descriptive Statistics of ICMV data during Mapping of HMA Lifts

Statistical Parameter	First HMA Lift				Second HMA Lift		
	Breakdown		Intermediate		Breakdown	Intermediate	
	Retrofit Kit on HAMM	HAMM OEM	Retrofit Kit on SAKAI	SAKAI OEM	CAT	Retrofit Kit on SAKAI	SAKAI OEM
Minimum	7.5	6.0	9.0	5.0	6.7	11.5	8.0
Maximum	104.7	100.0	83.5	100.0	100.6	66.3	100.0
Average	48.7	36.5	34.8	16.4	38.9	28.7	21.7
Standard Deviation	16.7	12.2	15.9	15.5	21.1	6.6	10.9
COV, %	34%	33%	46%	94%	54%	23%	50%

Soils Rodeo

The second equipment rodeo that was dedicated to soils was performed on a test section as part of the expansion of US 67 near Cleburne, Texas. The existing embankment layer was pre-mapped using the CAT, SAKAI and HAMM rollers equipped with the OEM, retrofit and UTEP DAQ. Again, since CAT rollers use a system similar to Trimble, there was no need to install the retrofit kit on that roller. Table 4.2.5 contains a summary of the collected IC data with the three rollers during this field operation.

Prior to the pre-mapping process at the second day of testing, a less stiff area toward the northeastern edge of the test section was created using a grader to assess the ability of the different IC systems to identify the less stiff spots during the compaction process. The pre-mapping of the existing embankment layer was carried out first. Figures 4.2.17 through 4.2.19 illustrate the spatial distributions of the CMVs from the retrofit systems on the HAMM and SAKAI smooth drum rollers (Day 2) as well as the CMVs collected with the CAT smooth drum roller (Day 1). Except for Figure 4.2.18, the same less stiff areas around the center and toward the south-eastern part of the test section are identified. The histograms and box plots of the ICMVs are summarized in Figure 4.2.20. Even though, the identical retrofit systems were installed on the HAMM and SAKAI rollers, the CMVs from the retrofit system on the SAKAI roller are significantly different than the CMVs from the other two rollers. The reason for this pattern is not known. The CMVs from the CAT roller and retrofit system on the HAMM roller are similar.

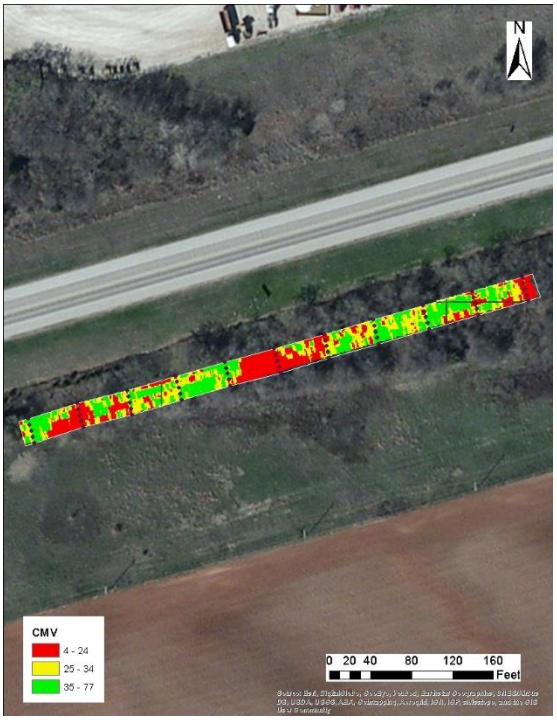

Figure 4.2.17. Spatial variation of CMV data from HAMM Retrofit system during pre-mapping (Day 2)

Figure 4.2.19. Spatial variation of CMV data from CAT smooth drum roller during pre-mapping (Day 1)

Figure 4.2.18. Spatial variation of CMV data from SAKAI Retrofit system during pre-mapping (Day 2)

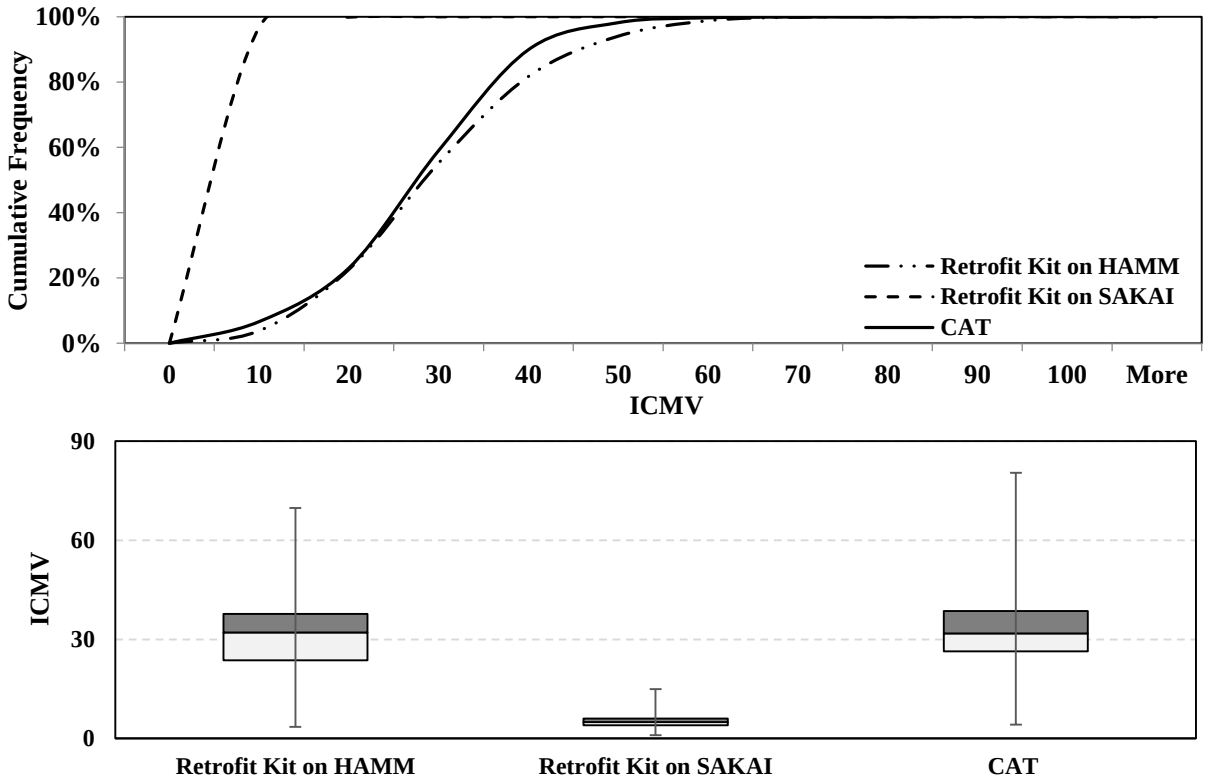

Figure 4.2.20. Comparison of CMV data from retrofit systems on SAKAI and HAMM rollers with CAT roller during pre-mapping of existing embankment layer

Table 4.2.5. Summary of IC data collected during the Soils equipment rodeo

Date	HAMM			SAKAI			CAT	
	OEM System	Retrofit System	Validation System	OEM System	Retrofit System	Validation System	OEM System	Validation System
Day 1 (Pre-Mapping)	Available	Not Collected	Not Collected	Not Collected	Not Collected	Not Collected	Available[1]	Available
Day 2 (Pre-Mapping)	Available	Available	Available	Available	Partially Available	Available	Available[1]	Available
Day 3 (Mapping)	Available	Available	Available	Available	Partially Available	Available	Available[2]	Available
Day 4 (Mapping)	Not Collected	Not Collected	Not Collected	Not Collected	Not Collected	Not Collected	Available[1]	Not Collected

[1] Smooth drum, [2] Padfoot

Figures 4.2.21 and 4.2.22 illustrate the spatial distributions of the ICMVs from the retrofit and OEM systems on the HAMM roller. Due to unknown reasons, only partial IC data was reported by the HAMM OEM system (see Figure 4.2.22). Therefore, a comprehensive comparison of these two systems is not possible. Figure 4.2.23 summarizes the distributions and box plots of the CMV and HMV data for the HAMM roller during pre-mapping on their common coverage area. Even though a small number of HMV data was collected, the trends of the two ICMVs are similar.

Figure 4.2.21. Spatial variation of CMV data from HAMM retrofit system during pre-mapping

Figure 4.2.22. Spatial variation of HMV data from HAMM OEM system during pre-mapping

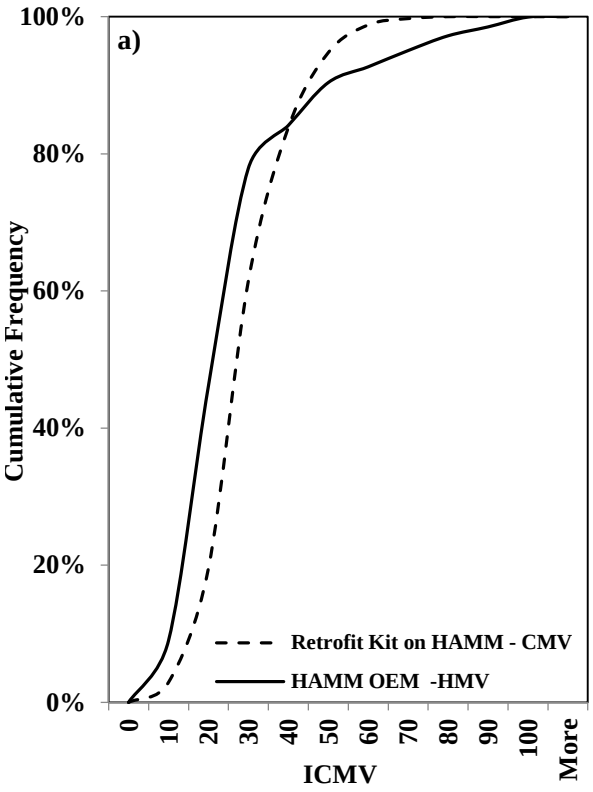

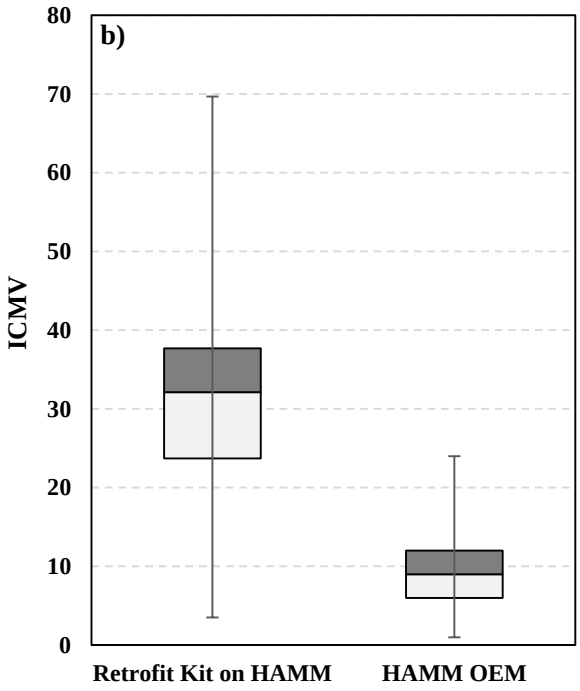

Figure 4.2.23. Comparison of ICMV data from retrofit and OEM systems on HAMM roller during pre-mapping of existing embankment layer

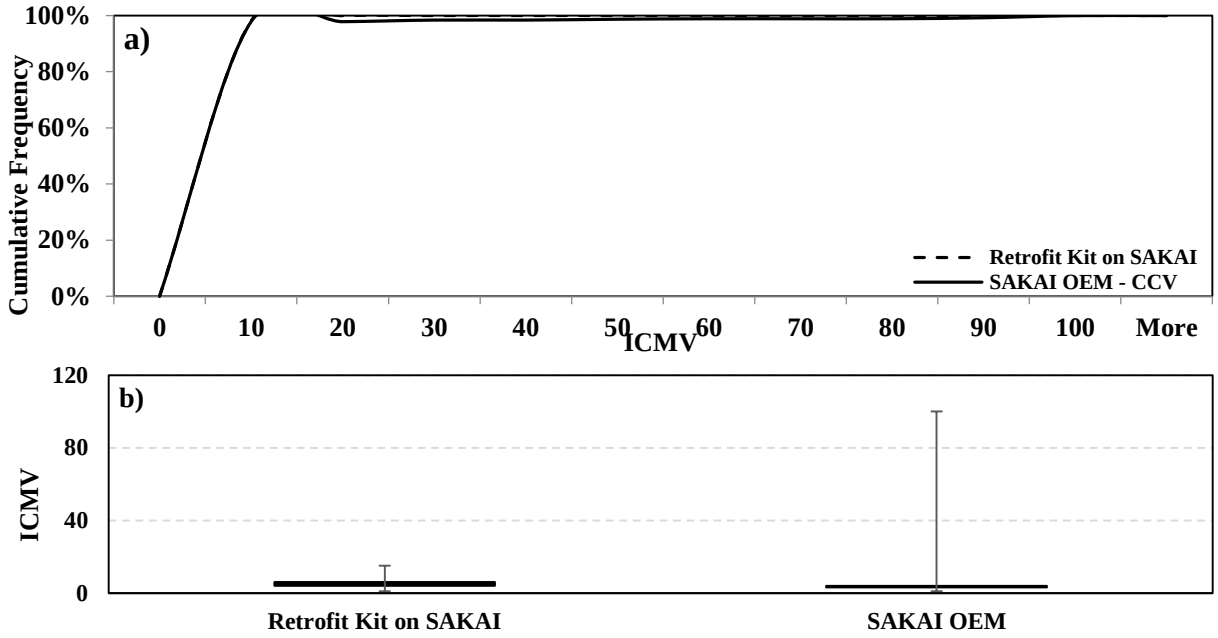

Figure 4.2.24. Graph. Comparison of ICMV data from retrofit and OEM systems on SAKAI roller during pre-mapping of existing embankment layer

Figure 4.2.24 compares the cumulative distributions and box plots of the CMVs from the retrofit systems with CCVs from the OEM system collected simultaneously with the SAKAI roller. The color-coded maps of the ICMVs during the pre-mapping process for each roller along with their statistical analyses followed by the detailed analyses of the UTEP embedded and roller sensors data on each roller are included in Appendix B. Due to technical issues related to reporting CMV data from the retrofit system, the comparison of these two systems are not quite comprehensive.

A 12-in.thick clayey subgrade material similar to the embankment material was placed on the existing embankment layer on the third day. The CAT roller with a padfoot shell was employed to compact the subgrade layer. The change in the dry density of the layer with the number of passes were monitored with an NDG as shown in Figure 4.2.25. The desired density was achieved after five passes of the roller.

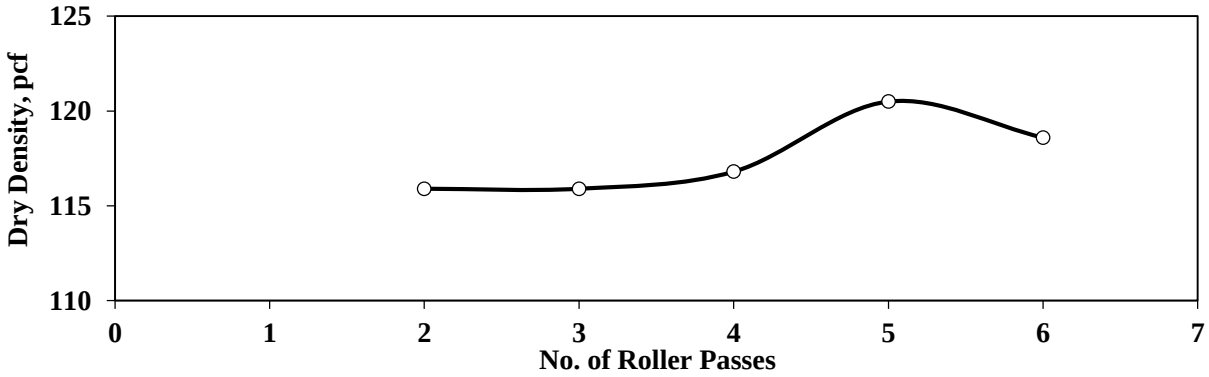

Figure 4.2.25. Variation of dry density during compaction of subgrade layer

After the completion of the compaction, the subgrade layer was mapped using the CAT, HAMM and SAKAI smooth drum rollers and CAT padfoot roller. Figures 4.2.26 through 4.2.28 illustrate the spatial variations of the CMVs from the retrofit systems on the HAMM and SAKAI rollers and from the OEM system on the padfoot and smooth drum CAT roller. The CMVs from all three systems demonstrate the less stiff area (the red zone towards the northeastern part of the test section). Another less stiff area around the central part of the test section is also identified in Figures 4.2.26 through 4.2.28. The range of CMV data from the retrofit system on the SAKAI roller seems to be associated with some technical difficulties as illustrated in Figure 4.2.27.

The CAT roller was converted to a smooth drum roller to map the compacted subgrade 18 hours after the compaction of the subgrade layer. Figure 4.2.30 shows the ICMVs during the mapping of the compacted subgrade with the CAT smooth drum roller 18 hrs after the compaction. The distributions of the CMVs from the CAT smooth drum roller and retrofit system on the HAMM roller (see Figure 4.2.26) are similar. To further compare the ICMV data from the three rollers during mapping of the subgrade layer are summarized in Figure 4.2.30. Figure 4.2.31 summarizes the CMV and HMV data collected with the retrofit and OEM systems on the HAMM smooth drum roller. Even though the process of estimating the HMV and CMV from the vibration data are similar (see Chapter 2), the two distributions are different. Figure 4.2.32 summarizes the ICMVs from the retrofit and OEM systems on the SAKAI roller during the mapping of the subgrade layer. Again, due to incomplete reporting of the CMV data from the retrofit system, a complete comparison of the OEM and retrofit systems is not feasible.

The ICMVs collected with the CAT smooth drum roller and the padfoot roller are compared in Figure 4.2.33. The subgrade surface seems stiffer than the initial compacted surface with the padfoot roller perhaps due the time between the completion of compaction and mapping.

Table 4.2.6 summarizes the ICMVs collected by the OEM and retrofit systems on the SAKAI, HAMM and CAT rollers during the pre-mapping of the embankment and mapping of the subgrade. The coefficients of variation and average CMVs from the CAT roller and the retrofit kit on the HAMM roller are similar. Furthermore, the average CMV from the SAKAI retrofit kit is lower than the HAMM retrofit kit and the CAT OEM system. The reason for that pattern, aside from the problems with collecting or retrieving the ICMV data, is unknown.

The ICMVs from the OEM and retrofit kit collected simultaneously with the HAMM roller are close, with the coefficient of variation from OEM being slightly greater than retrofit kit. The HAMM OEM data are also similar to those collected by the CAT roller during the pre-mapping. On the other hand, the SAKAI OEM data are different than the other ICMVs with a higher coefficient of variation. The same trends exist between almost all the IC systems during the mapping of the subgrade layer.

The observed differences between the data collected by the padfoot and smooth drum CAT rollers seems reasonable. The average CMV reported by the smooth drum roller is expectedly higher than that of the padfoot roller. Furthermore, the coefficient of variation of the CMVs from the smooth drum roller seems to be greater than that from the padfoot roller.

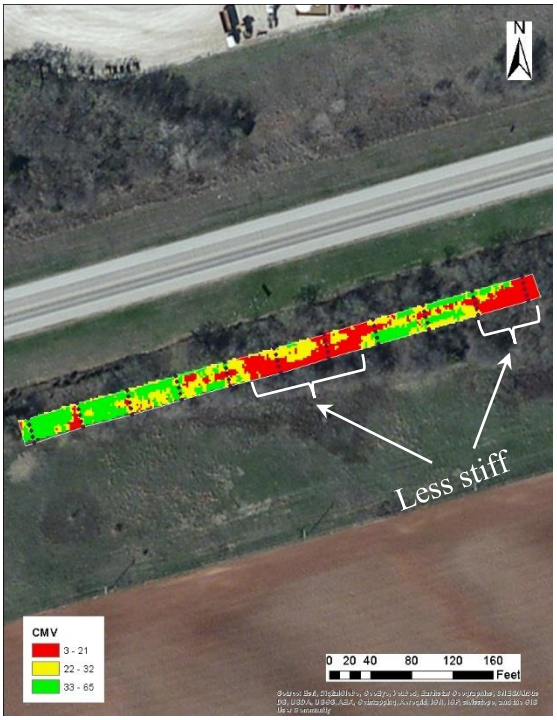

Figure 4.2.26. Spatial variation of CMV data from Retrofit system on HAMM smooth drum roller during mapping of subgrade layer

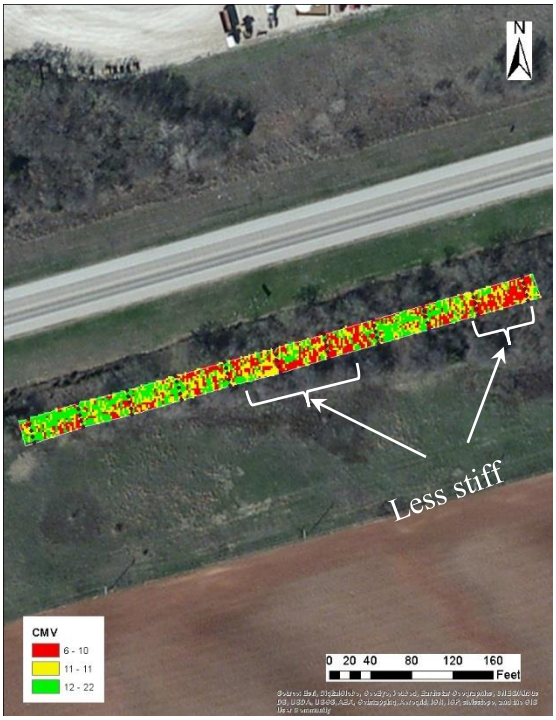

Figure 4.2.28. Spatial variation of CMV data from CAT padfoot roller after compaction of subgrade layer

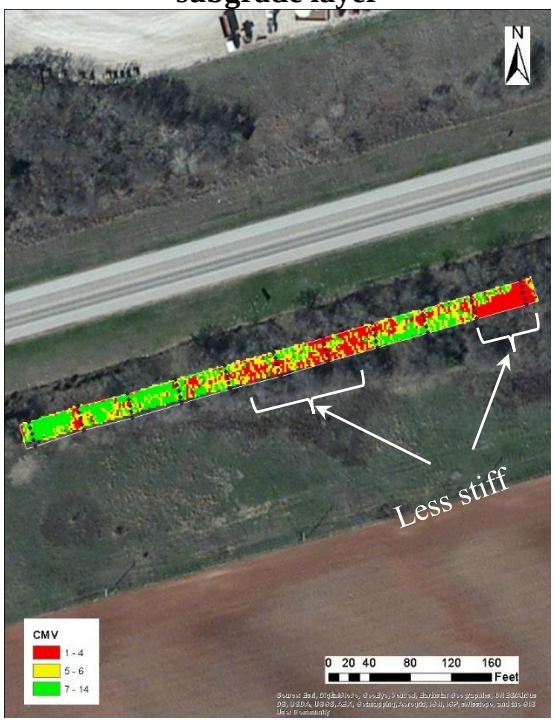

Figure 4.2.27. Spatial variation of CMV data from Retrofit system on SAKAI smooth drum roller during mapping of subgrade layer

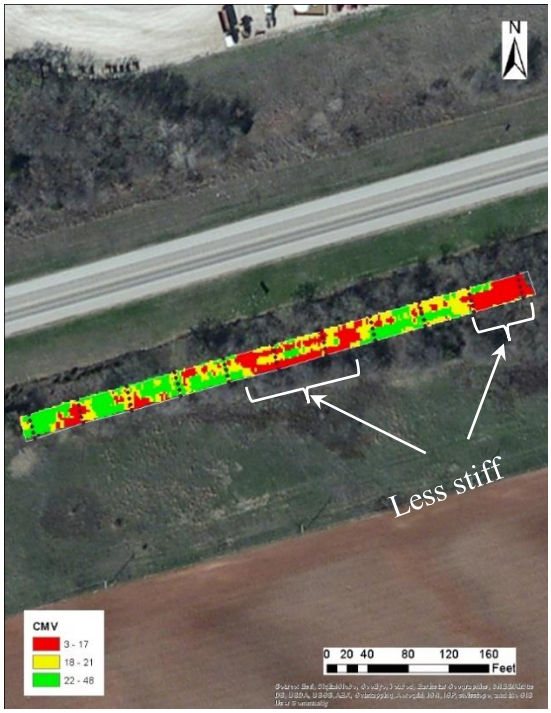

Figure 4.2.29. Spatial variation of CMV data from CAT smooth drum roller during mapping of subgrade layer

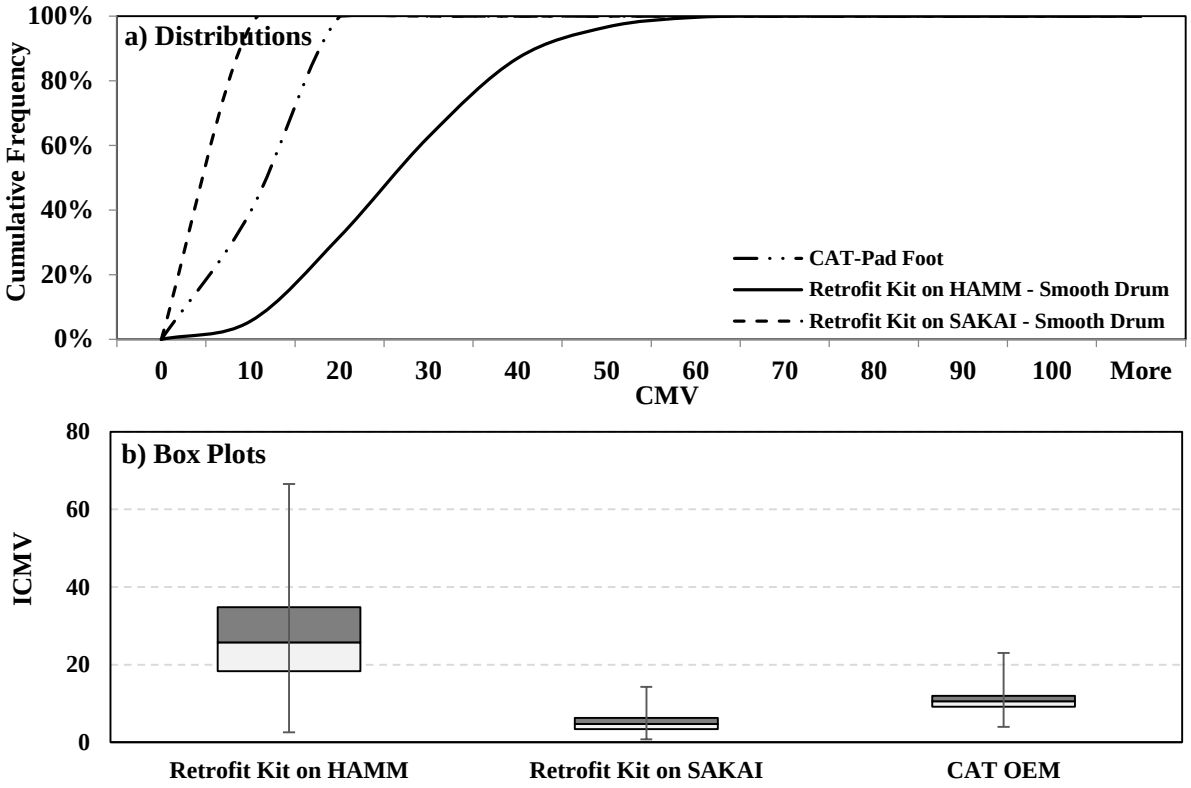

Figure 4.2.30. Comparison of CMV data from retrofit systems on SAKAI and HAMM rollers with OEM system on CAT roller during mapping of subgrade layer

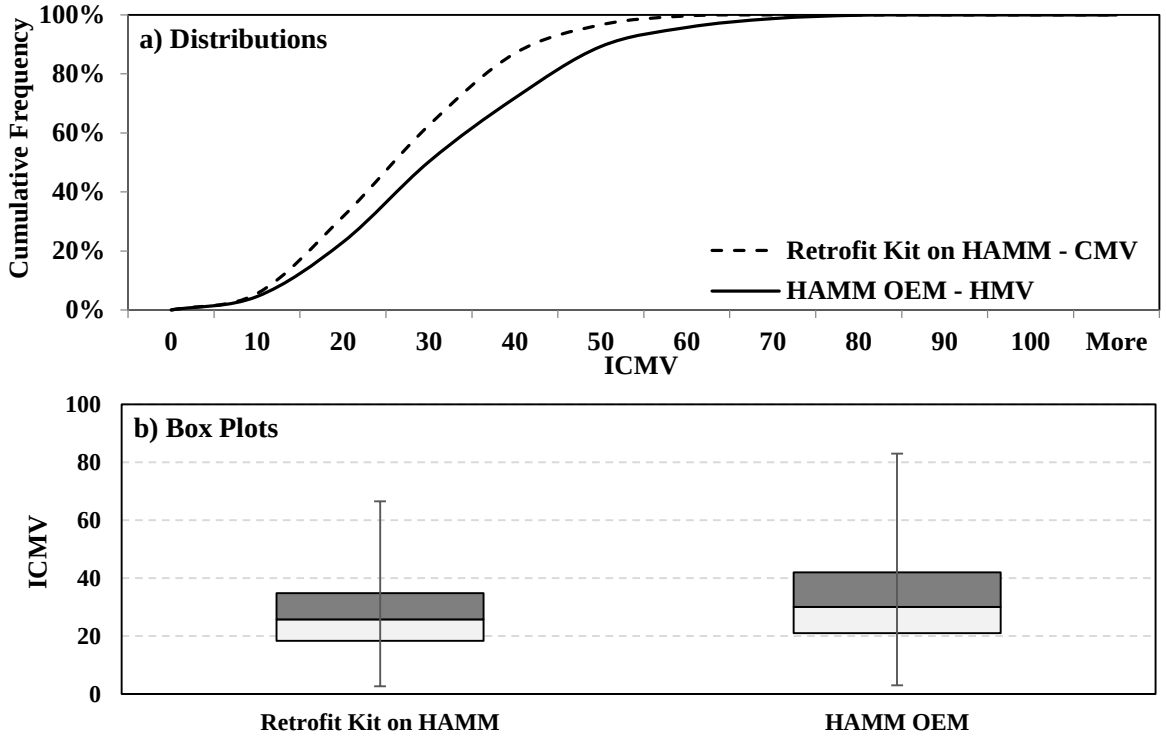

Figure 4.2.31. Comparison of CMV data from retrofit and OEM systems on HAMM roller during mapping of subgrade layer

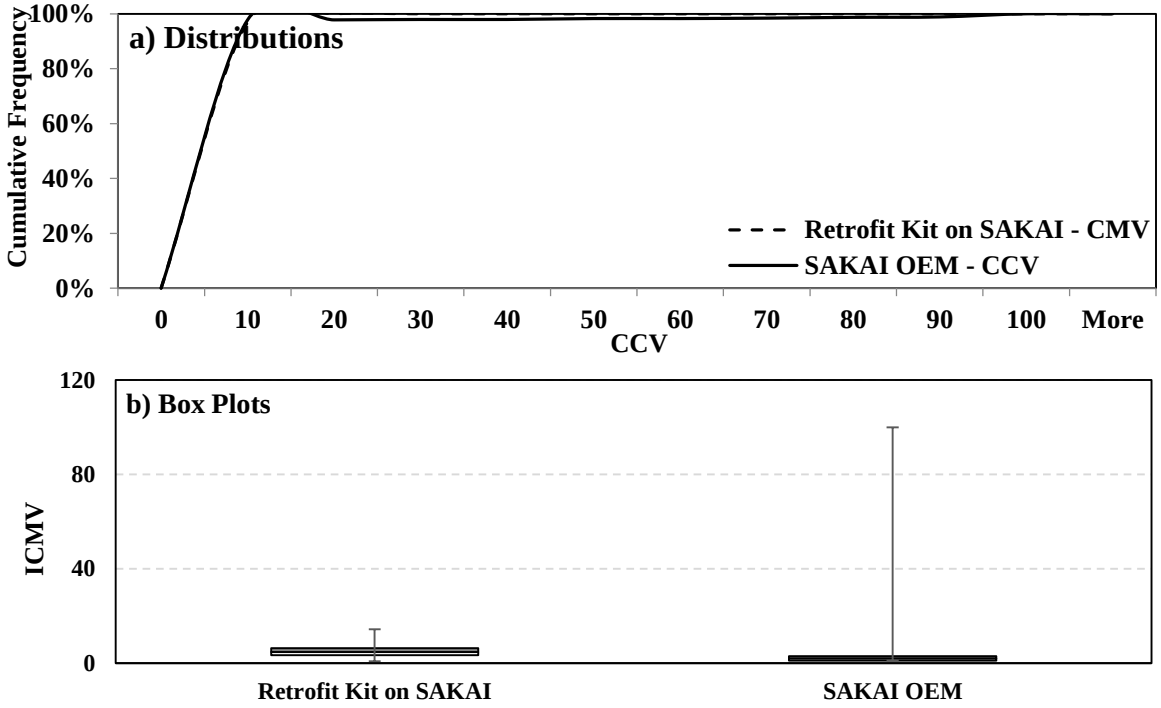

Figure 4.2.32. Comparison of CMV data from retrofit and OEM systems on SAKAI roller during mapping of subgrade layer

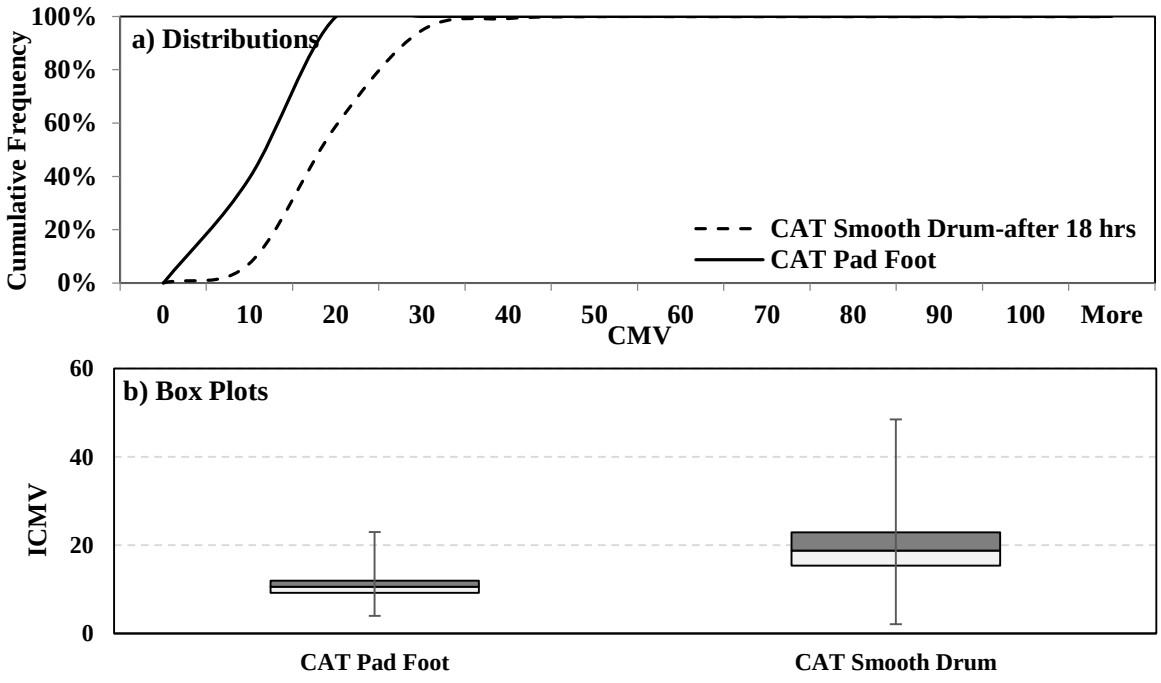

Figure 4.2.33. Comparison of CMV data from OEM system on CAT roller during mapping of subgrade layer with smooth drum and padfoot drum

Table 4.2.6. Descriptive Statistics of CMV data Collected by CAT Roller and Retrofit Kits on SAKAI and HAMM Rollers during Pre-Mapping of Embankment Layer and Mapping of Subgrade Layer

Statistical Parameter	Pre-Mapping of Embankment Layer					Mapping of Subgrade Layer					
	HAMM		SAKAI		CAT (smooth drum)	HAMM		SAKAI		CAT (padfoot drum)	CAT (smooth drum)
	Retrofit Kit	OEM	Retrofit Kit	OEM		Retrofit Kit	OEM	Retrofit Kit	OEM		
Minimum	3.5	2.0	1.1	1.0	4.2	2.6	3.0	0.8	1.0	4.0	2.1
Maximum	79.4	101.0	31.6	100.0	90.5	66.5	83.0	14.3	100.0	23.0	48.5
Average	29.6	26.8	4.9	3.3	27.6	26.9	32.1	5.0	4.5	10.7	19.2
COV	41%	68%	48%	317%	38%	43%	45%	44%	260%	20%	35%

4.3 ANALYSIS OF INFORMATION FROM VALIDATION SYSTEM

As discussed in Section 3.2, vibration data was also recorded using a validation system that was developed in this project for IC data collection parallel to the OEM and retrofit systems. This section is a report of the research team's efforts toward documenting the relationship between the raw vibration data collected during the vibratory compaction of different materials and different ICMVs collected by different vendors. Due to the highly technical nature of this study, the details of the data processing are included in Appendix C. Summary results of the reduced sensor data from the mounted accelerometers on the rollers and embedded geophones in the soil layers are summarized in the following sections. The detailed analyses of data collected with UTEP validation system are included in Appendices A and B for HMA and soils rodeos, respectively.

4.3.1 Initial Evaluation

The first set of initial evaluations refers to the stationary tests on the existing base layer in California. The stationary tests were performed at four different vibration settings. Figure 4.3.1 shows the frequency-domain vibration response during the stationary tests about 5 seconds after the start of the low frequency and low amplitude vibration measurement on the drum of the CAT roller (see Figure 4.3.2). As explained in Chapter 2, the accurate estimation of the forcing frequency and its multiples are of utmost importance for extracting accurate ICMVs. The vertical line in Figure 4.3.1 represents the forcing frequency of the drum vibration. The forcing frequency is about 42 Hz. The first harmonic frequency occurs at about 85 Hz. Some noise can also be observed in the data.

Figure 4.3.3 illustrates the spectrogram of the vibration of the drum at low frequency and low amplitude during the stationary test. A spectrogram is a graph of the amplitude spectra accumulated at different times during the vibration of the drum. The forcing frequency of vibration, which is shown as a darker strip around 42 Hz, is also visible.

Figure 4.3.4 shows the spectrogram of the vertical component of vibration response from the top embedded geophone at a depth of 12 in. in the base layer. A number of harmonic frequencies are noticeable in the spectrogram. The faded response areas at the bottom and top of the spectrogram represent the start and end of the roller vibration.

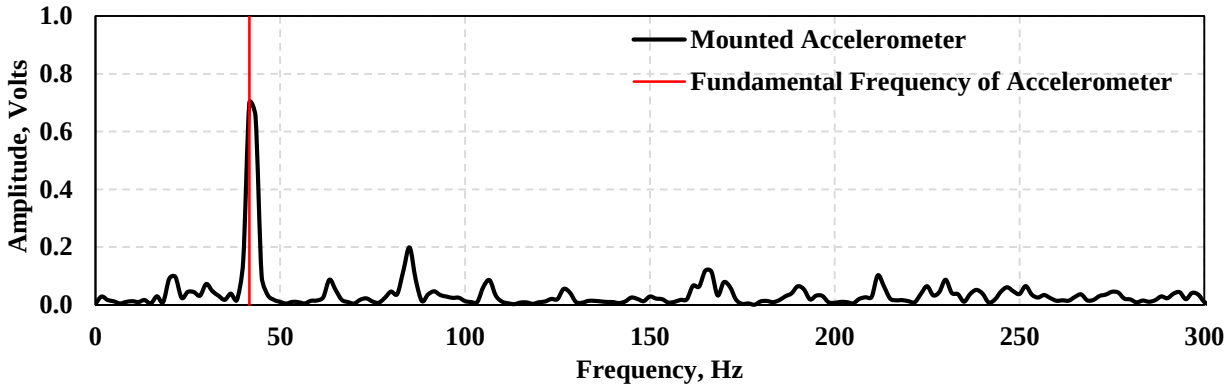

Figure 4.3.1. Response of mounted accelerometer on frequency domain during stationary test (CAT roller) – low frequency and low amplitude

Figure 4.3.2. Mounted accelerometer on drum surface

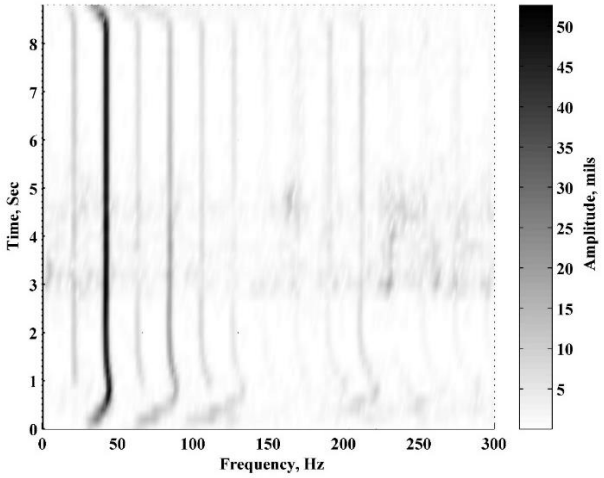

Figure 4.3.3. Spectrogram of mounted accelerometer response during stationary test (CAT roller) – low frequency and low amplitude

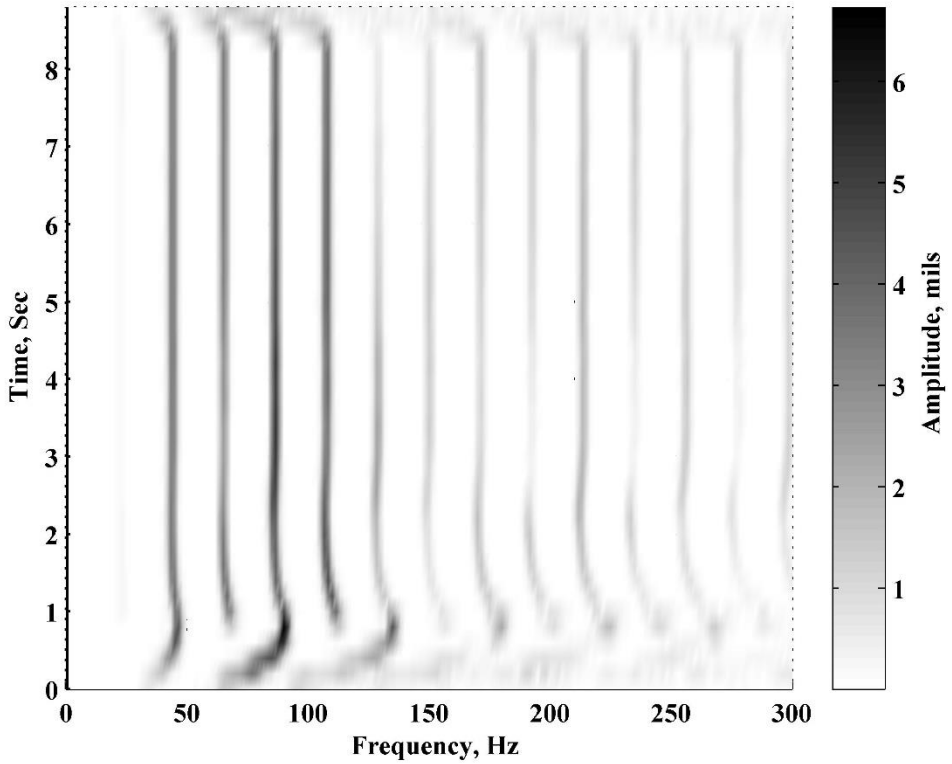

Figure 4.3.4. Spectrogram of vertical response from the top geophone during stationary test (CAT roller) – low frequency and low amplitude

Figure 4.3.5 summarizes the forcing frequency of the roller vibration during the four different vibration settings for the stationary tests. The low and high vibration frequencies can be distinguished in this figure. The start and end parts of each curve, represents the initiation and termination of vibration and the time that it took to reach (or leave) the steady state vibration. Each vibration test lasted less than 15 seconds.

The peak displacement amplitudes at the forcing frequencies during these tests are presented in Figure 4.3.6. Appropriate calibration factor and signal processing were applied to convert the raw voltage to displacement. The low and high amplitude levels of vibration amplitude are apparent in this figure.

Table 4.3.1, summarizes the forcing frequencies and their corresponding displacement amplitudes for the four vibration settings. Table 4.3.1 also contains the nominal values from the roller. The vibration frequencies from the mounted sensors match the roller values. However, the peak amplitudes are different from those specified as nominal machine specifications. This could be due to the stiffness of the compacted surface that causes frequent jumping of the drum during stationary vibrations. These extra movements could be dependent of the layer stiffness and might be lower on less stiff layers.

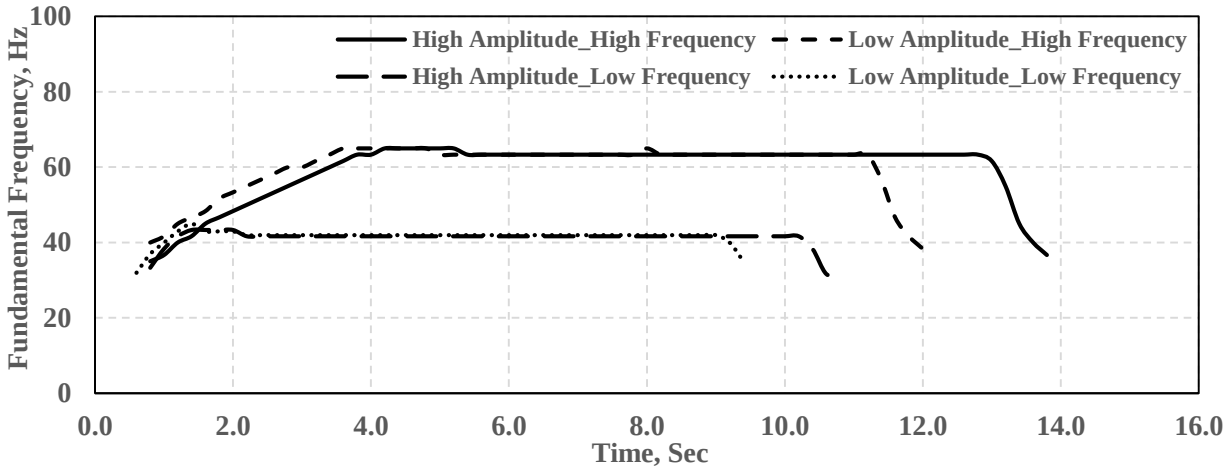

Figure 4.3.5. Comparison of forcing frequency of mounted accelerometer for different vibration settings during stationary tests (CAT roller)

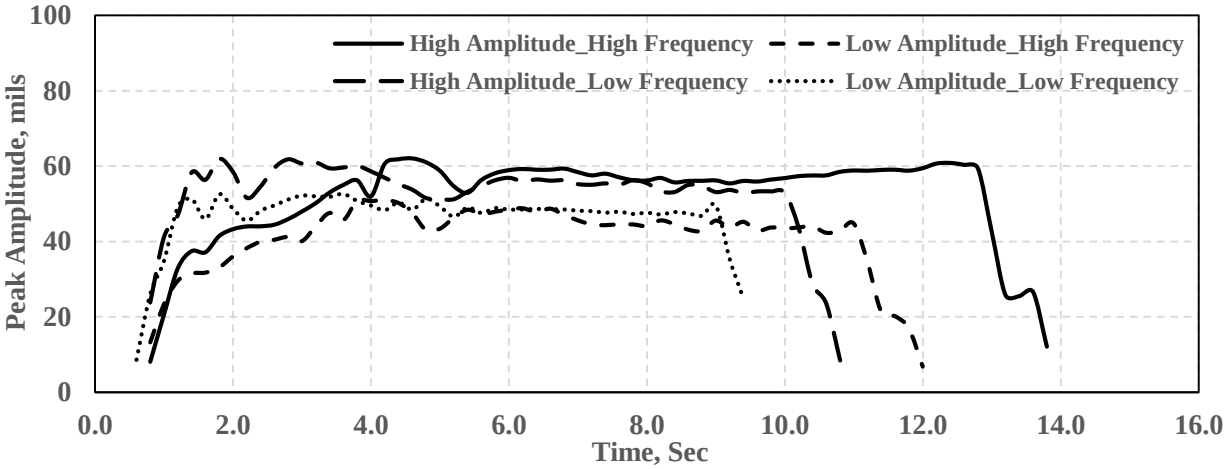

Figure 4.3.6. Comparison of peak amplitudes of mounted accelerometer for different vibration settings during stationary tests (CAT roller)

Table 4.3.1. Different vibration settings (acquired from validation system) during stationary tests (CAT roller)

Roller Vibration Setting	Accelerometer Forcing Frequency, Hz (vpm)	Peak Displacement Amplitude, mils	Nominal Frequency, Hz (vpm)	Nominal Amplitude, mils
High Frequency, High Amplitude	63.3 (3800)	57	63.3 (3800)	34
High Frequency, Low Amplitude	63.3 (3800)	44	63.3 (3800)	12
Low Frequency, High Amplitude	42 (2520)	56	42 (2520)	34
Low Frequency, Low Amplitude	42 (2520)	45	42 (2520)	12

Tables 4.3.2 and 4.3.3 summarize the measured and nominal vibration frequencies and amplitudes during stationary tests for the HAMM and SAKAI rollers. The SAKAI roller has an extra frequency setting as super high frequency that produces a nominal vibration frequency of 4000 vpm. The high frequency-high amplitude setting was skipped for HAMM roller since it was deemed damaging to the roller. For both rollers the vibration frequencies and amplitudes obtained from the mounted sensors are different from the nominal values.

Table 4.3.2. Different vibration settings (acquired from validation system) during stationary tests (HAMM roller)

Roller Vibration Setting	Accelerometer Forcing Frequency, Hz (vpm)	Peak Displacement Amplitude, mils	Nominal Frequency, Hz (vpm)	Nominal Amplitude, mils
High Frequency, High Amplitude	Not Collected	Not Collected	53.3 (3200)	34
High Frequency, Low Amplitude	67 (4000)	48	53.3 (3200)	18
Low Frequency, High Amplitude	45 (2700)	39	42 (2520)	34
Low Frequency, Low Amplitude	40 (2400)	32	42 (2520)	18

Table 4.3.3. Different vibration settings (acquired from validation system) during stationary tests (SAKAI roller)

Roller Vibration Setting	Accelerometer Forcing Frequency, Hz (vpm)	Peak Displacement Amplitude, mils	Nominal Frequency, Hz (vpm)	Nominal Amplitude, mils
High Frequency, High Amplitude	46.7 (2800)	38	Not Provided	25
High Frequency, Low Amplitude	46.7 (2800)	33	Not Provided	13
Low Frequency, High Amplitude	38.3 (2300)	41	42 (2520)	25
Low Frequency, Low Amplitude	40 (2400)	25	42 (2520)	13
Super High Frequency, Low Amplitude	65 (3900)	65	67 (4000)	13

Spectrograms of the vibration data collected with the UTEP DAQ on the CAT, HAMM and SAKAI rollers are included in Appendix A. Since the rollers were not designed to operate and collect vibration data during the stationary mode, there was no retrofit nor OEM data available during these tests.

Table 4.3.4 demonstrates the spectrograms of vibration responses for the three rollers during the stationary tests. Tables 4.3.5 and 4.3.6 summarize the vibration frequency and peak displacement amplitude of each roller during the stationary vibration tests. The forcing frequency is clearly recognizable as the darkest strip in each spectrogram. Furthermore, the number of discernable harmonic frequencies is higher in the case of high amplitude vibration as compared to the low amplitude settings (see the second and third columns in the tables). As shown in Tables 4.3.5 and 4.3.6, the vibration frequency of the CAT roller in the high frequency mode is 63 Hz as compared

to 47 Hz for the SAKAI roller. The peak displacement amplitude of these two rollers are 57 and 38 mils, respectively. Moving to the low frequency and high amplitude setting, the HAMM roller reflects the highest vibration frequency followed by the CAT and SAKAI.

Table 4.3.4. Vibration Response of Different Rollers during Stationary Vibration Tests

	High Frequency, High Amplitude	Low Frequency, High Amplitude	High Frequency, Low Amplitude	Low Frequency, Low Amplitude
CAT	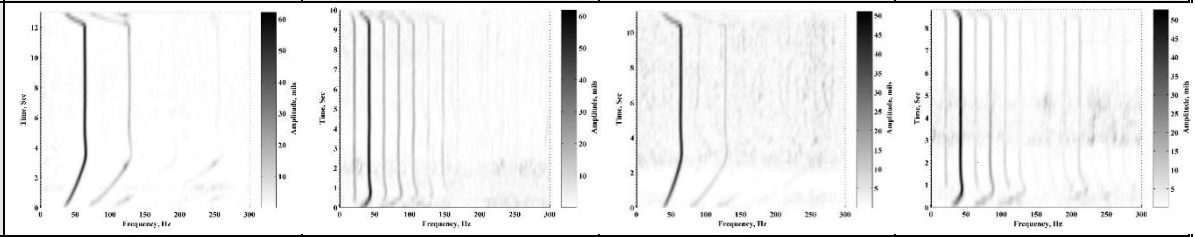			
SAKAI	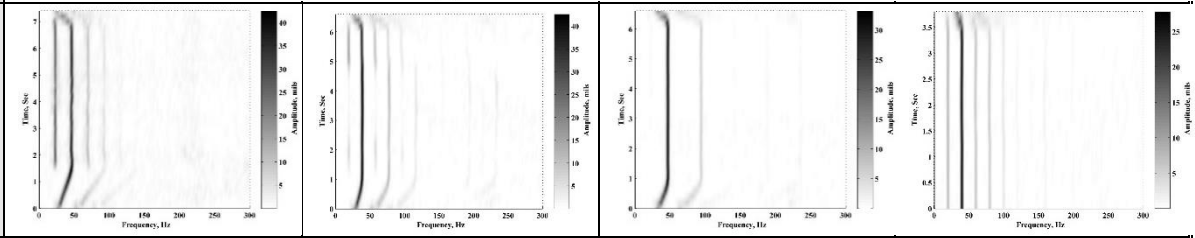			
HAMM	Not Collected	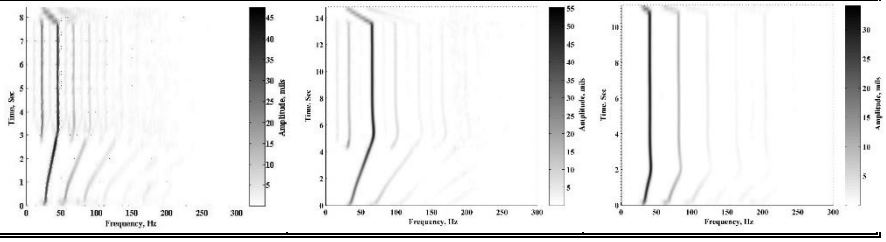		

Table 4.3.5. Vibration Frequency of Different Rollers during Stationary Vibration Tests

Roller	Vibration Frequency, Hz			
	High Frequency, High Amplitude	**Low Frequency, High Amplitude**	**High Frequency, Low Amplitude**	**Low Frequency, Low Amplitude**
CAT	63.3	42	63.3	42
SAKAI	46.7	38.3	46.7	40
HAMM	Not Collected	45	67	40

Table 4.3.6. Peak Displacement of Different Rollers during Stationary Vibration Tests

Roller	Peak Displacement Amplitude, mils			
	High Frequency, High Amplitude	**Low Frequency, High Amplitude**	**High Frequency, Low Amplitude**	**Low Frequency, Low Amplitude**
CAT	57	56	44	45
SAKAI	38	41	33	25
HAMM	Not Collected	39	48	32

To further study the responses of the underlying layers during the stationary roller vibration, the vertical responses of the top and bottom geophones during different vibration settings are summarized in Figures 4.3.7 and 4.3.8. Since the durations of vibration were not identical, each curve in these figures ends at a different time. The y-axis represents the geophones' displacements at the forcing frequency as illustrated before in Figure 4.3.1. The top and bottom geophone responses follow the same trend. A number of abrupt jumps are observed in the geophone responses at high frequency and low amplitude experiment. This phenomena could be due to decoupling of the roller from the soil surface. The same jumps are also evident when the roller is vibrating at high frequency and high amplitude. Further analysis of the geophone responses for the equipment rodeo in California are included in Appendix A.

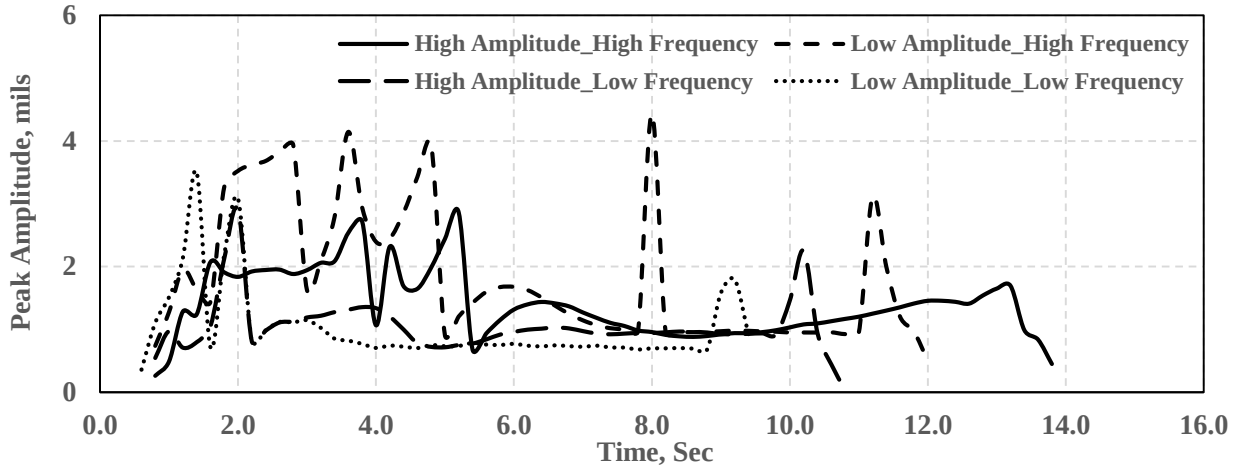

Figure 4.3.7. Comparison of amplitudes (vertical response) of top embedded geophone for different vibration settings during stationary tests (CAT roller)

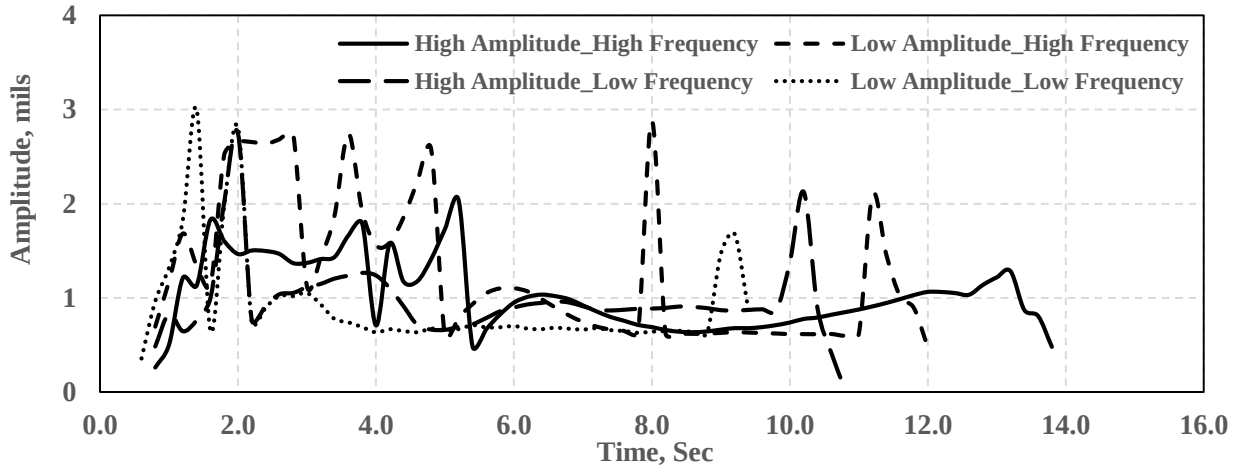

Figure 4.3.8. Comparison of amplitudes (vertical response) of bottom embedded geophone for different vibration settings during stationary tests (CAT roller)

Table 4.3.7 summarizes the response of the top embedded geophone during the stationary vibrations. The differences between the high and low frequency vibrations are clearly identified from the ground response spectrograms as the high frequency vibration creates less dense dark strips (harmonics of forcing frequency exerted from the drum vibration) compared to low frequency vibrations. Furthermore, at the same level of vibration setting on the rollers, the ground

response is quite different considering the fact that the vibration frequency and amplitude of the rollers, as well as their vibration mechanisms, are not similar.

Table 4.3.7. Response of Top Embedded Geophone during Stationary Vibration Tests

	High Frequency, High Amplitude	Low Frequency, High Amplitude	High Frequency, Low Amplitude	Low Frequency, Low Amplitude
CAT	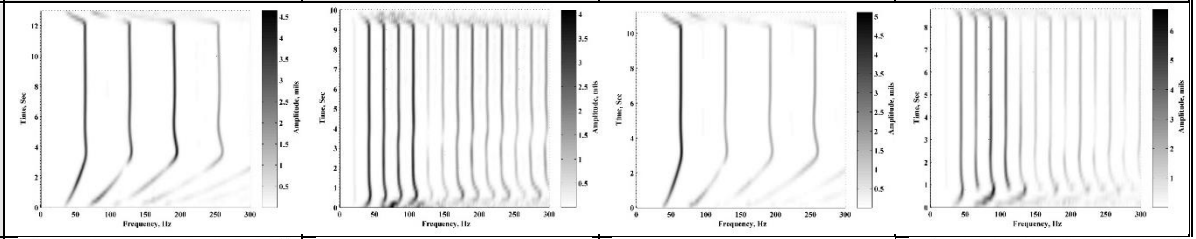			
SAKAI	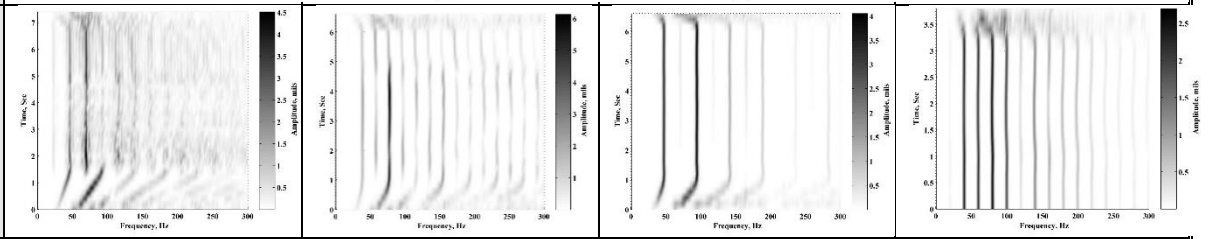			
HAMM	Not Collected	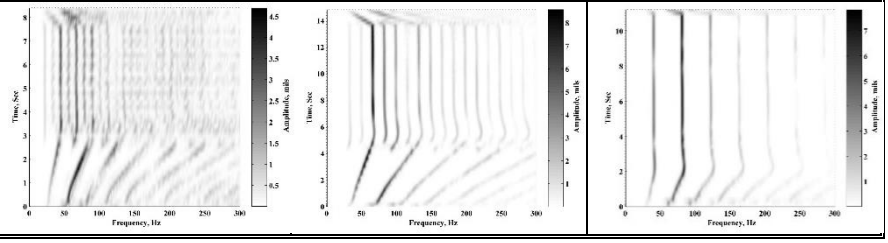		

Figure 4.3.9 compares the drum deflection at the soil surface with geophone deflections at the 12 in. and 20 in. depths. The deflection data was captured 5 seconds after the initiation of the stationary vibration at low frequency and low amplitude setting with the CAT roller on top of the geophone location. The depth of influence, defined as the depth that the deflection becomes 10% of the surface deflection, is also depicted in Figure 4.3.9. The difference between the top and bottom geophones' deflections are small as compared to the surface displacement of the drum. However, the displacement of the drum on top of the soil surface is not necessarily identical to the surface deflection of the soil due to jumping of the drum on top the soil surface. Further analysis of the geophone displacements during the equipment rodeo in California is included in Appendix A.

Table 4.3.8 summarizes the surface and ground deflections during the stationary tests. The depth of influence is dependent on the vibration setting. The influence depth of the CAT roller, on the existing base layer, is from 11 to 14 in. while these values for the SAKAI roller are in the range of 14 to 18 in. for the different vibration settings. The estimated influence depth from the HAMM roller are from 18 to 36 in. based on the vibration amplitude and frequency. These fairly low values of influence depth compared with those in literature could be due to the excessive stiffness of the existing base layer as observed during the testing process that affect the roller drum rebound behavior.

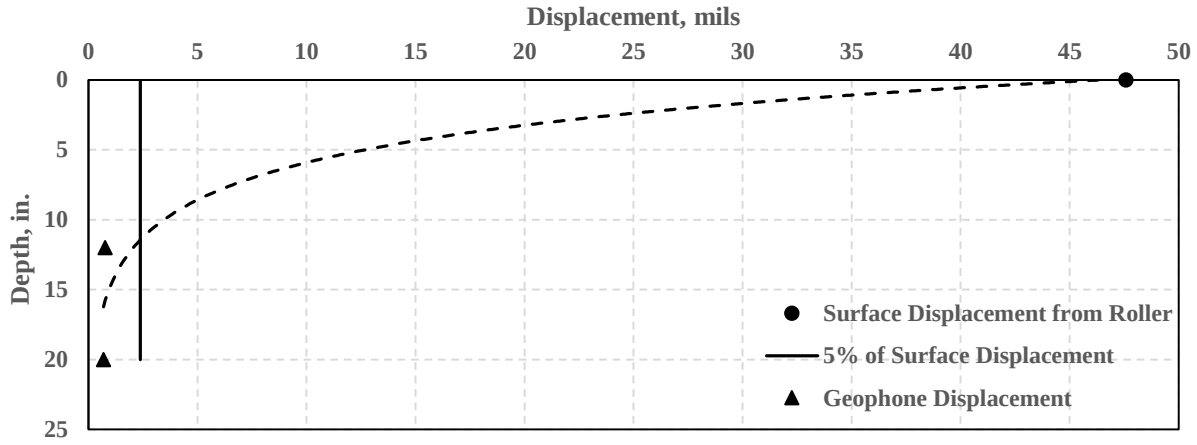

Figure 4.3.9. Comparison of surface roller displacement with deflection of soil layers from embedded geophones at 5 seconds after initiation of low amplitude and low frequency stationary vibration (CAT roller)

Table 4.3.8. Peak Displacement Amplitude of Different Rollers during Stationary Vibration Tests

Parameter	CAT				SAKAI				HAMM			
	H Freq. H Amp.	L Freq. H Amp.	H Freq. L Amp.	L Freq. L Amp.	H Freq. H Amp.	L Freq. H Amp.	H Freq. L Amp.	L Freq. L Amp.	H Freq. H Amp.	L Freq. H Amp.	H Freq. L Amp.	L Freq. L Amp.
Deflection at Surface, mils	57	56	44	45	38	41	33	25	Not Collected	39	48	32
Deflection at 12 in Deep, mils	1.2	0.9	1.7	0.8	2.2	1.1	1.3	1.7		8.6	3.5	4.3
Deflection at 12 in Deep, mils	0.8	0.9	1.1	0.7	1.7	1.0	1.1	1.5		6.2	2.9	3.4
5% of Surface Deflection, mils	2.9	2.8	2.2	2.3	1.8	1.8	1.6	1.3		2.1	2.3	1.5
Estimated Depth of Influence, in.	11.7	11.6	13.5	11.4	16.4	13.6	14.5	17.5		35.8	18.1	24.0

Soils Rodeo

Figure 4.3.10 illustrates the forcing frequency of the two accelerometers mounted on the SAKAI roller during one of the stationary tests during the Texas rodeo on top of the embedded geophones. This test was performed at 1800 vpm and low amplitude according to the roller settings. However, the forcing frequency of vibration obtained from the validation system is 32 Hz, equivalent to 1900 vpm. The forcing frequency captured from the accelerometers on both sides of the drum are almost identical.

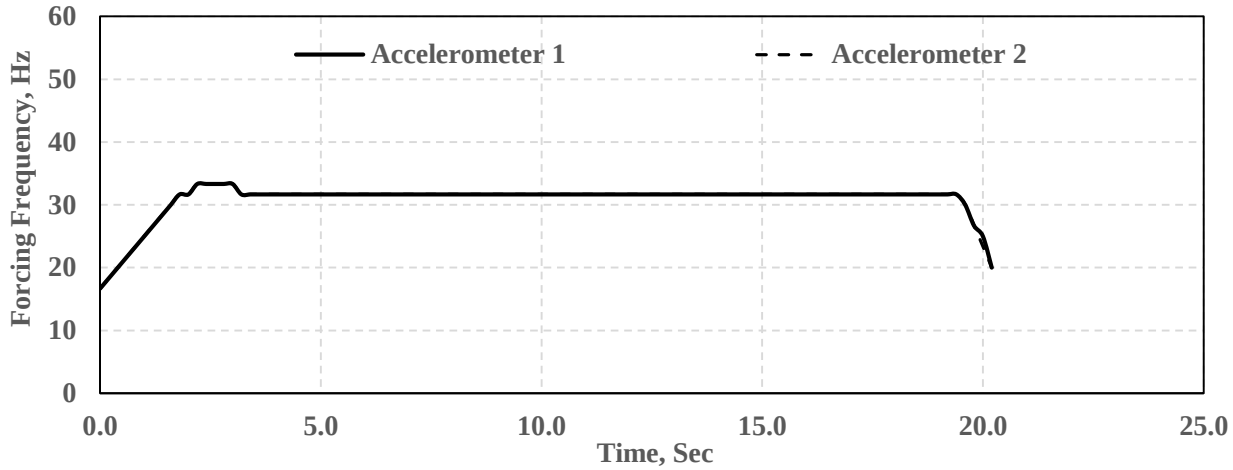

Figure 4.3.10. Forcing frequency of mounted accelerometer from SAKAI roller during stationary test on existing embankment layer

Figure 4.3.11 illustrates the peak vibration amplitudes during the same stationary test for the two accelerometers. The peak amplitude is about 20 mils after the vibration signal reaches the steady state about 3 seconds after the initiation of vibration. Again, the peak amplitudes of the two accelerometers are similar.

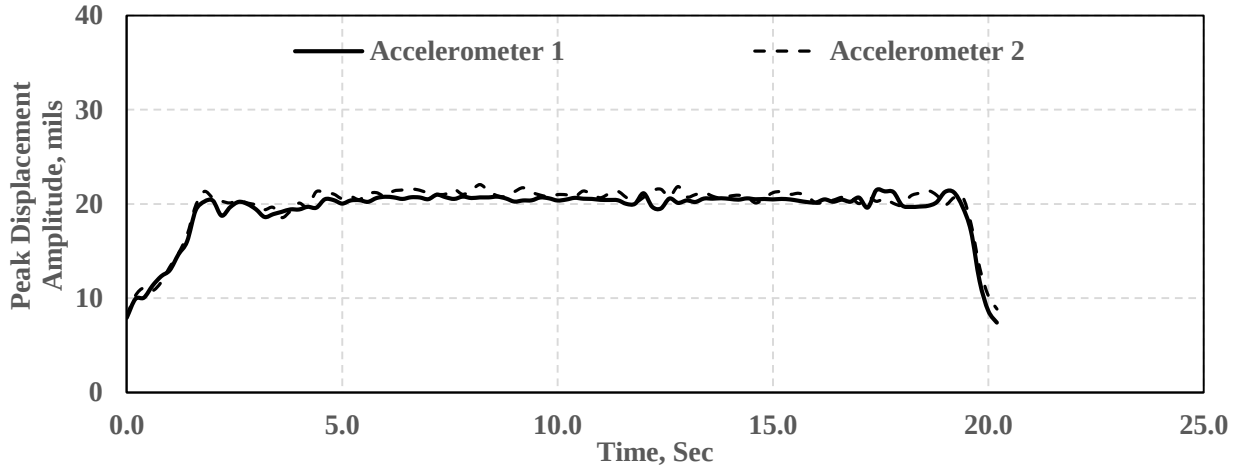

Figure 4.3.11. Peak amplitude of mounted accelerometer from SAKAI roller during stationary test on existing embankment layer

Figure 4.3.12 summarizes the deflections of the soil layers at two depths from the embedded geophones. The deflection of the top geophone is about 60% greater than the deflection obtained from the bottom geophone.

Table 4.3.9 summarizes the responses of the top embedded geophone (at 24 in. depth) during the stationary tests by the different rollers under the different vibration settings. The CAT and HAMM rollers did not perform the high amplitude and high frequency tests to avoid excessive load on their rollers. The responses of the top embedded geophone during the high frequency vibrations of the SAKAI roller exceeded the maximum range (clipped). The effect of the vibration frequency and amplitude is noticeable from the spectrograms.

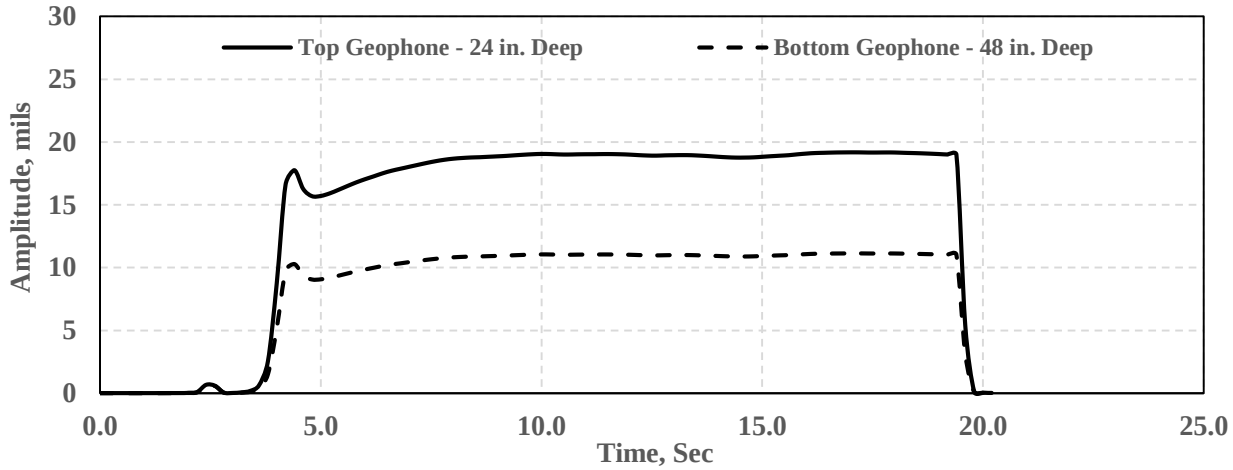

Figure 4.3.12. Peak amplitude of embedded geophones during stationary test on existing embankment layer with SAKAI roller

Table 4.3.9. Response of Top Embedded Geophone during Stationary Vibration Tests

	High Frequency, High Amplitude	Low Frequency, High Amplitude	High Frequency, Low Amplitude	Low Frequency, Low Amplitude
CAT	Not Collected	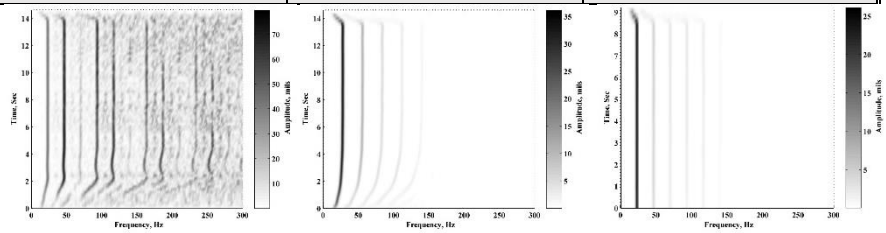		
SAKAI	Signal Clipping	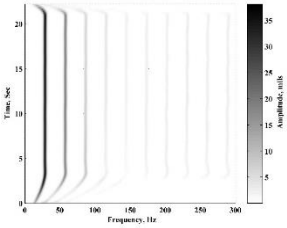	Signal Clipping	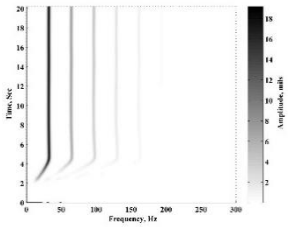
HAMM	Not Collected	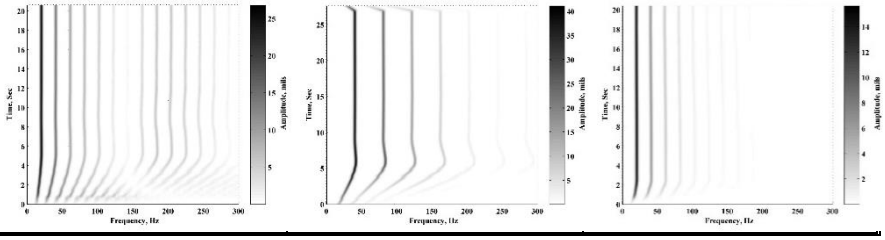		

Figure 4.3.13 compares the deflection of the roller captured from the mounted accelerometers with the deflection of the soil layers from the embedded geophones at the two depths. The deflection data were obtained 6 seconds after the initiation of the vibration, so that the drum vibration would be in a steady state mode. At this specific moment, the deflection of the drum on the soil surface is 21 mils while the deflections of the ground are 17 and 10 mils at 24 and 48 inches deep, respectively. Considering the 10% of surface deflection as the criterion, the estimated influence

depth would be much deeper than 50 in. Further analyses of vibration data during the equipment rodeo in Texas are included in Appendix B. Comparing such estimations with those illustrated in Figure 4.3.9, the depth of influence of the drum vibration may depend on the stiffness of the compacted layer.

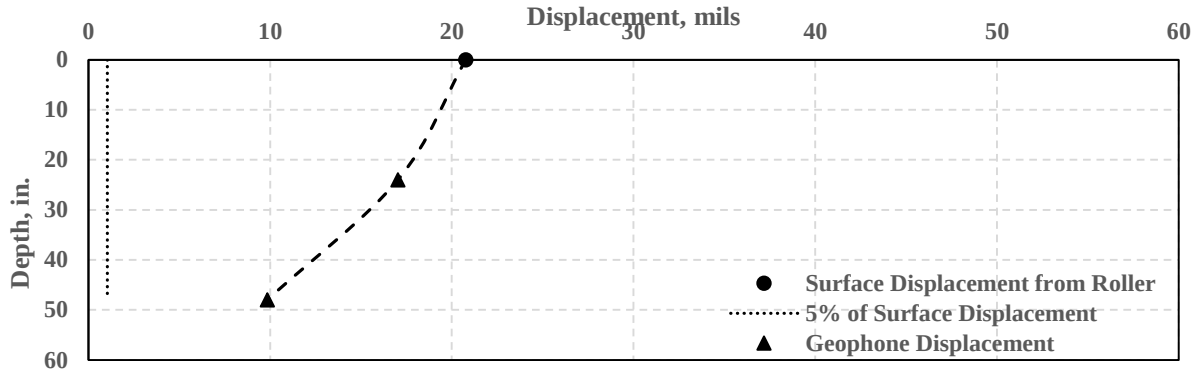

Figure 4.3.13. Comparison of surface roller displacement with deflection of soil layers from embedded geophones at 6 seconds after initiation of vibration (SAKAI roller)

Table 4.3.10 summarizes the results of the stationary tests during the soils rodeo. The deflections of the ground were estimated at two depths (24 in. and 48 in.) and the surface deflection was calculated using the response of the mounted accelerometer on the roller drum. The influence depth during these tests was extrapolated as between 65 in. and 83 in. Comparing these influence depths with the results from the very stiff base land subgrade from the first rodeo shows that the influence depth is dependent of the layer stiffness as well as the vibration settings.

Table 4.3.10. Peak Displacement Amplitude of Different Rollers during Stationary Vibration Tests

Parameter	CAT				SAKAI				HAMM			
	H Amp. H Freq.	L Amp. H Freq.	H Amp. L Freq.	L Amp. L Freq.	H Amp. H Freq.	L Amp. H Freq.	H Amp. L Freq.	L Amp. L Freq.	H Amp. M Freq.	L Amp. H Freq.	H Amp. L Freq.	L Amp. L Freq.
Deflection at Surface, mils	Not Collected	28.5	39.2	30.0	Signal Clipping	Signal Clipping	35.1	21.2	Not collected	40.0	30.8	16.1
Deflection at 24 in Deep, mils		25.8	32.6	26.0			32.1	18.9		37.4	26.8	15.1
Deflection at 48 in Deep, mils		11.5	20.0	11.8			17.7	10.1		16.5	13.2	7.7
5% of Surface Deflection, mils		1.4	2.0	1.5			1.8	1.1		2.0	1.5	0.8
Estimated Depth of Influence, in.		65.0	82.6	65.3			74.5	72.5		64.7	68.6	70.4

4.3.2 Vibration Evaluation due to Moving Rollers

The moving vibration tests were performed along a 100-ft-long section of each test section in California and Texas. Vibration data were simultaneously collected from the accelerometers mounted on the rollers and the two embedded geophones. The data summarized in this section mainly corresponds to the SAKAI roller. Similar results from the HAMM roller are included in Appendices A and B. The UTEP accelerometers could not be installed on the double-drum CAT roller during the California rodeo due to its special configuration. The vibration data from the single-drum CAT roller used in Texas are summarized in Appendix B.

HMA Rodeo

Figure 4.3.14 illustrates the roller path with respect to the location of the embedded geophones during the moving vibration tests in California. Since during the compaction process, an area equal to the width of the drum is covered in each pass, the GPS coordinates had to be gridded. The gridded area is compared with the measured GPS locations in Figure 4.3.15.

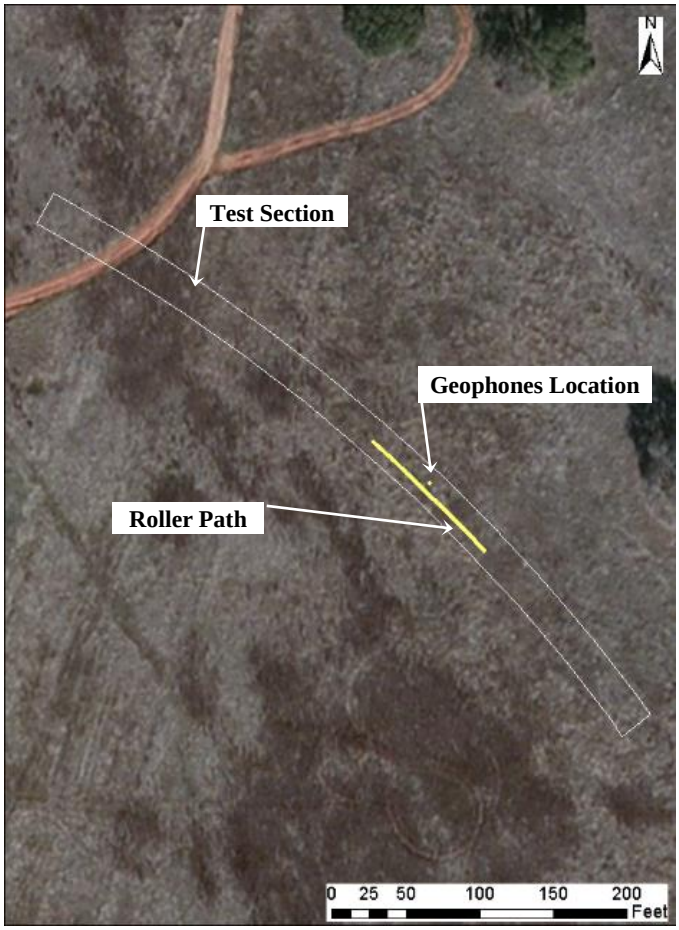

Figure 4.3.14. Roller path with respect to geophones locations within the test section in California (SAKAI roller)

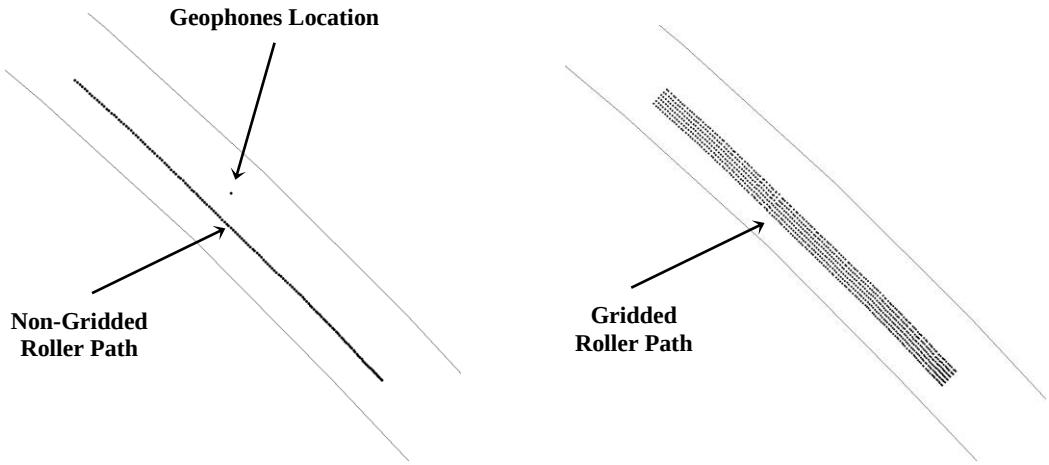

Figure 4.3.15. Gridded data points compared to the original GPS locations

The vibration frequency and amplitude as well as the estimated ICMVs were extended to the width of the roller at each point. The spatial analyses were performed on the gridded data hereafter. The following sections include the details of the vibration data from mounted accelerometers and embedded geophones followed by their spatial analyses.

Figure 4.3.16 illustrates an example of frequency spectrum from the accelerometer data during the moving vibration tests. The forcing frequency and the first harmonic component of the vibration are identified in the figure. The acceleration amplitudes at these two frequencies were utilized to estimate the stiffness in terms of the CMV.

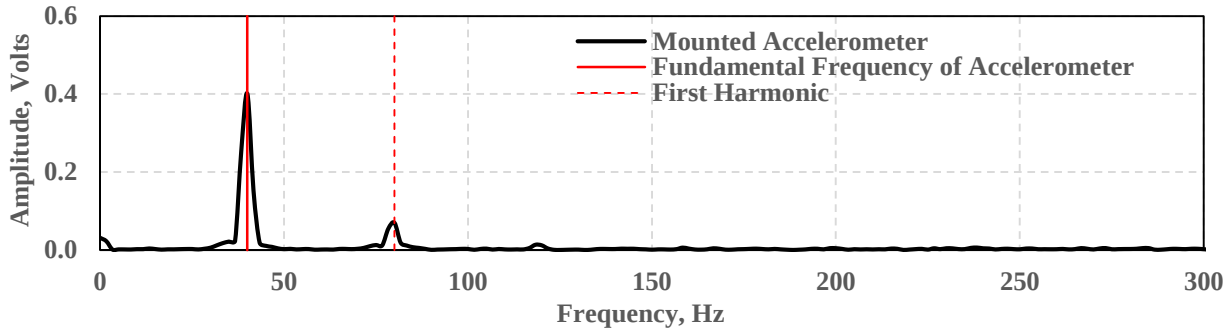

Figure 4.3.16. An example of vibration data from mounted accelerometer

Figure 4.3.17 demonstrates the spectrogram of the accelerometer data during the moving vibration test with the SAKAI roller. The y-axis denotes the distance of the roller from the location of the embedded geophones. The negative distances correspond to the data before the roller arrived at the geophone location. Again, the forcing and first harmonic modes are evident. The faded areas in the bottom and top of this figure represents the initiation and the termination of roller vibration.

The corresponding vibration data spectrogram from the top vertical geophone, during the same pass of the SAKAI roller is shown in Figure 4.3.18. The vibration response gets stronger as the roller gets closer to the geophones, and weaker as the roller moves away from the geophones. The number of harmonic modes represented as dark strips in Figure 4.3.18 is greater as compared to the roller accelerometer data.

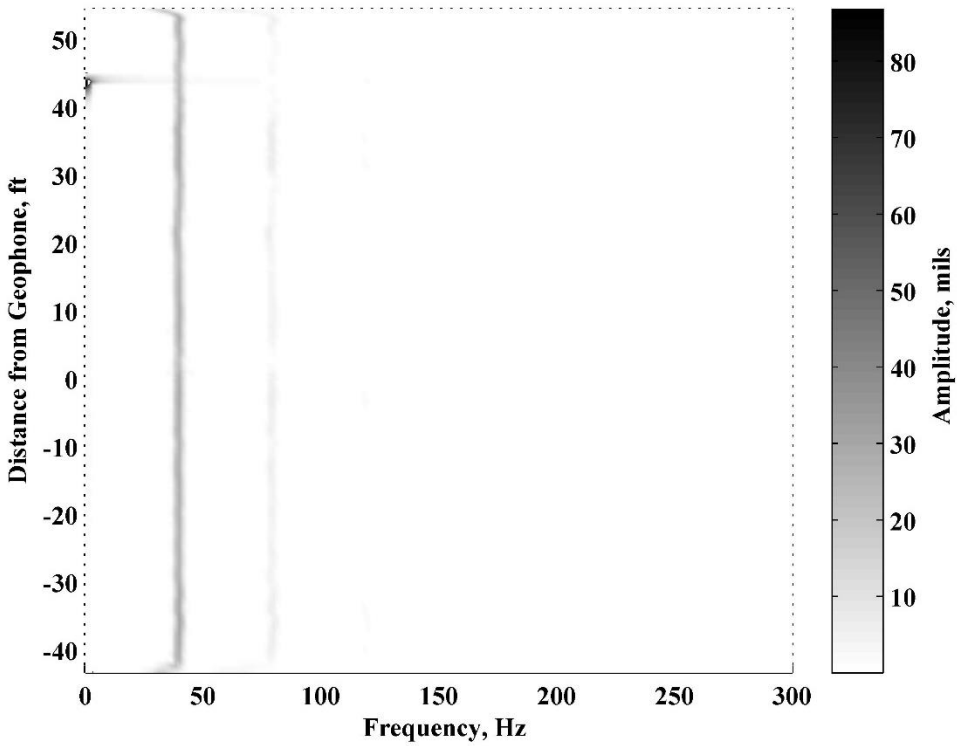

Figure 4.3.17. Spectrogram of vibration data from mounted accelerometer for one roller pass (SAKAI roller)

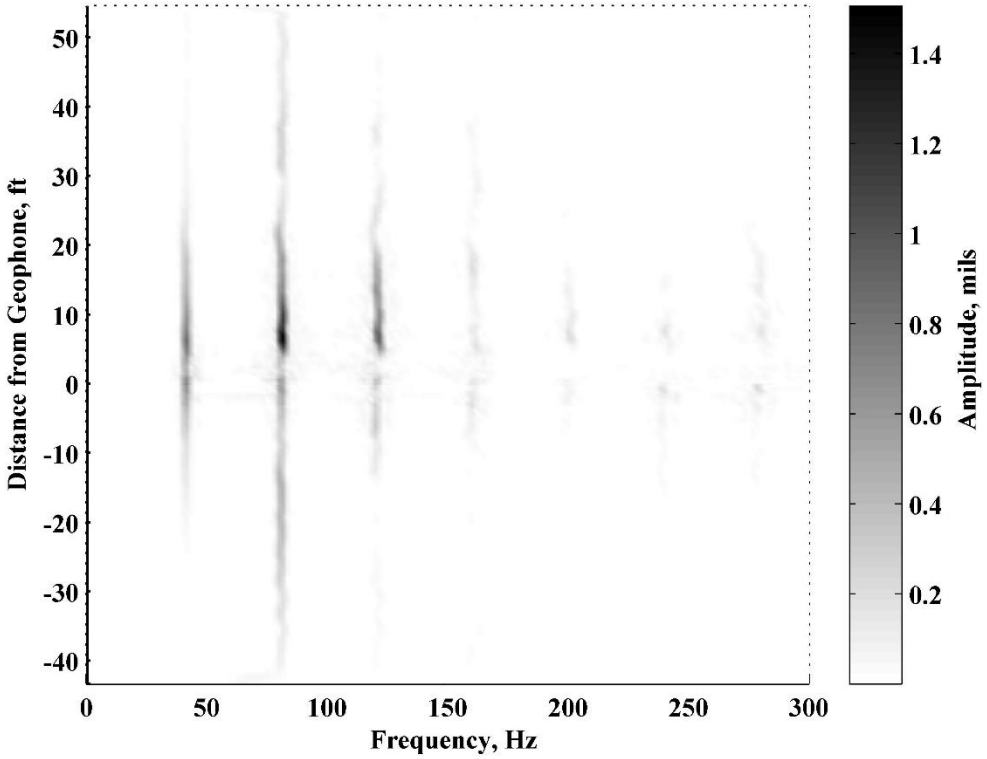

Figure 4.3.18. Spectrogram of vibration data from top embedded geophone for one roller pass (SAKAI roller)

The vibration data from the UTEP system were then compared with the data collected from the retrofit kit installed on the SAKAI roller. Figure 4.3.19, which summarizes the forcing frequencies from the UTEP system and the retrofit kit, indicates that the forcing frequencies differ only slightly considering the expanded range of the y-axis in this figure. Furthermore, the peak amplitudes corresponding to the forcing frequencies from the two systems also compare well (see Figure 4.3.20). The minor differences could be associated with the position of the mounted sensors and differences in data analysis parameters.

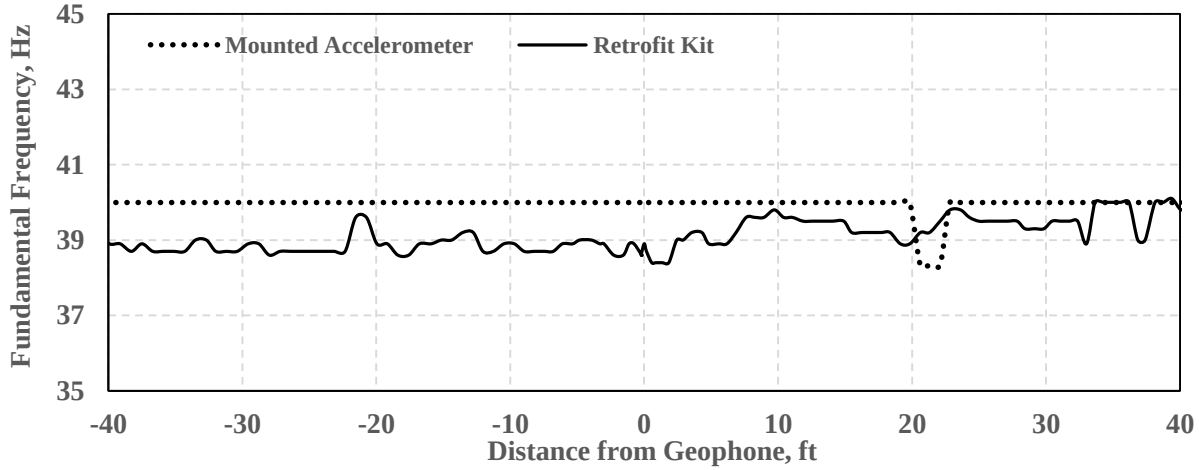

Figure 4.3.19. Comparison of vibration frequency data from validation system with retrofit kit for one roller pass (SAKAI roller)

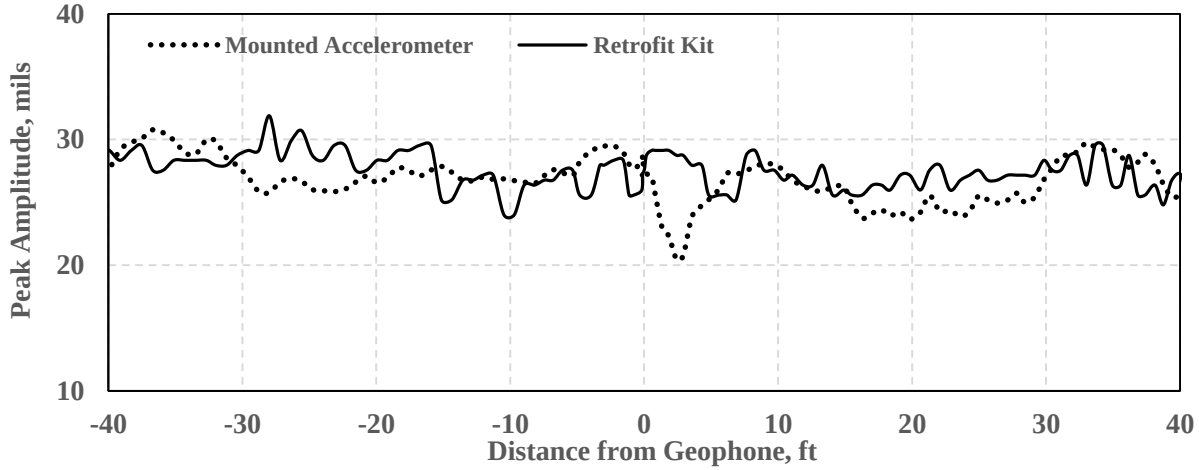

Figure 4.3.20. Comparison of vibration amplitude data from validation system with retrofit kit for one roller pass (SAKAI roller)

The CMVs calculated using the vibration data from the validation system are compared with the reported CMVs by the retrofit kit in Figure 4.3.21. The results from the two systems are somehow different. But both systems show a less stiff area (lower CMVs) about 40 ft past the geophone location. But the less stiff area close to the sensor is sensed by the mounted accelerometer but not the retrofit kit. A part of such differences could be associated with the different data processing parameters used as discussed in Appendix C. These data may also show that the calculated CMVs are sensitive to the position of the vibration sensor and how well the sensor is attached to the drum.

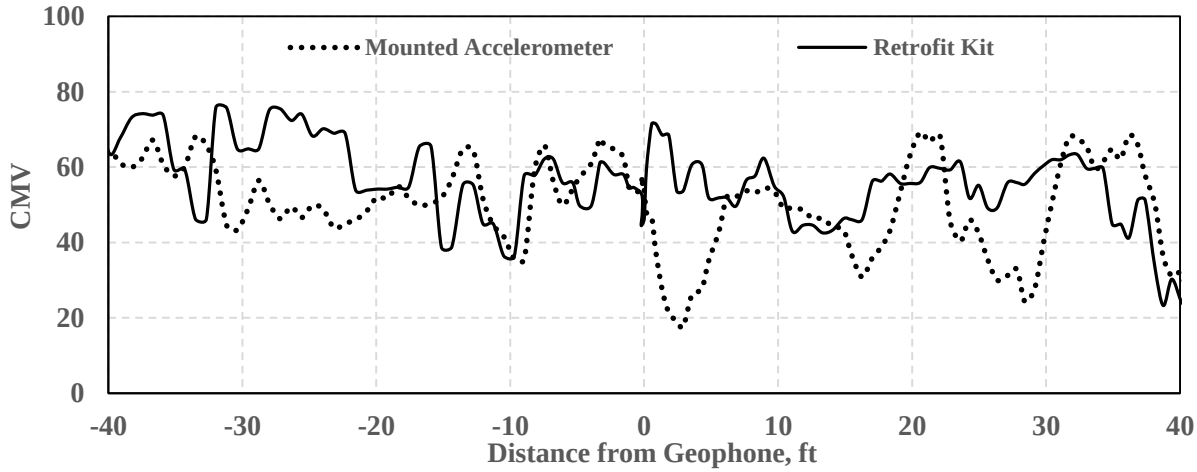

Figure 4.3.21. Comparison of CMV data from validation system and retrofit kit for one roller pass (SAKAI roller)

The vertical accelerations at the forcing frequency of vibration from the two embedded geophones with respect to the distance of the roller from the geophones are presented in Figure 4.3.22. The magnitudes of the geophone responses increase as the roller becomes closer to the geophone location. The sudden drop in the amplitudes of the vertical acceleration on the positive side of the x-axis could be due to the lower stiffness of that particular section. Furthermore, there are minor differences between the vertical responses of the top and bottom geophones. This is perhaps because of the extremely stiff nature of the subgrade at this location that prevents the attenuation of the signals within the ground. The transversal and longitudinal responses summarized in Figures 4.3.23 and 4.3.24 show the same trends except that the vertical amplitudes are greater than the transversal and longitudinal responses.

Figure 4.3.25 compares the distributions of the CMVs from the UTEP and retrofit systems on the SAKAI roller during the pre-mapping of the base layer. Both systems seem to provide similar distributions of the CMVs. However, the CMVs from the retrofit system are slightly greater than those estimated from the UTEP system. Further analyses of the vibration data during the equipment rodeo in California are included in Appendix A.

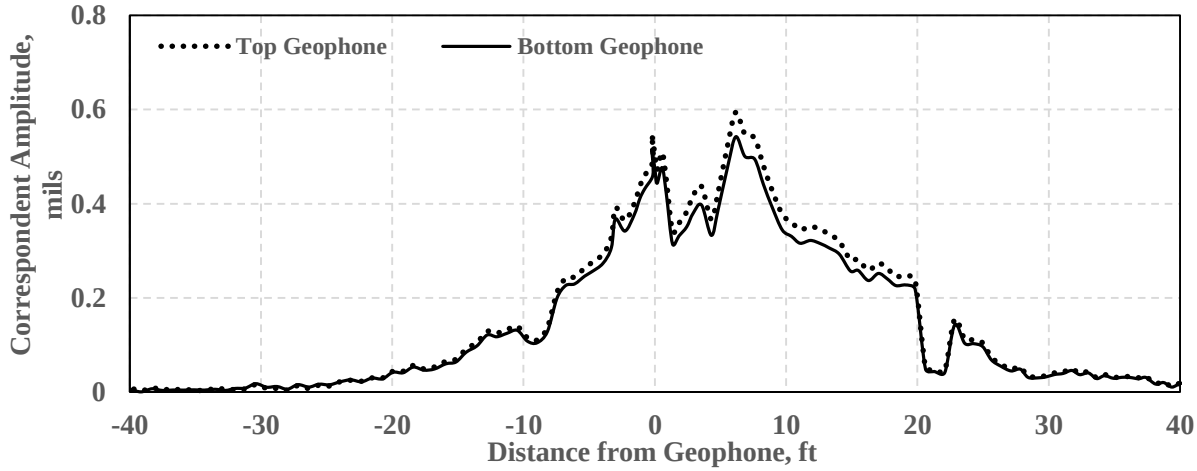

Figure 4.3.22. Vertical response of geophones during one roller pass (SAKAI roller)

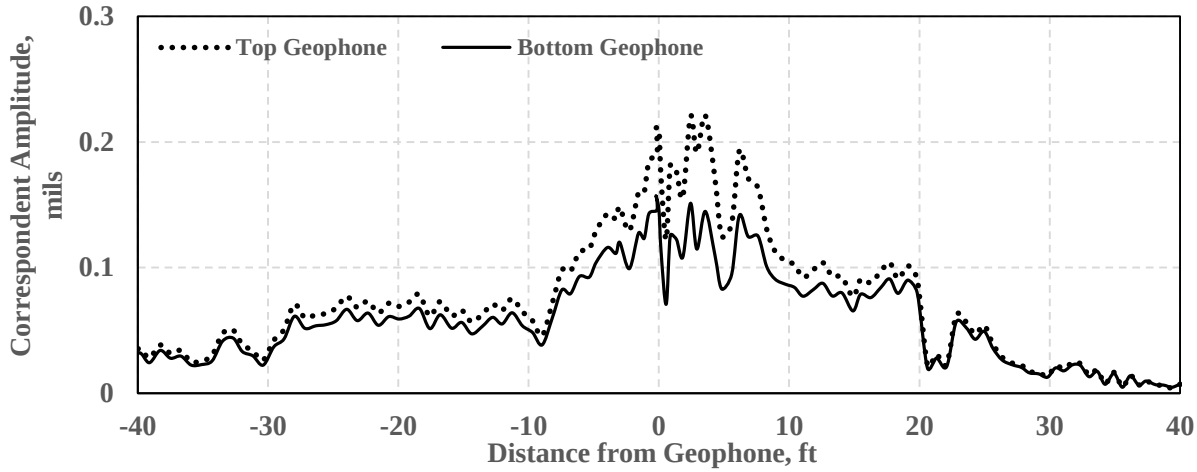

Figure 4.3.23. Transversal response of geophones during one roller pass (SAKAI roller)

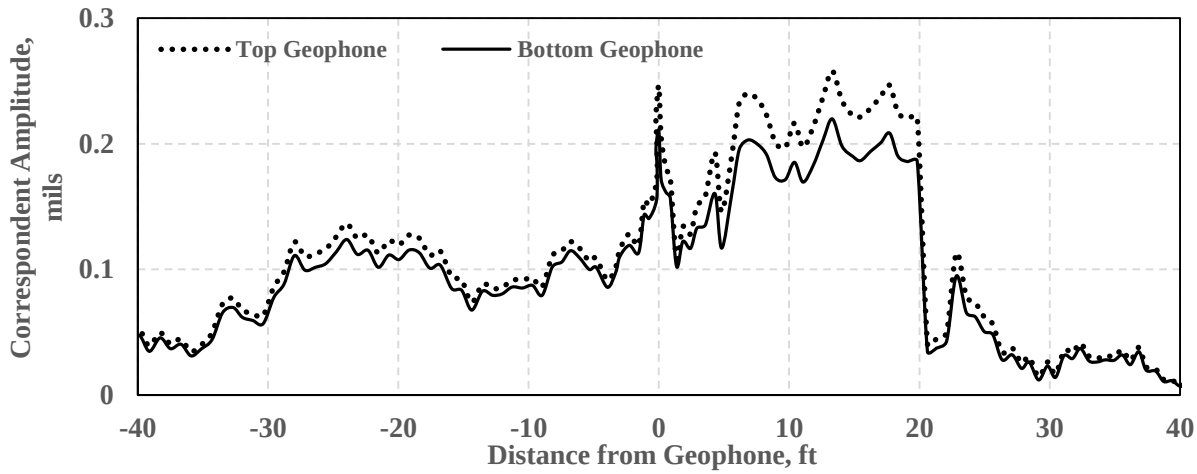

Figure 4.3.24. Longitudinal response of geophones during one roller pass (SAKAI roller)

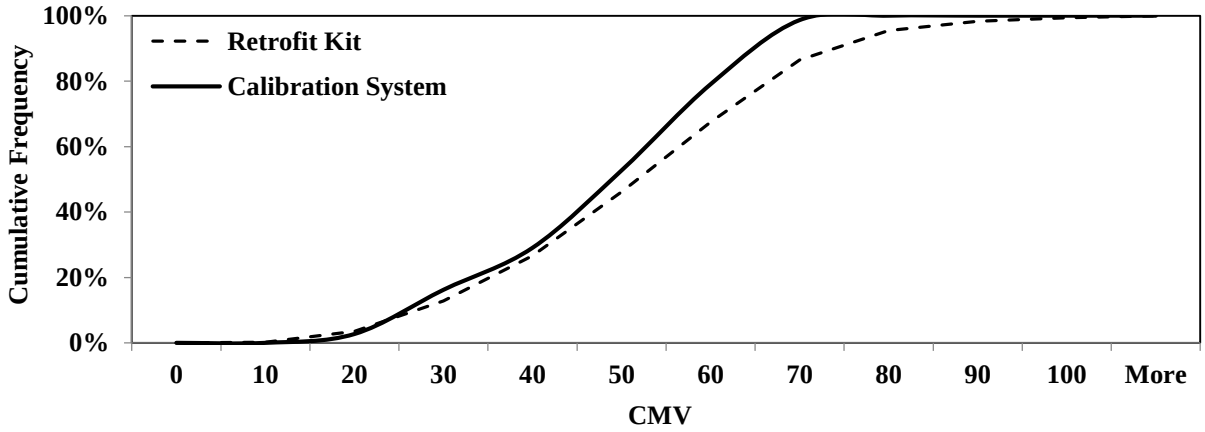

Figure 4.3.25. Comparison of CMV data from validation system and retrofit kit on SAKAI roller during pre-mapping of base layer

Tables 4.3.11 through 4.3.13 summarize the responses of the mounted accelerometer and top embedded geophone for the moving vibration tests during pre-mapping of the base layer and mapping of the first and second HMA lifts. It was not feasible to instrument CAT roller during this equipment rodeo. As reflected in Table 4.3.11, the forcing frequencies of the vibration and the numbers of harmonic frequencies as measured by mounted accelerometers are different for the SAKAI and HAMM rollers. The responses of the embedded geophone is also different under different vibration settings for different rollers.

Table 4.3.11. Response of Mounted Accelerometer and Top Embedded Geophone during Moving Vibration Tests, Pre-Mapping of Base Layer

	Low Frequency, High Amplitude – SAKAI High Frequency, High Amplitude – HAMM		Low Frequency, Low Amplitude	
	Geophone	**Accelerometer**	**Geophone**	**Accelerometer**
SAKAI	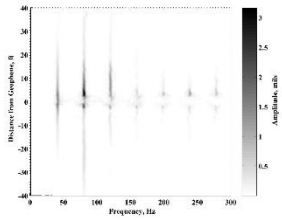	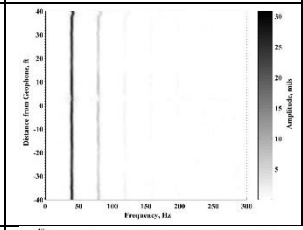	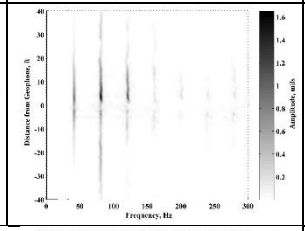	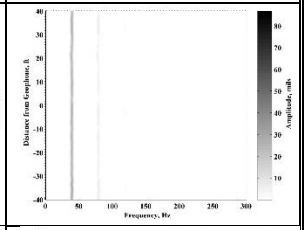
HAMM	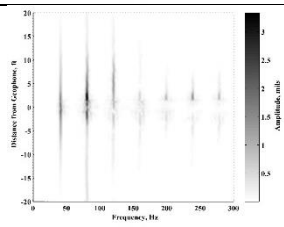	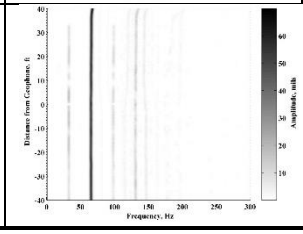	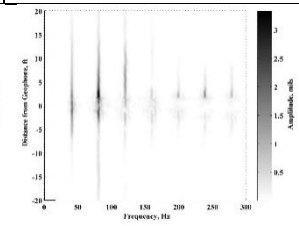	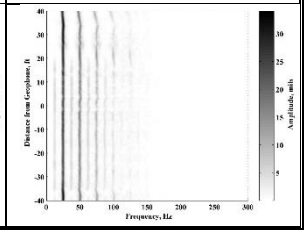

Responses of the mounted accelerometer on the SAKAI roller as well the embedded geophone are summarized in Tables 4.3.12 and 4.3.13 for the mapping of the first and second HMA lifts. Similar information from other rollers is not available because only the SAKAI roller was instrumented during the mapping of the HMA lifts. Again, the impact of the vibration settings on the response of the accelerometer and geophones is reflected in these spectrograms. The number of harmonic frequencies in accelerometer and geophone spectrograms are different as shown in Table 4.3.12 due to the different vibration amplitude and frequency. Furthermore, the displacement amplitudes of the two spectrograms during the mapping of the second HMA lift is different than the spectrogram of the response on the first HMA lift.

Soils Rodeo

Vibration evaluation was also performed during the second equipment rodeo in Texas on soil layers. Figure 4.3.26 shows the location of one SAKAI roller pass during the pre-mapping process with respect to the location of the embedded geophones and the boundaries of the test section.

Figure 4.3.27 summarizes the forcing frequencies of the two accelerometers mounted on the two sides of the SAKAI roller during the pre-mapping of the existing embankment layer in Texas. The vibration frequencies were almost constant at 1900 vpm (32 Hz) during the pre-mapping process. The corresponding peak amplitudes are depicted in Figure 4.3.28 for the same pass of the SAKAI roller. The displacements of the drum from both accelerometers are about 20 mils.

Table 4.3.12. Response of Mounted Accelerometer and Top Embedded Geophone during Moving Vibration Tests, Mapping of First HMA Lift

	Low Frequency, High Amplitude		High Frequency, Low Amplitude	
	Geophone	**Accelerometer**	**Geophone**	**Accelerometer**
SAKAI	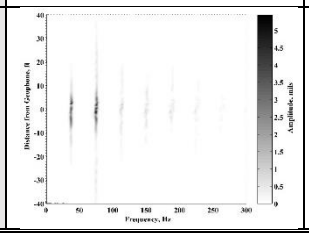	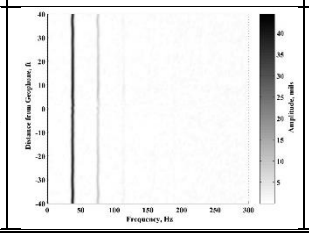	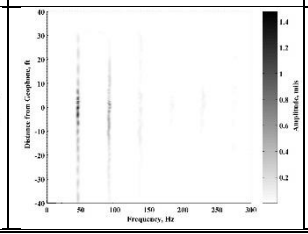	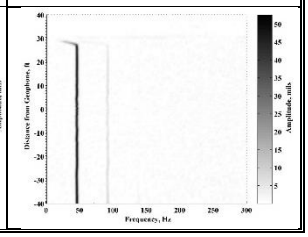

Table 4.3.13. Response of Mounted Accelerometer and Top Embedded Geophone during Moving Vibration Tests, Mapping of Second HMA Lift

	High Frequency, High Amplitude		High Frequency, Low Amplitude	
	Geophone	**Accelerometer**	**Geophone**	**Accelerometer**
SAKAI	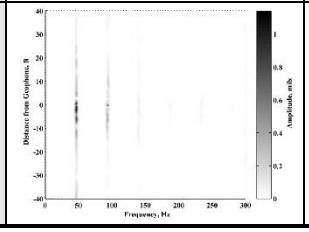	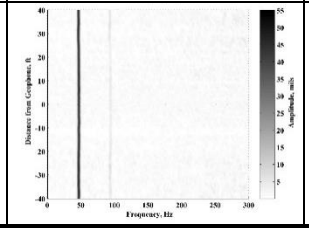	Data Not Collected	

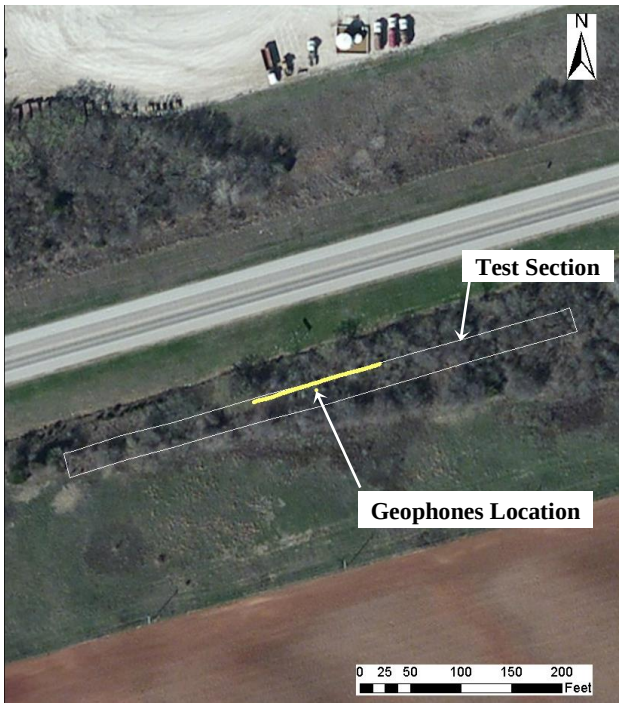

Figure 4.3.26. Location of roller pass with respect to geophone locations and tests section in Texas

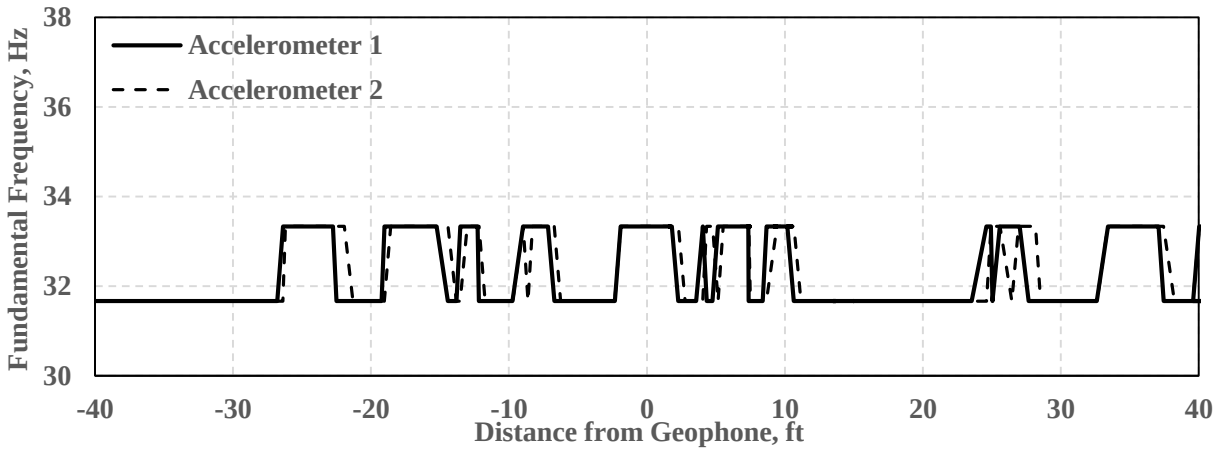

Figure 4.3.27. Forcing frequency of roller vibration from mounted accelerometers on SAKAI roller during pre-mapping

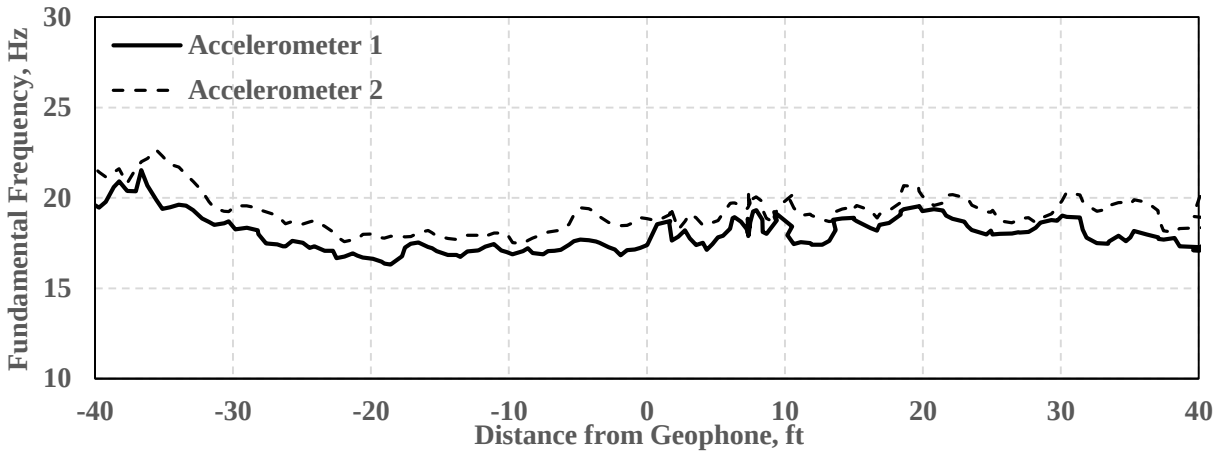

Figure 4.3.28. Peak amplitude of roller vibration from mounted accelerometers on SAKAI roller during pre-mapping

Figure 4.3.29 summarizes the vibration frequencies from the three systems mounted on the SAKAI roller during the pre-mapping of the embankment. The forcing frequencies obtained from the retrofit and validation systems agree. The vibration frequencies of the OEM system is about 4 Hz less than the other two systems. Such effects are further discussed in Appendix C.

Figure 4.3.30 demonstrates the vibration amplitude of the drum during the pre-mapping with the SAKAI roller. The OEM system seems to report a constant number while the retrofit kit and the validation system are more sensitive to the changes in vibration amplitude. There is a sudden increase in the amplitude of the retrofit system between the -52 ft to -19 ft point from the geophone location. The reason for this change is not known.

Figure 4.3.31 compares the calculated CMVs from the UTEP system and the retrofit kit. The trends of the two sets of CMVs are similar. Figure 4.3.32 summarizes the estimated CCVs from the UTEP system along with the reported CCVs from the OEM system. Same as the vibration amplitude, the CCVs seem to be fairly constant while the calculated CCVs from the validation system are more sensitive to the minor changes in the stiffness. Again, this can be due to the selection of analysis parameters as discussed in Appendix C.

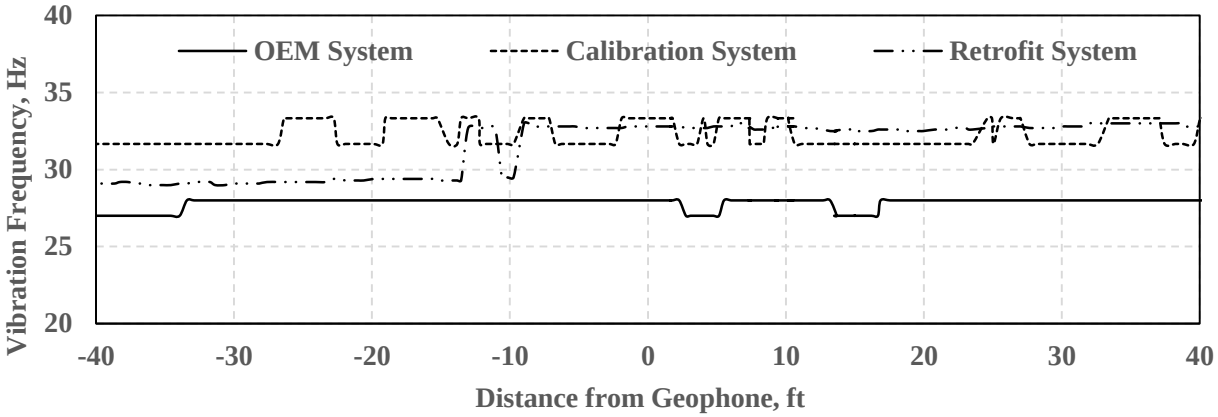

Figure 4.3.29. Comparison of vibration frequency between OEM, retrofit and validation systems on SAKAI roller during pre-mapping

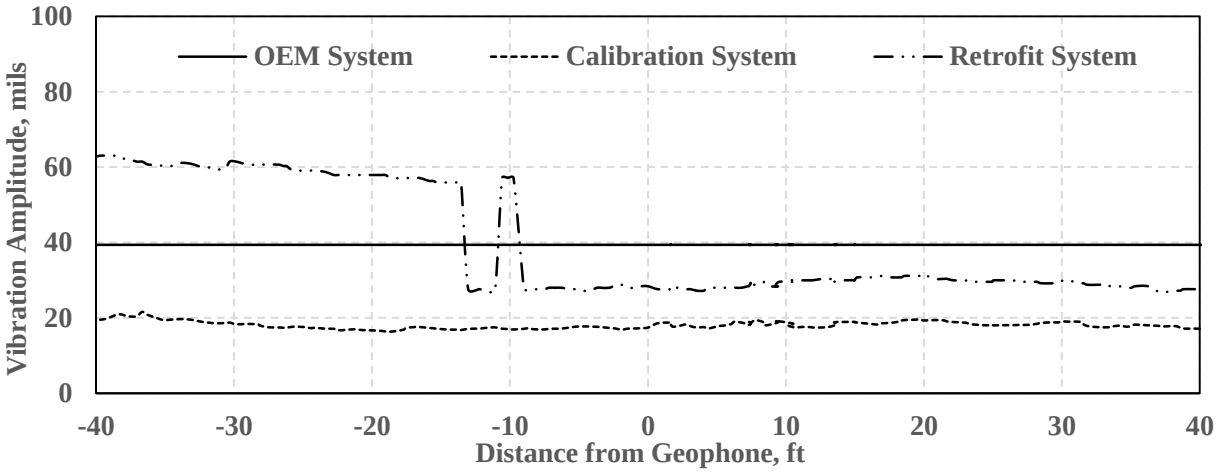

Figure 4.3.30. Comparison of vibration amplitude between OEM, retrofit and validation systems on SAKAI roller during pre-mapping

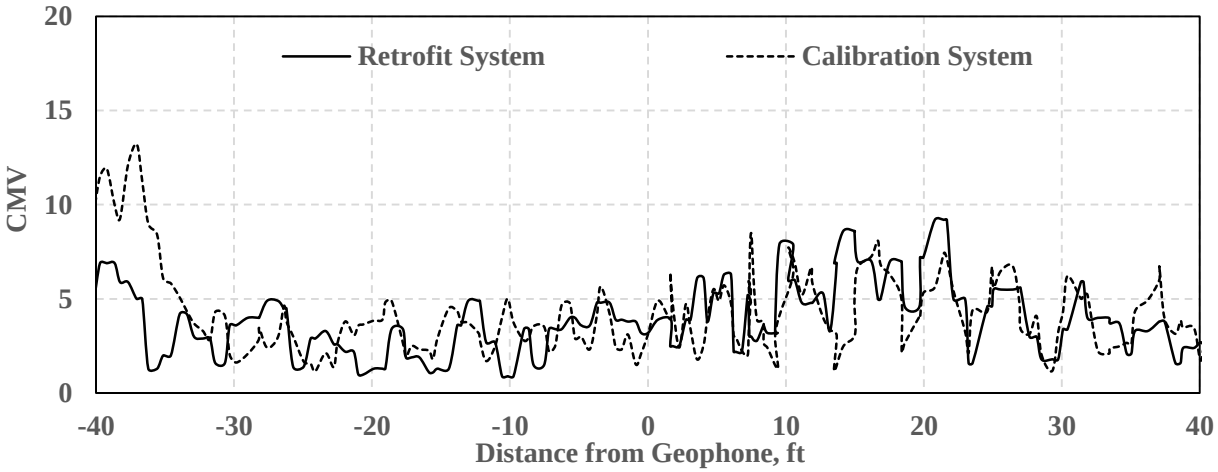

Figure 4.3.31. Comparison of CMVs from retrofit and validation systems on SAKAI roller during pre-mapping

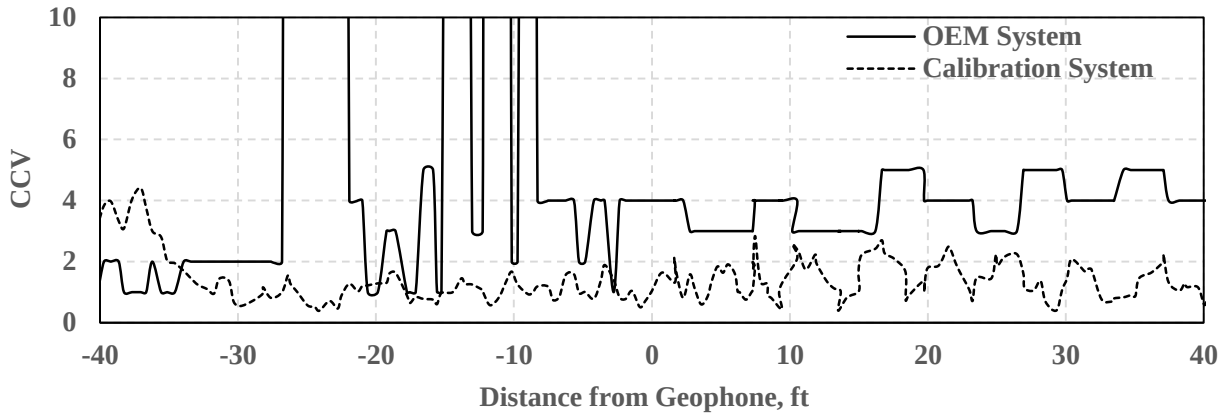

Figure 4.3.32. Comparison of CCVs from OEM and validation systems on SAKAI roller during pre-mapping

Figures 4.3.33 through 4.3.35 illustrate the vertical, transversal and longitudinal components of the response of the embedded geophones during the pre-mapping of the existing embankment layer with the SAKAI roller. The vertical deflections of the top geophone are about 50% more than the bottom one. The transversal components of the deflections are small as compared to the vertical ones. However, the longitudinal responses of the embedded geophones, which is along with the roller path, is noticeable. Further analysis of the vibration data collected from the equipment rodeo in Texas are included in Appendix B.

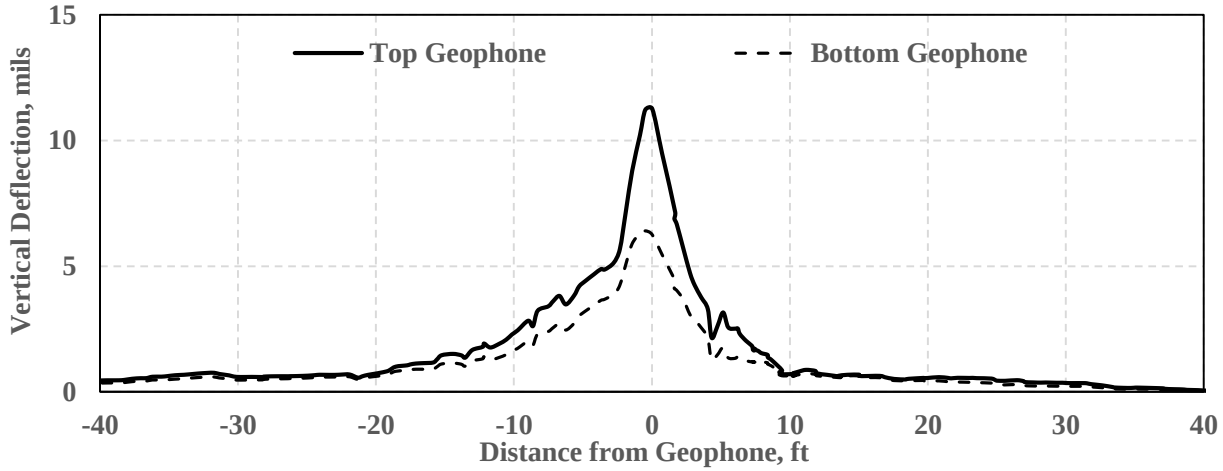

Figure 4.3.33. Vertical component of the response of top and bottom embedded geophones during pre-mapping of embankment layer

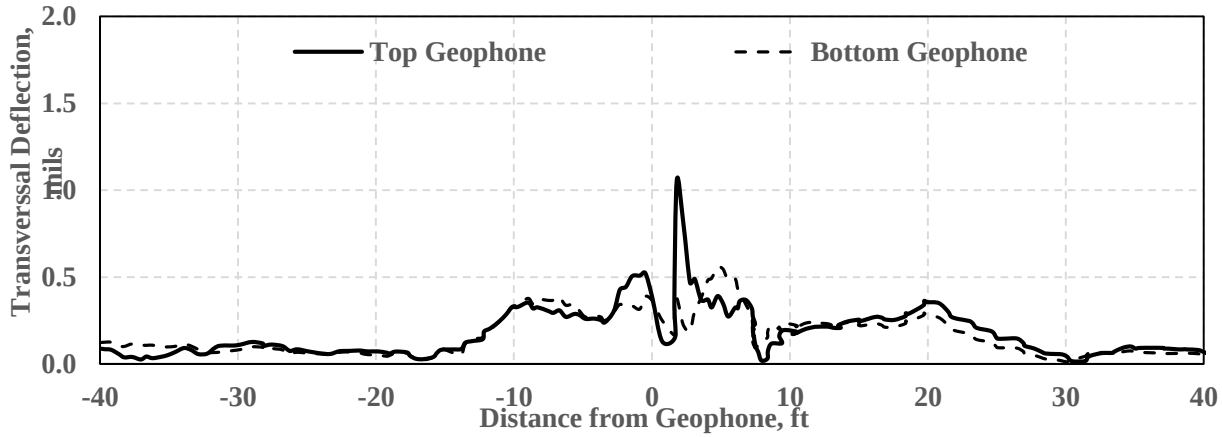

Figure 4.3.34. Transversal component of the response of top and bottom embedded geophones during pre-mapping of embankment layer

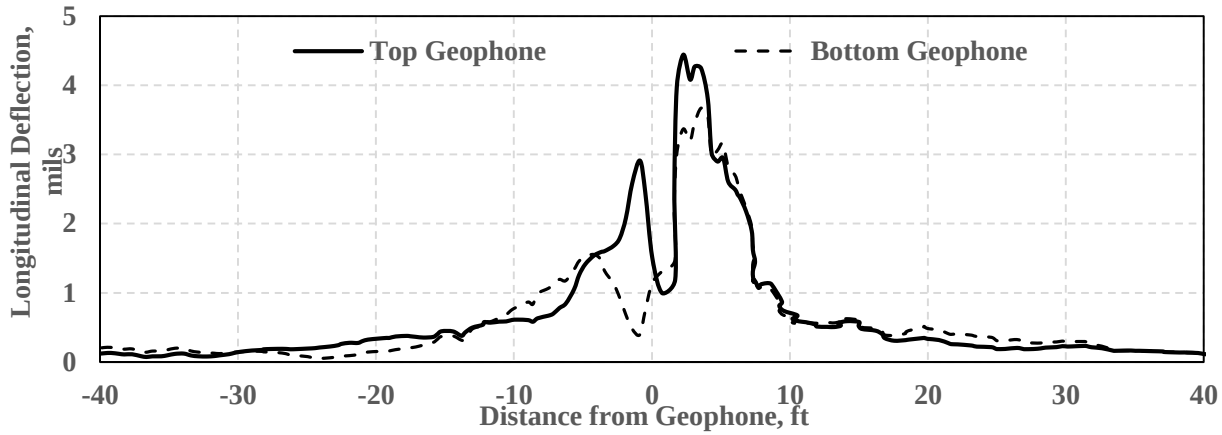

Figure 4.3.35. Longitudinal component of the response of top and bottom embedded geophones during pre-mapping of embankment layer

Table 4.3.14 summarizes the responses of the mounted accelerometers and top embedded geophone during IC data collection by the three rollers. The moving vibration tests were performed under two vibrations settings as low frequency-high amplitude and low frequency-low amplitude. The spectrograms of the accelerometer responses show that the forcing frequency of the SAKAI roller is somehow higher than the CAT and HAMM rollers. Furthermore, under high amplitude vibration, there are more harmonic frequencies in the spectrogram of the geophone response as compared to the low amplitude vibration. The white area in the spectrogram of the accelerometer and geophone responses for the HAMM roller during the low frequency and low amplitude vibration shows the period of time that the vibration was turned off on the machine.

4.4 CORRELATION OF SPOT TESTS AND IC DATA

As discussed earlier, a number of modulus/stiffness-based spot tests were performed during both equipment rodeos. One of the main parameters that should be considered during evaluation of spot tests and prior to the comparison of their results with IC data, is the influence depth of each device.

Since each device uses a different mechanism to estimate the modulus/stiffness, the influence depths are different. Figure 4.4.1 illustrates the influence depth of different devices compared to

Table 4.3.14. Response of Mounted Accelerometer and Top Embedded Geophone during Moving Vibration Tests (soils rodeo)

	Low Frequency, High Amplitude		Low Frequency, Low Amplitude	
	Accelerometer	Geophone	Accelerometer	Geophone
CAT (pre-mapping)	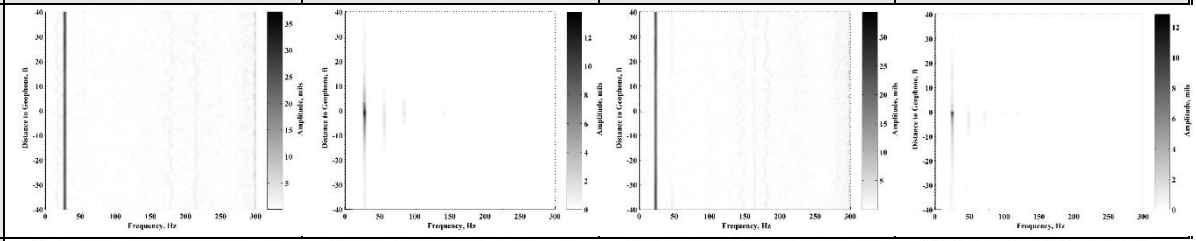			
SAKAI (mapping)	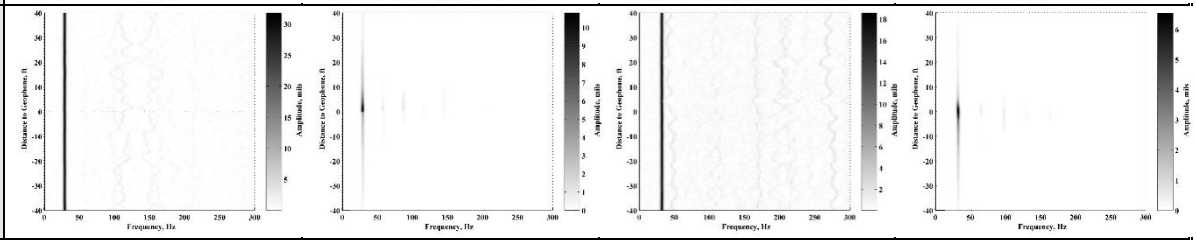			
HAMM (pre-mapping)	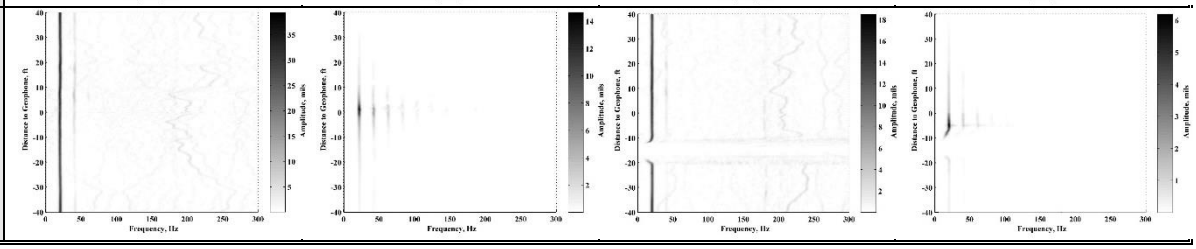			

the IC roller on top of an unbound geomaterial layer. Both nuclear density gauge and soil stiffness gauge (which was not employed in this study) are limited to the top 1 ft of the geomaterial layer. The influence depth of the dynamic cone penetrometer (DCP) is based on the penetration of the DCP rod. However, the typical penetration is about 3 to 4 ft with extension up to 10 ft. The reported influence depths of the falling weight deflectometer (FWD) and the light weight deflectometer (LWD) are different based on the research results in the literature. However, the typical values for both deflection-based devices are illustrated in Figure 4.4.1. The same uncertainty exists in the determination of the influence depth for the IC rollers. A typical value based on the results found in the literature is illustrated in Figure 4.4.1. However, the investigation of the influence depths of the IC rollers in still undergoing.

HMA Rodeo

The results of the spot tests performed on the compacted base layer were correlated with the IC data collected during the pre-mapping process. Figures 4.4.2 and 4.4.3 summarize the relations of the PSPA and LWD moduli with the CMVs obtained from the retrofit system on the SAKAI roller. Clear relationships between the spot tests and IC data are not observed. However, the LWD results seems to relate closer to the collected CMV data due to the deeper influence depth of the device as compared to the PSPA that is layer-specific. Considering the strong correlations observed between the ICMVs from the retrofit and OEM systems, the stiffness values from the OEM system also do

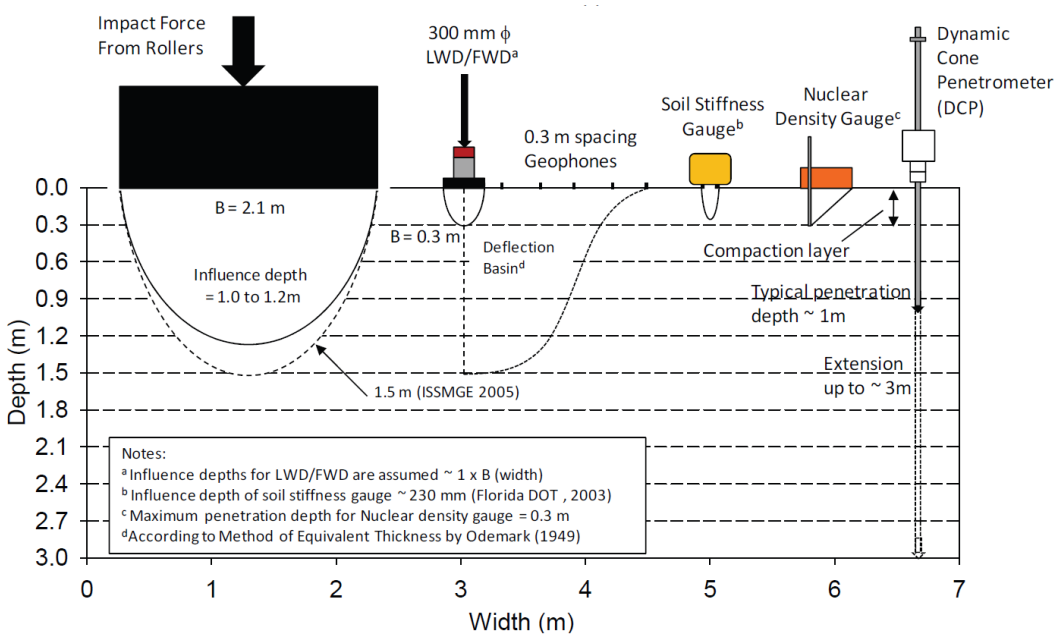

Figure 4.4.1. Comparing influence depth of spot tests with IC roller (Chang et al, 2011)

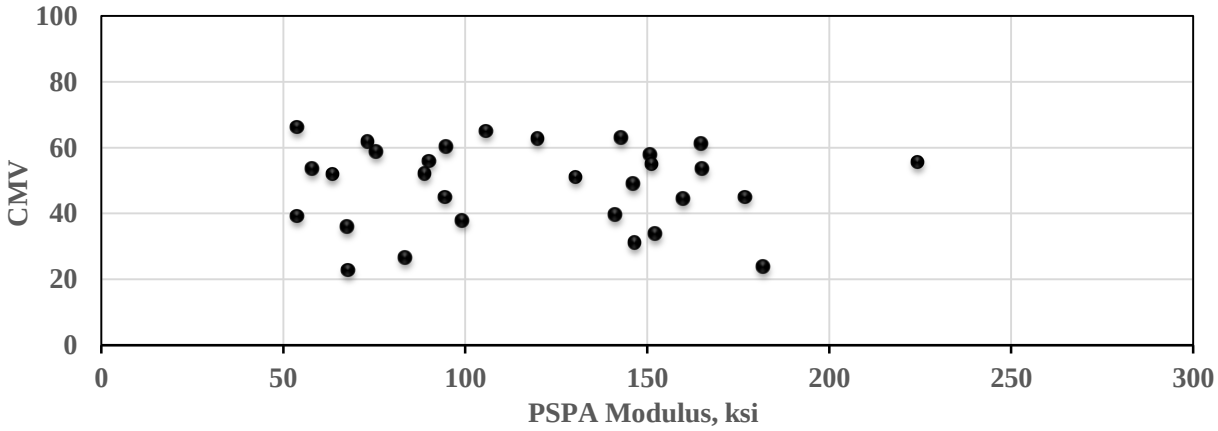

Figure 4.4.2. Correlation of CMVs from retrofit system on SAKAI roller with PSPA moduli on base layer

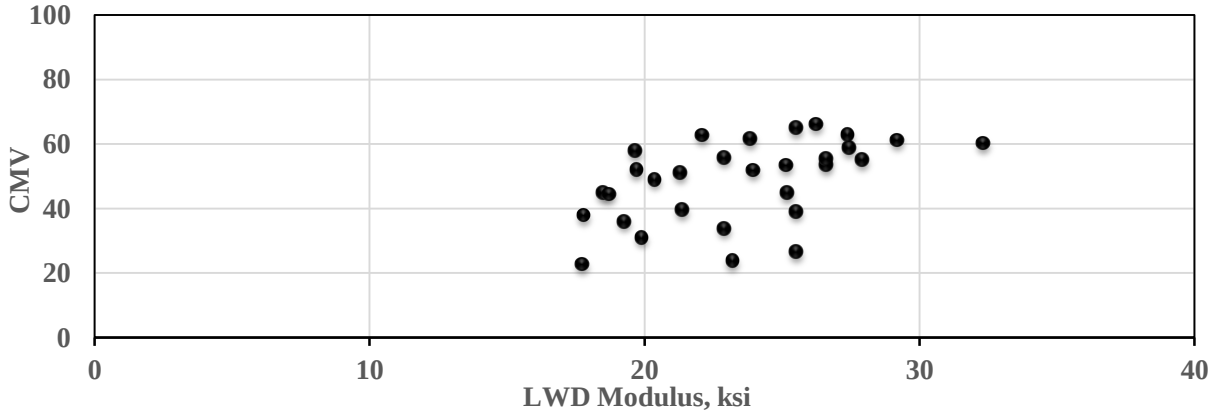

Figure 4.4.3. Correlation of CMVs from retrofit system on SAKAI roller with LWD moduli on base layer

not seem to have a relationship with the spot test results. The complete analyses of the spot tests and their correlations with collected IC data from different rollers during the California rodeo are included in Appendix A.

Table 4.4.1 summarizes the results of the spot tests during the pre-mapping of the existing base layer and mapping of the first and second HMA lifts. Again, since PSPA estimates the low-strain linear elastic modulus of the top layer, its moduli are greater as compared to the LWD test results on the existing base layer. The coefficients of variation of both devices seem reasonable considering the higher variability of the soil layer as compared to the HMA. Comparing the PSPA results between the first and second HMA lifts, it is clear that the asphalt layer gets stiffer after placing and compacting the second HMA lift.

Table 4.4.1. Descriptive Statistics of Spot Test Results during Pre-Mapping of Base Layer and Mapping of HMA Lifts

Statistical Parameter	Base Layer		First HMA Lift	Second HMA Lift
	PSPA Modulus, ksi	LWD Modulus, ksi	PSPA Modulus, ksi	PSPA Modulus, ksi
Minimum	54	17	302	392
Maximum	224	32	532	560
Average	121	23	400	499
COV	36%	16%	13%	8%

Soils Rodeo

Figures 4.4.4 through 4.4.6 summarize the correlations between the spot tests with the CMVs obtained from the retrofit system on the HAMM roller for the subgrade layer during the equipment rodeo in Texas. Again, strong relations could not be observed between the spot tests and the stiffness data from the IC roller. Further analyses of the results from other IC rollers are included in Appendix B.

Figure 4.4.7 illustrates the variation of the representative CMVs from the retrofit system on the HAMM roller with the moisture content of the subgrade layer at different spots within the test section. The soil samples were extracted from the compacted subgrade layer to obtain laboratory oven-dry moisture contents. A strong correlation between the CMV and moisture content is not observed. However, the LWD moduli seem to be related to the estimated moisture contents of the subgrade layer as shown in Figure 4.4.8. The stiffness increases as the moisture content decreases.

Table 4.4.2 summarizes the spot test results during the pre-mapping of the embankment layer and the mapping of the subgrade layer. Spot tests on the subgrade layer were performed about 18 hrs after completing the compaction process. Both the LWD and DCP devices exhibit high variability on the embankment and subgrade layers. This could be partially associated with the uncertainty of the device measurement and partially due to the variation of the soil properties throughout the test section. The varying range of subgrade moisture content between 12.7% and 19.6% could be a source of the variability in soil properties. Almost none of the devices show a noticeable difference between the stiffness of the embankment layer and the compacted subgrade layer.

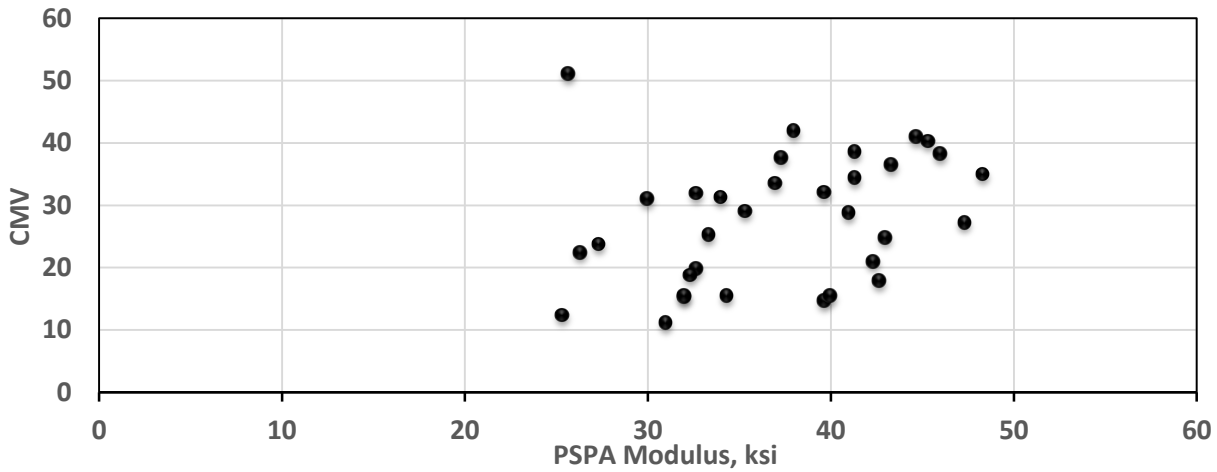

Figure 4.4.4. Correlation of CMVs from retrofit system on HAMM roller with PSPA moduli on subgrade layer

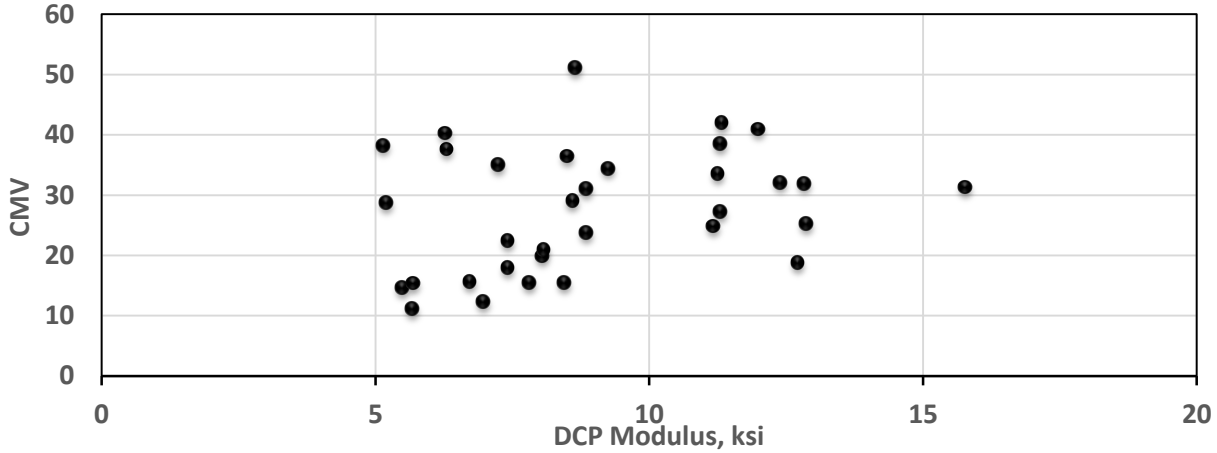

Figure 4.4.5. Correlation of CMVs from retrofit system on HAMM roller with DCP moduli on subgrade layer

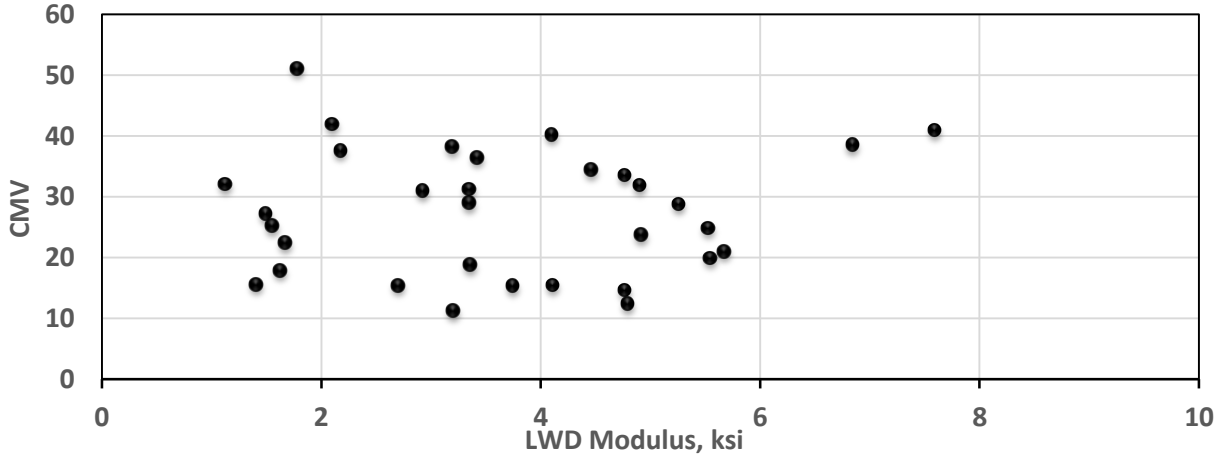

Figure 4.4.6. Correlation of CMVs from retrofit system on HAMM roller with LWD moduli on subgrade layer

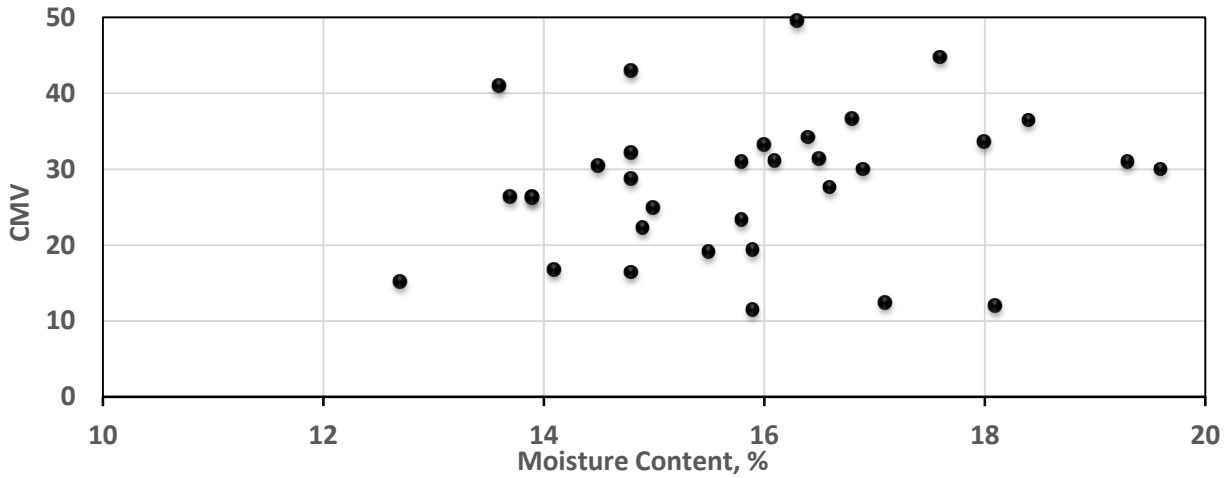

Figure 4.4.7. Correlation of CMVs from retrofit system on HAMM roller with moisture content of subgrade layer

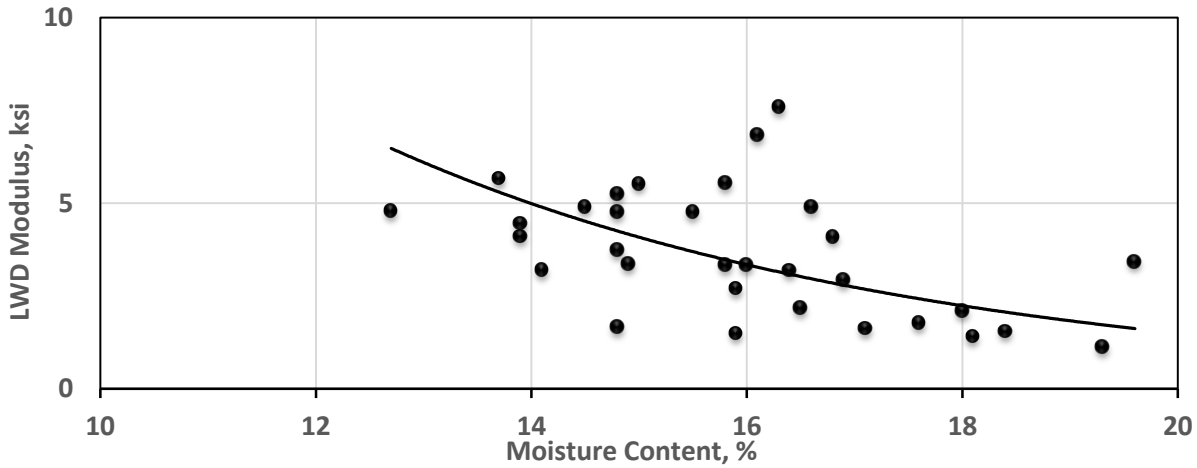

Figure 4.4.8. Correlation of LWD moduli with moisture content of subgrade layer

Table 4.4.2. Descriptive Statistics of Spot Test Results during Pre-Mapping of Embankment and Mapping of Subgrade Layer

Statistical Parameter	Embankment Layer			Subgrade Layer			
	PSPA Modulus, ksi	LWD Modulus, ksi	DCP Modulus, ksi	PSPA Modulus, ksi	LWD Modulus, ksi	DCP Modulus, ksi	Moisture Content, %
Minimum	23	1.2	1.6	25	1.1	5.2	12.7
Maximum	52	15.2	14.7	48	14.0	15.8	19.6
Average	38	5.8	8.4	37	4.0	9.0	15.9
COV	17%	67%	46%	17%	60%	30%	10%

CHAPTER 5. CONCLUSIONS AND RECOMMENDATIONS

The deliverables, products and activities associated with them are as follows:

- *Development of at least two equipment rodeos in two different locations across the country*. Two equipment rodeos were arranged to evaluate the performance and reliability of the IC retrofit kits. The first rodeo was dedicated to asphalt materials on a test section in California while the second rodeo was focused on soils and was conducted on as a part of a construction project of US 67 near Cleburne, Texas. Appendices A and B provide detailed information about these activities. Side-by-side comparison of the IC-retrofitted rollers with the factory supplied IC rollers was carried out. CAT, HAMM and SAKAI participated in the two rodeos with their factory-installed OEM IC rollers. They provided their double-drum rollers for the asphalt rodeo, and their single-drum rollers for the soils rodeo. The HAMM and SAKAI rollers were also retrofitted with the aftermarket IC retrofit kits provided by Trimble. The performance of the equipment was evaluated on hot mix asphalt, base, and subgrade.
- *Development of a validation procedure for IC retrofits commercially available at the time of the rodeos*: A validation process was prototyped through an independent data acquisition system to collect vibration data from accelerometers mounted on rollers and geophones embedded in the subsurface soil during the field studies. Appendix C contains appropriate information about that system.
- *Recommendation with respect to proper installation of retrofit kits*: Appendix D contains a multimedia presentation showing the step-by-step installation process for the retrofit kit. The first part of the Appendix includes the summary guidelines for the following items:
    - Introduction to the IC retrofit kit
    - Components of the IC retrofit kit
    - How the IC retrofit kit works
    - Features, benefits and limitations of the IC retrofit kit
    - Comparison of retrofitted and OEM IC rollers
    - Operational steps for installation of the retrofit kit
    - Initial setup of the IC retrofit kit

  The research team also produced an instructional video representing the general steps in installation of the IC retrofit kit. It is strongly recommended that the installation of the IC retrofit kit be performed by a certified technician.
- *Updated generic specification for the use of IC with asphalt pavements, base, and subgrade*: The AASHTO PP 81-14 specification was studied to accommodate the use of the IC retrofit kit based on the findings and results of this study. No change in the specifications is necessary, except FOR incorporating a section about the validation of proper installation of hardware and software. The development of a validation system is encouraged.
- *Frequently asked questions (FAQ) and answers on the use and operation of the IC retrofit kits, including lessons learned from the rodeos*. A list of FAQs regarding the installation and operation of the IC retrofit kit is included in Appendix E.

Upon completion of the two equipment rodeos (one on asphalt and another one on soils) and analyses of the collected data from the OEM systems, retrofit kits and the developed data acquisition system, the following observations and conclusions are presented:

- ***Retrofit Kits*:** The only commercially-available retrofit kit during the conduction of the two rodeos was developed by Trimble. The installation of the retrofit kit on conventional rollers needs special configuration and installation processes that should be planned in advance of their use. The roller model and its serial number are required prior to installation of the retrofit kit to accommodate for any special equipment and installation process.

  Since TOPCON launched its retrofit kit after the completion of the two rodeos, that system was not evaluated by the research team. However, the OEM systems on the SAKAI IC rollers under this study used a partial TOPCON retrofit system but with SAKAI's CCV system.

- ***IC Measurement Values and Units***: As included in the main report and further discussed in the appendices, each IC system estimates the stiffness using a different definition. The retrofit kit provided by Trimble measures the stiffness as Compaction Meter Value (CMV), which is the same as the OEM system on the CAT roller. The SAKAI OEM system reports the stiffness as Compaction Control Value (CCV). The OEM system on HAMM estimates the stiffness as HAMM Measurement Value (HMV). The recently launched retrofit kit by TOPCON, for which the results are not included in this study, reports the stiffness as CMV with an option to use any IC vendor's measurement system. All the above ICMVs are unitless. On the other hand, the roller-integrated soils stiffness K_b value and vibration modules E_{vib}, which were not evaluated under this study, use physical units of stiffness. The vibration data collected with the data acquisition system developed for this study are in terms of raw vibration signals that can be used to calculate CMV, CCV or HMV as necessary.

- ***Retrofit Kit Installation:*** The findings from the experience gained during the installation process at the two rodeos are as follows:

  - The research team strongly suggests that the installation process of the retrofit kit to be performed by an experienced technician certified by the developer of the retrofit kit.
  - Training materials provided as part of this project should be reviewed to ensure that the vibration sensor (accelerometer) is installed properly and securely in a way that it captures the "true" vibration of the drum.
  - A trial run a few days before the start of the work is strongly recommended to make sure that the hardware and software components are properly installed and function properly.
  - Since operational malfunction or missing data without the knowledge of the QC manager/ technician is not uncommon, the collected data should be downloaded daily, either from the cloud storage or locally using a thumb drive, and checked to ensure integrity of the data.
  - Frequent data quality checks during the first few days of the operation is strongly recommended.
  - The availability of a certified and knowledgeable technician should be ensured throughout the project but especially during the first few days of the operation.
  - The GPS coverage and calibration should be performed prior to the start of the IC data collection.

- A local GPS base station or a virtual base station could be used to provide correctional signals to the retrofit kit GPS receiver in order to achieve real time kinematic (RTK) accuracy.
- The Virtual Reference System (VRS) and Texas Real-Time Network (RTN) were employed in this project and the results were satisfactory. Upon establishment of connection with the base station channel, the roller should move slightly to stabilize the header computation of the GPS coordinates according to the recommended procedure in the FHWA Generic IC Specification.
- The coordinates of both sides of the drum contact with the surface should then be measured using a handheld GPS rover to calculate the coordinates of the drum center.
- The reported GPS coordinate by the IC system (either OEM system or retrofit kit) should be within 12 in. of the calculated coordinate using a handheld rover. If the validation fails, troubleshooting should be made to resolve this issue. No work should be proceeded before this issue is resolved.

- ***Geospatial Analysis of IC Data*:** The findings from the experienced gained during the data analyses from data collected at the two rodeos are as follows:
  - Shortly after the completion of the IC operation, the collected data should be analyzed as an expedited quality control tool.
  - One pragmatic way of almost real time use of the data, given the current complications with setting the target ICMV, is to observe the average ICMV of the last pass which is accessible on the control box of the IC kit. This average value can be used as the reference value to spatially locate relatively less stiff areas by the contractor.
  - The data transfer process was evaluated in this study using the cloud storage and a thumb drive. Downloading the collected IC data through each vendor's online data management system (e.g., VisionLink for Trimble/CAT, SiteLink3D for Topcon/Sakai and HAMM Compaction Quality navigator) seems to be more straightforward.
  - Since IC data are associated with GPS coordinates, geospatial and geostatistical data analyses should be performed on collected data. Veta is a standard tool required in the FHWA, AASHTO, and many DOT IC specifications to view IC data on the map and perform statistical analysis on the collected data. More advanced analysis can be conducted using the ArcGIS package on collected IC data and provides a complete range of coordinate system to locate IC data on different types of geographical and satellite maps while correcting for any possible data offsets. Using this tool requires basic knowledge of ArcGIS and its definitions.

- ***IC Data Analysis and Interpretation*:** The spatial interpretation of the IC data in terms of color-coded maps is dependent on the classification algorithm employed. The interpretation of color-coded maps also rely on the selected statistical parameters. Since the estimation of the ICMV target values is not very straightforward yet, a standardized statistical method should be employed to interpret the spatial distribution of the ICMV data, and furthermore, to identify the under-compacted areas. The standard quantile method was employed in this study to statistically classify the ICMV data and assign three colors (red, green and yellow) to the data points. The generated color-coded maps were then evaluated to identify the less stiff spots. In this method, the ICMV data are grouped into three different classes in the way that there are the same number of data points in each group. This classification method is independent of the statistical parameters of each set of collected ICMV data and do not require a target ICMV.

Classification methods based on defined target ICMV can be standardized in future research efforts. However, utilization of classification based on the statistical distribution of ICMV population seems reasonable at this time.

The performance of the Trimble IC retrofit kit mounted on two different types of rollers based on the color-coding criteria discussed were similar. However, depending on the vibration settings and vibration mechanisms of different rollers used in this study, the reported raw ICMV data were somewhat different.

- ***HMA Rodeo:*** The following specific items were observed during the HMA rodeo:
  - The spatial distributions of the ICMVs from all systems during pre-mapping of the existing base layer in terms of color-coded maps showed similar less stiff areas.
  - The cumulative distribution of the ICMVs collected with the retrofit systems on the HAMM and SAKAI rollers during the pre-mapping of the existing base layer were similar. However, the CAT roller showed a different trend for the cumulative distribution of collected CMVs.
  - The distributions of the ICMVs from the OEM system and retrofit kit on the HAMM roller were similar. The IC data from the SAKAI OEM system were not available for comparison purposes.
  - The ICMVs from the mapping of the HMA layers with the two retrofit systems mounted on the HAMM and SAKAI rollers were slightly different. This could be due to the different coverage area and change of HMA stiffness between the breakdown and intermediate compaction.
  - The OEM and retrofit systems on the HAMM roller showed that the ICMVs were similar during mapping of the HMA layer. The differences could be due to different algorithms that the two systems use to estimate CMV and HMV.
  - The OEM and retrofit systems on the SAKAI roller reported significant different ICMVs. However, the range of reported CMVs from the retrofit kit on the SAKAI roller agrees with that reported from the retrofit kit on the HAMM roller. The same pattern exists for the results of the OEM system on the SAKAI roller during the mapping of the second HMA lift.
- ***Soils Rodeo:*** The following items were observed during the soils rodeo:
  - From monitoring the density changes during the compaction process, the desired density was achieved after five passes. This is significantly less than ten or more passes that the contractors usually used.
  - The coverage of the collected IC data during the soils rodeo were more consistent and comprehensive since all rollers reported the IC results for almost 100% of the test section.
  - The ICMV results during the pre-mapping of the existing embankment layer with the retrofit kit mounted on the HAMM roller and the OEM system on the CAT roller were similar. The ICMV data collected from the retrofit kit mounted on the SAKAI roller were lower than those reported by the HAMM retrofit and CAT OEM systems. This could be due to an unidentified malfunction in transmitting or transferring the associated data.
  - The ICMV data from the retrofit kit and the OEM system on the HAMM roller showed reasonably similar trends with some differences that could be due to the data processing algorithms used by each of the two systems.

- The spatial distributions of the CMVs in the color-coded maps from the retrofit system on HAMM roller and the OEM system on the CAT roller are similar as they identified similar less stiff areas.
- The color-coded map of CMV from mapping the compacted subgrade layer with the padfoot roller was not as clear in identifying less stiff areas as compared to the results from the same roller with a smooth-drum. The color-coded map from the retrofit systems on the HAMM and SAKAI smooth-drum rollers, similar to the CAT OEM system, exhibited more homogenous distributions of stiffness data with clear distinction of the less stiff areas.
- The ICMV distributions between the retrofit and OEM systems on the HAMM roller were similar despite the fact that they use different algorithms to analyze the vibration data.
- The cumulative distributions of the ICMV data from the retrofit system on the HAMM roller and the OEM system on the CAT smooth drum roller were similar
- During the mapping of the compacted subgrade layer, the retrofit kit and the OEM system on the SAKAI roller did not provide comparable data.

- ***Data Acquisition (DAQ) System:*** The data acquisition system developed in this study was utilized to collect vibration data parallel to the OEM and retrofit systems to evaluate the performance of the retrofit kits during the IC data collection process. Furthermore, additional 3D sensors were embedded in the ground to monitor the response of the subsurface and estimate the influence depth of the IC rollers. Two sets of vibration tests, stationary and moving, were performed to monitor the ground response with more detail. he following items were observed from the utilization of the DAQ system:

  - The proper positioning of the accelerometers is crucial in capturing the proper vibration energy. This is especially important for rollers with special configurations of the drums and with dynamic vibration mechanisms.
  - The vibration responses of the two accelerometers mounted on the opposite sides of the drum were similar with typically less than 4% difference.
  - The algorithm employed to reduce and analyze the vibration data can affect the reported ICMV. Therefore, understanding the data processing algorithms within each IC system, either OEM or retrofit, is crucial in understanding and interpreting the reported ICMVs.
  - One of the main factors affecting the analysis of the vibration data is the gridding algorithm to transform the raw GPS-recorded coordinates to a gridded network and assigning ICMV data to the gridded points. Some of the differences observed in the mapping results can be due to different gridding algorithms used by different vendors.
  - Identifying the fundamental (vibration) frequencies and their multiple harmonics from the vibration data properly is essential in calculating the appropriate ICMVs. The data analysis algorithms also impact the reported ICMVs. A harmonization of the data reduction among different vendors is desirable.
  - Based on the measurements and analyses of the drum vibrations in the stationary position at different vibration settings, the following items were observed:
    - The reported operational frequencies are consistent. However, the nominal vibration frequencies and actual ones in some instances are different.
    - The influence depth of the roller vibration is dependent of the layer stiffness as well as the vibration settings. Based on the field data in this study, the influence depth could

be as shallow as 20 in. for a very stiff granular layer over bedrock and deeper than 5 ft for a less stiff clayey material. Such results could be verified with analytical simulation data.

- The cumulative distributions of the calculated ICMVs between the retrofit kit and the DAQ system were similar with minor differences. The ICMVs from the retrofit kit on the SAKAI roller during the soils rodeo was not comparable to the ICMVs of the other retrofit kit on the HAMM roller and the OEM system on the CAT roller.
- The reported vibration frequencies from the DAQ system during the moving vibration tests agree with those reported as the roller specifications. However, the captured amplitudes from the DAQ system were different from the nominal vibration amplitudes reported in the vendor specifications. Such differences are dependent on the layer stiffness and roller speed during the operation.

- ***Investigating correlation between selected nondestructive test (NDT) results and IC data:*** Three types of stiffness-based spot tests (Portable Seismic Property Analyzer, PSPA; Light Weight Deflectometer, LWD; and Dynamic Cone Penetrometer, DCP), along with density tests with NDG, were densely employed in this study. The PSPA and LWD were utilized during both the asphalt and soils rodeos, but the DCP was used during the soils rodeo only. At each stage 33 points were tested with the relevant devices. The corresponding ICMVs from the different rollers at each point were also extracted for comparison.

  A strong correlation among any of the spot tests and ICMV data during the soils or asphalt rodeo was not observed. From the PSPA measurements that correspond to the stiffness of the top layer, it was concluded that the ICMVs are indicative of the stiffness of the pavement system, and not the layer being compacted alone. Due to deeper depth of measurement, the LWD and DCP results show slightly closer correlations to the corresponding ICMVs. The color-coded map of stiffness variation based on the LWD and DCP results are more similar to the color-maps created from IC data.

Recommendations

- The installation of the IC retrofit kit should be performed by a certified technician at least a few days before the start of the project. Furthermore, the installed system should be carefully checked to ensure that the components are properly connected and that the vibration sensor is mounted vertically, securely and in a position that can capture the actual vibration of the drum.
- The roller configuration and installation parameters should be defined as part of the installation of the in-cab control box. In some IC systems, the design file could be uploaded for better understanding of the roller position during the operation.
- The GPS calibration process should be performed prior to any data collection. Either a physical or virtual base station along with a hand-rover could be utilized to perform the calibration process. The corrected GPS coordinates should be applied to the in-cab control settings.
- Even though transferring collected IC data through a thumb drive is included in the retrofit kit options, it is recommended to download the IC data through the cloud storage and export them to a specific file format for further analysis.
- For a reasonable geospatial interpretation of the collected IC data, using a color-coded map is recommended. Even though different color levels could be used based on various statistical parameters, the results of this study recommends the use of three colors (green, yellow and red) based on the concept that green areas represent the higher level of stiffness while the red

areas representing the less stiff areas. It is recommended to color-code the ICMV using the quantile classification method as discussed earlier in this report. However, such criteria is just a recommendation and has not been standardized yet.

- In most of the IC operations, the IC data are available both for all passes and for the final pass. However, for quality control purposes, it is recommended to use the data from the final coverage file. The mapping process is recommended to be performed at low frequency and low amplitude and a constant speed between 2.5 to 3.0 mph. The operator should be reminded that the vibration mode should be turned on in order to collect IC data.
- Both the OEM and retrofit kit manufacturers should improve the robustness of their systems. Even the expert operators continued operating the rollers without knowing that their rollers where not collecting data properly.
- The gridding algorithms of the IC systems and the retrofit kit could be improved to provide more reliable results. Furthermore, employing a harmonized gridding algorithm by the IC system vendors would be desirable to avoid any miscommunication among different systems.
- The format of the reported IC data could be unified among the IC system vendors so that the analysis of the data can be simplified.
- Standardization of ICMV among different manufacturers is desirable.
- Further correlation of stiffness parameters with soil properties and developing a database of ICMVs on different soil types would also be beneficial to IC users.
- A unified process for presentation of collected IC in a color coded format is desirable
- Even though the use of virtual base stations was successfully conducted in this study, it is recommended to use a survey-grade handheld rover to accurately calibrate the GPS units of the IC systems prior to the field operations.
- Development of a low cost validation system that could be easily mounted on the roller is desirable to monitor and validate the collected IC data.

REFERENCES

Adam, D., and Kopf, F. (2000). Sophisticated roller compaction technologies and roller-integrated compaction control. Compaction of Soils, Granulates and Powders, 3(113).

AMMANN (2003). "ACE-Soil Compaction and Compaction Control," CD, AMMAN Verdichtung AG, Langenthal, Swiss.

Anderegg, R., and Kaufmann, K. (2004). "Intelligent compaction with vibratory rollers feedback control systems in automatic compaction and compaction control." Transportation Research Record, Journal of the Transportation Research Board, 1898, 124-134.

Briaud, J. L., & Seo, J. (2003). Intelligent compaction: overview and research needs. Texas A&M University, College Station, TX.

Chang, G., Xu, Q., Rutledge, J., Horan, B., Michael, L., White, D., and Vennapusa. P.K.R. (2011). Accelerated Implementation of Intelligent Compaction Technology for Embankment Subgrade Soils, Aggregate Base, And Asphalt Pavement Materials. Federal Highway Administration (FHWA), Report No. FHWA-IF-12-002, Washington, D.C.

Gallivan, V. L., Chang, G. K., and Horan, D. R. (2011). "Intelligent compaction for improving roadway construction." Geotechnical special publication, American Society of Civil Engineers, 218, 117-124.

Geodynamik ALFA-030. Compactometer, Compaction Meter for Vibratory Rollers, ALFA-030-51E/0203, Geodynamik AB, Stockholm, Sweden.

Hossain, M., Mulandi, J., Keach, L., Hunt, M., and Romanoschi, S. (2006). "Intelligent compaction control." Airfield and Highway Pavements, American Society of Civil Engineers, 304-316.

Mooney, M. A., Rinehart, R.V., Facas, N.W., Musimbi, O. M., White, D., and Vennapusa, P. K. R. (2010). Intelligent soil compaction systems. National Cooperative Highway Research Program (NCHRP) Report No. 676, Transportation Research Board, Washington, D.C.

Nazarian, S., Yuan, D., and Tandon, V. (1999). Structural field testing of flexible pavement layers with seismic methods for quality control. Transportation Research Record: Journal of the Transportation Research Board, (1654), 50-60.

Nazarian, S., Mazari, M., Abdallah, I. N., Puppala, A. J., Mohammad, L. N., and Abu-Farsakh, M. (2014). Modulus-based construction specification for compaction of earthwork and unbound aggregate. National Cooperative Highway Research Program (NCHRP), Transportation Research Board, Washington, D.C.

Petersen, D. L., and Peterson, R. (2006). "Intelligent compaction and in-situ testing at MnDOT TH53." Minnesota Department of Transportation, MN/RC – 2006-13.

Tirado, C., Mazari, M., Carrasco, C., and Nazarian, S. (2015). Simulating Response of Different Lightweight Deflectometer Testing Using Finite Element Modeling. Transportation Research Board 94th Annual Meeting, Washington D.C.

White, D. J., Morris, M., and Thompson, M. J. (2006). "Power-based compaction monitoring using vibratory pad foot roller." Geo Congress 2006, American Society of Civil Engineers, 1-6.